On the Origin of Natural Antibody

by

Alexander E. Reynolds

Department of Immunology
Duke University

Date:_____

Approved:

_____
Garnett Kelsoe, Supervisor

_____
Michael S. Krangel, Chair

_____
Michael D. Gunn

_____
R. Lee Reinhardt

_____
Soman Abraham

Dissertation submitted in partial fulfillment of
the requirements for the degree of Doctor
of Philosophy in the Department of
Immunology in the Graduate School
of Duke University

2016

ABSTRACT

On the Origin of Natural Antibody

by

Alexander E. Reynolds

Department of Immunology
Duke University

Date:_____

Approved:

_____
Garnett Kelsoe, Supervisor

_____
Michael S. Krangel, Chair

_____
Michael D. Gunn

_____
R. Lee Reinhardt

_____
Soman Abraham

An abstract of a dissertation submitted in partial fulfillment of the requirements for the degree of Doctor of Philosophy in the Department of Immunology in the Graduate School of Duke University

2016

Abstract

Natural IgM (nIgM) is constitutively present in the serum, where it aids in the early control of viral and bacterial expansions. nIgM also plays a significant role in the prevention of autoimmune disease by promoting the clearance of cellular debris. However, the cells that maintain high titers of nIgM in the circulation had not yet been identified. Several studies have linked serum nIgM with the presence of fetal-lineage B cells, and others have detected IgM secretion directly by B1a cells in various tissues. Nevertheless, a substantial contribution of undifferentiated B1 cells to nIgM titers is doubtful, as the ability to produce large quantities of antibody (Ab) is a function of the phenotype and morphology of differentiated plasma cells (PCs). No direct evidence exists to support the claim that a B1-cell population directly produces the bulk of circulating nIgM. The source of nIgM thus remained uncertain and unstudied.

In the first part of this study, I identified the primary source of nIgM. Using enzyme-linked immunosorbent spot (ELISPOT) assay, I determined that the majority of IgM Ab-secreting cells (ASCs) in naïve mice reside in the bone marrow (BM). Flow cytometric analysis of BM cells stained for intracellular IgM revealed that nIgM ASCs express IgM and the PC marker CD138 on their surface, but not the B1a cell marker CD5. By spinning these cells onto slides and staining them, following isolation by fluorescence-activated cell sorting (FACS), I found that they exhibit the typical

morphological characteristics of terminally differentiated PCs. Transfer experiments demonstrated that BM nIgM PCs arise from a progenitor in the peritoneal cavity (PerC), but not isolated PerC B1a, B1b, or B2 cells. Immunoglobulin (Ig) gene sequence analysis and examination of B1-8i mice, which carry an Ig knockin that prohibits fetal B-cell development, indicated that nIgM PCs differentiate from fetal-lineage B cells. BrdU uptake experiments showed that the nIgM ASC compartment contains a substantial fraction of long-lived plasma cells (LLPCs). Finally, I demonstrated that nIgM PCs occupy a survival niche distinct from that used by IgG PCs.

In the second part of this dissertation, I characterized the unique survival niche of nIgM LLPCs, which maintain constitutive high titers of nIgM in the serum. By using genetically deficient or Ab-depleted mice, I found that neither T cells, type 2 innate lymphoid cells, nor mast cells, the three major hematopoietic producers of IL-5, were required for nIgM PC survival in the BM. However, IgM PCs associate strongly with IL-5-expressing BM stromal cells, which support their survival *in vitro* when stimulated. *In vivo* neutralization of IL-5 revealed that, like individual survival factors for IgG PCs, IL-5 is not the sole supporter of IgM PCs, but is likely one of several redundant molecules that together ensure uninterrupted signaling. Thus, the long-lived nIgM PC niche is not composed of hematopoietic sources of IL-5, but a stromal cell microenvironment that provides multiple redundant survival signals.

In the final part of my study, I identified and characterized the precursor of nIgM PCs, which I found in the first project to be resident in the PerC, but not a B1a, B1b, or B2 cell. By transferring PerC cells sorted based on expression of CD19, CD5, and CD11b, I found that only the $CD19^{+}CD5^{+}CD11b^{-}$ population contained cells capable of differentiating into nIgM PCs. Transfer of decreasing numbers of unfractionated PerC cells into Rag1 knockouts revealed an order-of-magnitude drop in the rate of serum IgM reconstitution between stochastically sampled pools of 10^{6} and $3x10^{5}$ PerC cells, suggesting that the $CD19^{+}CD5^{+}CD11b^{-}$ compartment comprises two cell types, and that interaction between the two necessary for nIgM-PC differentiation. By transferring neonatal liver, I determined that the early hematopoietic environment is required for nIgM PC precursors to develop. Using mice carrying a mutation that disturbs cKit expression, I also found that cKit appears to be required at a critical point near birth for the proper development of nIgM PC precursors.

The collective results of these studies demonstrate that nIgM is the product of BM-resident PCs, which differentiate from a PerC B cell precursor distinct from B1a cells, and survive long-term in a unique survival niche created by stromal cells. My work creates a new paradigm by which to understand nIgM, B1 cell, and PC biology.

To my mother and father, who taught me to always do my best, to never give up, and to maintain purpose and perspective in all that I do. Thank you for your love and encouragement.

Contents

List of Tables

List of Figures

List of Abbreviations

7-AAD	7-Aminoactinomycin D
Ab	antibody
Ad	adherent
ADCC	antibody-dependent cellular cytotoxicity
Ag	antigen
AID	activation-induced cytidine deaminase
AP	alkaline phosphatase
APC	allophycocyanin
APRIL	a proliferation-inducing ligand
ASC	antibody-secreting cell
B6	C57BL/6
BAFF	B cell-activator of the tumor necrosis factor family
Bcl6	B-cell lymphoma 6
BCMA	B-cell maturation antigen
BCR	B cell receptor
Blimp-1	B lymphocyte induced maturation protein 1
BM	bone marrow
bp	base pair

BrdU	bromodeoxyuridine
BSA	bovine serum albumin
C	constant
CCR	C-C chemokine receptor
CD	cluster of differentiation
cDNA	complementary DNA
CDR	complementarity-determining region
ChoP	phosphorylcholine
cIgM	cytoplasmic IgM
CLP	common lymphoid progenitor
CMP	common myeloid progenitor
CSR	class-switch recombination
CXCL	C-X-C chemokine ligand
CXCR	C-X-C chemokine receptor
d	day
D	diversity
DAPI	4′,6-diamidino-2-phenylindole
DC	dendritic cell
dsDNA	double-stranded DNA
DZ	dark zone

E	embryonic day
ELISA	enzyme-linked immunosorbent assay
ELISPOT	enzyme-linked immunosorbent spot
EPT	end-point titer
ER	endoplasmic reticulum
FACS	fluorescence-activated cell sorting
FBS	fetal bovine serum
Fc	crystalizable fragment
FC	flow cytometry
FcR	Fc receptor
FDC	follicular dendritic cell
FITC	fluorescein isothiocyanate
FSC	forward scatter
GC	germinal center
HC	heavy chain
HRP	horseradish peroxidase
HSC	hematopoietic stem cell
IFNγ	interferon γ
Ig	immunoglobulin
IL	interleukin

IL-5Rα	interleukin 5 receptor α subunit
ILC2	type 2 innate lymphoid cell
IMDM	Iscove's Modified Dulbecco's Medium
i.p.	intraperitoneal
IRF4	interleukin regulatory factor 4
Iso	isotype control antibody
i.v.	intravenous
J	joining
Lat	linker for activation of T cells
LC	light chain
LLPC	long-lived plasma cells
LN	lymph node
LPS	lipopolysaccharide
LSK	Lineage$^-$Sca-1$^+$cKit$^+$
LZ	light zone
MC	mast cell
Mcl-1	myeloid cell leukemia protein 1
MCp	mast cell precursor
MF	mature follicular
MHC	major histocompatability complex

MHCII	major histocompatability complex class II
mIgM	membrane-bound IgM
mRNA	messenger RNA
MZ	marginal zone
N	non-templated
N-Ad	non-adherent
n.d.	not detected
nIgM	natural IgM
NL	neonatal liver
NS	not significant
OD	optical density
OxLDL	oxidized low-density lipoprotein
PAMP	pattern-associated molecular pattern
PAX-5	paired box 5
PB	plasmablast
PBS	phosphate-buffered saline
PC	plasma cell
PCR	polymerase chain reaction
PE	phycoerythrin
PerC	peritoneal cavity

pMHC	peptide-loaded major histocompatability complex
pre-B cell	precursor B cell
pre-BCR	pre-B cell receptor
pro-B cell	progenitor B cell
PRR	pattern recognition receptor
RA	rheumatoid arthritis
RAG	recombination-activating gene
RORα	retinoic acid receptor-related orphan receptor α
RSS	recombination signal sequence
S	switch
SLC	surrogate light chain
SLE	systemic lupus erythematosus
SPL	spleen
SSC	side scatter
TCR	T cell receptor
TD	thymus-dependent
TdT	terminal deoxynucleotidyl transferase
T_{FH} cell	follicular helper T cell
T_H cell	helper T cell
Thy1.2	thymocyte differentiation antigen 1.2

TI	thymus-independent
TI-1	thymus-independent type 1
TI-2	thymus-independent type 2
TLR	Toll-like receptor
TNF	tumor necrosis factor
TT	tetanus toxoid
V	variable
WT	wild type
XBP1	X box-binding protein 1
μHC	IgM heavy chain

Acknowledgements

This dissertation would not have been possible without the assistance, collaboration, guidance, and support of many wonderful people. First, I thank my mentor Dr. Garnett Kelsoe for his tireless commitment to my intellectual growth and development as a scientist. His training and encouragement have driven me toward excellence in all that I do, both in and out of the lab. Dr. Masayuki Kuraoka, both a colleague and friend, has also been a tremendous source of knowledge and guidance as I navigated the studies presented here. I am grateful for the countless hours we spent discussing my work over the past six years. The foundation of much of my technical skill I owe to Dr. Derek Cain, whose patient, thoughtful instruction helped to develop my confidence and proficiency at the bench during my first years in the lab.

Several others have directly assisted me in performing experiments. I am indebted to Kristen Hopper and Jose Torres-Castillo for carrying out some of the histology work presented here, Dr. Pilar Snowden for providing data on serum IgM levels in MyD88-deficient mice, and Michael Cunningham and Sergio Sanders for aiding me with organ harvests on numerous occasions. I owe my independence at the flow cytometer to Patrice (Patti) McDermott, who both trained and assisted me throughout my time in the graduate program. The majority of the cell sorting required to perform my experiments was carried out by R. Ian Cumming, who has become a friend. His

dependability and cheerful attitude on the countless occasions I arrived late, or ran long into the evening have taught me a great deal about work ethic and selflessness. I am grateful for the collaboration of Dr. Anton Jetten, who kindly provided RORα-deficient mice for one of my projects.

I am sincerely thankful for all the members of the Kelsoe Lab, past and present, who have made our group into a family. Deborah Feyes, T. Matt Holl, Takuya Nojima, Xiaoe Liang, Xiao-Yan Nie, Margaret Barker, Wen-Li Zhang, Ann Miller, Joel Finney, Chen-Hao Yeh, and Hanqing Peng have been a delight to work alongside. I am especially grateful for the camaraderie of Dongmei Liao, Mandy Womble, Mengfei Liu, and Akiko Watanabe. Finally, I thank Pilar Snowden, Guang Yang, Kuei-Ying Su, Michael "Montana" Cunningham, Sergio Sanders, and Jose Torres-Castillo, who have become lifelong friends that I cherish deeply.

1. Introduction

1.1 Antibody

During the Peloponnesian War, nearly two-and-a-half thousand years ago, a plague struck the people of Athens. Greek historian Thucydides made the observation that the "same man was never attacked twice – never at least fatally," thus marking the first record of what we now know as immunity [1]. How such protection is mediated remained a mystery for centuries, but it is now known that the body defends itself by means of both cells and secreted molecules, which together form the immune system. Chief among immune molecules is an extraordinary protein called immunoglobulin, or antibody (Ab). Ab underlies the protective effect of essentially all current vaccines, which collectively represent one of the greatest public health achievements [2, 3].

Ab was discovered in 1890 by Behring and Kitasato, who reported the existence of a factor in blood serum that neutralized diphtheria and tetanus toxins. Transfer of serum from immunized to unimmunized animals protected the latter during subsequent toxin injection, thus proving that the body produced a soluble substance in response to initial exposure [4]. Forty-nine years later, the protective factor was found to exist in the third globulin fraction of electrophoretically separated serum, called "gamma" [5]. This led to the term "gamma globulin", eventually changed to immunoglobulin G (IgG).

Individual Abs react with a single or very limited set of determinants, while as a collection Abs are capable of recognizing an array of targets that is essentially limitless.

This attribute, together with the ability to reach targets at great distances from the cell that produced them, places Abs among the most potent protective elements of the immune system. Unsurprisingly, Ab exists in all vertebrate species yet examined [6].

1.1.1 Structure

Immunoglobulin (Ig) is a Y-shaped molecule comprising four protein chains: two longer chains described as heavy (HC), and two shorter light chains (LC) (Figure 1A). Each individual chain has two distinct regions. The amino-terminal domain differs between individual Ab molecules, and is thus referred to as the "variable" (V) region, while the rest of the chain is always one of five isotypes (IgM, IgD, IgG, IgA, IgE) and is thus called "constant" (C) (Figure 1B) [7, 8]. LCs each have a single C domain, while HCs have three or four and sometimes include a hinge region between the first and second C domains (Figure 1B). HCs are about 55 kDa, whereas LCs have a mass of approximately 25 kDa [9]. Igs are glycoproteins, with some isotypes more heavily glycosylated than others. Glycans help maintain Ig solubility and conformation, facilitate secretion, and mediate effector function [10].

By digesting Ig molecules with various enzymes it was discovered that the two branches of the Y, through their variable regions, are the parts of the Ab that interact with target molecules. The C-terminal base of the Y, called the crystalizable fragment (Fc), does not. Instead, it mediates functional effects [11]. Molecules bound by Abs are referred to as antigens (Ag), for their role in stimulating antibody generation. The site on

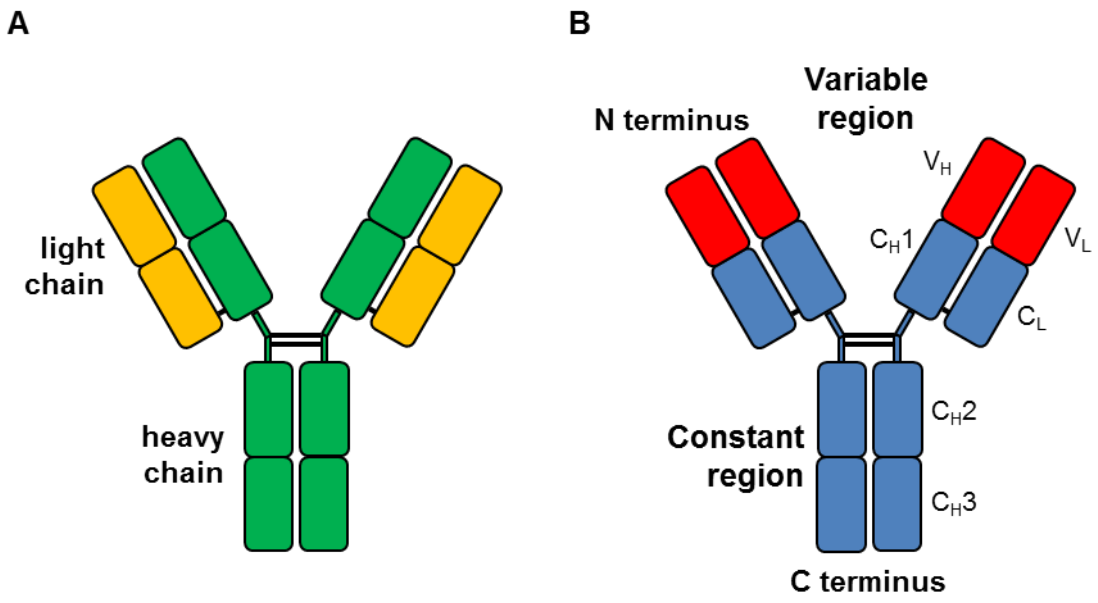

Figure 1: Structure of an antibody molecule

Schematics of a typical antibody molecule, showing (**A**) heavy (green) and light (yellow) chains, and (**B**) N-terminal variable (red) and C-terminal constant (blue) regions. Each colored box represents a domain; labels indicate domain name. Designed after Janeway's immunobiology [8].

an Ab at which it binds to Ag is referred to as the paratope, whereas the portion of the Ag bound by the Ab is called the epitope. As most Ags are made up of numerous epitopes, one Ab can discriminate between two Ags that differ at a single site, or bind different Ags that share only a small region of similarity.

1.1.2 Function

Ab mediates host protection most potently though neutralization, where Ab coats and renders toxic substances inert, or blocks host-binding determinants on pathogens to prevent infection. Ab-coated pathogens can also be targeted for cytolytic destruction by immune effector cells through a process called Ab-dependent cellular cytotoxicity (ADCC). Opsonization is a similar function, wherein phagocytic cells eat and destroy Ab tagged Ags (opson being the ancient Greek meal component that consisted of a savory side dish). Ab-Ag complexes also bind C1q, thereby triggering activation of the classical complement cascade, leading directly to target lysis or engulfment by complement receptor-expressing phagocytes (also a form of opsonization). Direct interactions between Ig and immune cells are facilitated by receptors that bind specifically to the Fc region of Ig molecules. Such "Fc receptors" (FcRs) exist for all Ig isotypes and mediate phagocytosis of opsonized particles, recognition of targets for ADCC, and regulation of immune cell activity.

Each Ig isotype exhibits distinct functional activity, contributing to the immune system's capacity to effectively defend against a range of insults. IgG is the most

predominant Ig in humans, and comes in four forms: IgG1, IgG2, IgG3, and IgG4 (IgG1, IgG2a, IgG2b, and IgG3 in mice), according to their decreasing prevalence in the circulation. Though all neutralize toxins and viruses, each sub-isotype has other distinct functional activities and is bound with different affinities by the Fcγ receptors. Whereas IgG4 does not fix complement, the other three bind C1q to varying degrees and thereby activate the classical pathway or act as opsonins. Nearly all hematopoietic cells, with the notable exception of T cells, express FcγRs. Of the three FcγR classes, I is high affinity, while II and III are low affinity and bind to IgG only when aggregated in Ab-Ag complexes (also called immune complexes). FcγRII and FcγRIII each have two forms, A and B. Engagement of FcγRI, FcγRIIA, or FcγRIIIA triggers activating signals; FcγRIIB sends an inhibitory signal, and FcγRIIIB none at all [9, 11, 12].

Though present at low levels in the serum, IgA is the most abundant Ig at mucosal surfaces and in secretions, such as tears, saliva, intestinal fluid, and breast milk. Here IgA is generally found as a dimer, connected by a linker called a joining (J) chain, though it is a monomer in the serum. The two subtypes of IgA, IgA1 and IgA2, differ in that IgA1 is more common in the serum and has a longer hinge region that allows greater flexibility and thus Ag binding, but also greater vulnerability to bacterial proteases. IgA2, predominant in the mucosae, has a shorter hinge and is thus less susceptible to such degradation [13]. Nevertheless, the high avidity of polymeric IgA enables it to play a critical role in neutralization of toxins and pathogens in the mucosae,

blocking their respective absorption by or adherence to mucosal surfaces. Engagement of FcαR induces phagocytosis or ADCC by the cells that express it [9].

The rarest form of Ig is IgE. Although it has strong anti-helminth properties, IgE is perhaps best known for its pathogenic role in hypersensitivity and allergy. This is partially due to the cross-reactivity of parasite determinant-specific Abs with allergy-generating Ags (allergens) [14]. IgE mediates its effects primarily when bound to the surface of mast cells (MCs) and basophils, which express high levels of the high-affinity IgE receptor FcεRI. Crosslinking of surface-bound IgE molecules by Ag induces the degranulation of MCs and basophils. FcεRI is also expressed at lower levels on Langerhans cells, monocytes, and eosinophils. The low-affinity receptor FcεRII, also called cluster of differentiation (CD) 23, is found on mature B cells [15].

IgM is plentiful in the circulation where it acts primarily a neutralizer, opsonin, and extremely efficient complement-fixing agent. These functions are linked to the pentameric (decavalent) structure of secreted IgM, which consists of five IgM molecules linked by a J-chain (Figure 2). Indeed, the high avidity of IgM often confers polyreactivity (the ability to bind multiple epitopes) [16]. Most IgM is produced constitutively as a form of pre-existing immune protection, and plays an important role in preventing infection and maintaining tissue homeostasis. These are discussed in detail below in section 1.1.3.

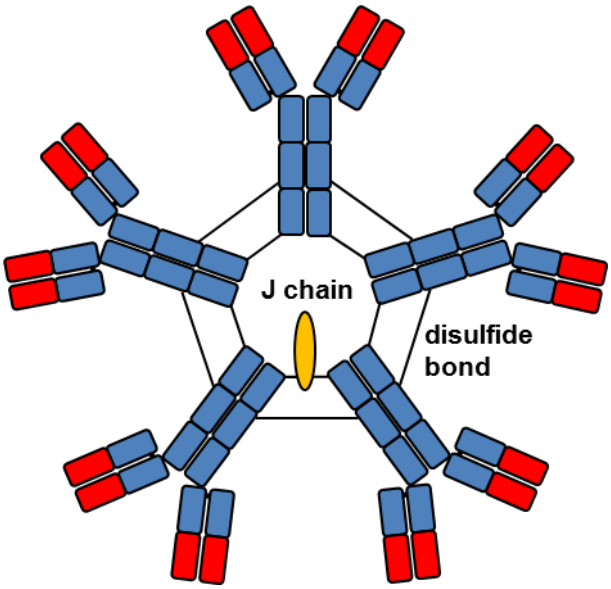

Figure 2: Pentameric IgM structure

Schematic of a pentameric IgM molecule, showing five individual IgM molecules connected by disulfide bonds (lines) and a J chain (yellow oval). The ten Ag-binding V-regions are colored red. Designed after Janeway's immunobiology [8].

1.1.3 Natural IgM

In contrast to other isotypes, secreted IgM is present in the serum even in the absence of exposure to external Ag. Not only is the quantity of IgM similar between germ-free mice and those housed under specific pathogen-free conditions, but the Ag-binding repertoire is largely unchanged as well [17, 18]. Such Igs are referred to as "natural Ab" or "natural IgM" (nIgM), and are present in the sera of all vertebrates, including neonatal and adult humans [19, 20]. Levels can vary more than 100-fold between individuals, though they remain relatively constant throughout the life of an organism [21, 22]. The unique binding pattern of nIgM is also conserved between individuals, and even species, and is focused primarily on common pathogen Ags and apoptotic cell determinants [20, 23-28]. These specificities endow nIgM with its two primary functions: prevention of infection and maintenance of tissue homeostasis.

nIgM binds viral and bacterial toxins, as well as directly to pathogens through conserved molecular structures, such as phospholipids, carbohydrates, and nucleic acids, allowing it to broadly recognize and block harmful substances and invading microorganisms never before encountered [24, 29, 30]. By virtue of its highly valent pentameric structure, nIgM easily neutralizes and agglutinates its targets, thereby defusing their harmful effects and infective capabilities, as well as promoting their destruction [16]. Studies have demonstrated the critical role of nIgM in protection against viruses such as influenza, bacteria such as *Streptococcus pneumonia*, fungi such as

Cryptococcus neoformans, and parasites such as *Brugia pahangi* [31-36]. nIgM not only clears these infectious agents from the circulation and tissues, but also carries them to lymphoid tissues to enhance the subsequent development of specific immunity, which is discussed below in section 1.3 [24]. The powerful ability of nIgM to clear pathogens has been harnessed in treatments such as Pentaglobin®, an IgM-enriched intravenous Ig (IVIG) infusion, which is highly effective in managing sepsis [19, 37].

The other major set of nIgM targets comprises apoptotic cell-associated, oxidation-specific Ags [25, 26]. The central protruding region of the mushroom-shaped pentameric IgM molecule binds with high affinity to C1q, which acts as an opsonizing "eat-me" signal for phagocytic uptake [19, 38, 39]. Through this mechanism, nIgM is a critical mediator of apoptotic cell clearance [40-42]. The removal of apoptotic debris is essential to maintaining tissue homeostasis, and is one of the most fundamental functions of the immune system. Every day billions of cells in the human body die and are replaced by fresh ones. To prevent these dying cells from inducing inflammation and immune activation, their death occurs in a controlled manner called apoptosis, whereby they shrink, their DNA is broken down, and their plasma membrane altered to form immunologically inert particles. If not cleared, apoptotic debris can progress to secondary necrosis where self-Ags and inflammatory mediators, such as high-mobility group box 1 (HMGB-1), are released [19]. Indeed, the defect in apoptotic cell clearance caused by C1q deficiency is associated with lupus-like disease in both humans and mice

[19]. Two primary dead-cell targets are recognized by nIgM: phosphorylcholine (ChoP), a phospholipid head group which is exposed during apoptosis, and phosphatidylcholine, a determinant on senescent red blood cells [19, 43, 44]. In addition to directing the removal of dead cell debris, nIgM also promotes the formation of an anti-inflammatory environment by modulating the phagocytes that take them up [45].

The scavenger role of nIgM has a profound impact on the maintenance of tissue homeostasis and immune tolerance to self Ags. In the absence of secreted IgM, mice spontaneously develop self-reactive IgG, and in autoimmune prone strains, accelerated disease [46, 47]. In humans, higher levels of IgM reactive with the apoptotic cell determinants PC and oxidized low-density lipoprotein (OxLDL) are found in systemic lupus erythematosus (SLE) patients with more mild disease, as well as healthy twins in SLE discordant twin studies [26, 48]. Though anti-double-stranded DNA (dsDNA) IgG is a hallmark of SLE and a mediator of disease, IgM against dsDNA, as well as other self-determinants such as beta-2-glycoprotein I and cardiolipin, correlates with reduced occurrence of renal disease in SLE patients [48-51]. High levels of IgM binding to atherosclerotic plaques, which contain OxLDL, are associated with reduced atherosclerotic disease in humans and LDL-receptor deficient mice [52-54]. A number of studies in Sweden have revealed inverse correlations between ChoP-reactive IgM levels and the incidences of stroke, heart attack, and even Alzheimer's disease [55-57]. These striking findings are supported by successful attempts to treat autoimmune diseases

such as atherosclerosis, SLE, and rheumatoid arthritis (RA) with nIgM, either through direct infusion or vaccine-induced expansion of nIgM specificities [58-61].

For all its powerful health-promoting attributes, nIgM also has negative qualities. Inflammation and tissue damage are higher in IgM-sufficient mice compared to their deficient counterparts in models of myocardial infarction and intestinal ischemia-reperfusion injury [62, 63]. In malaria infection, Plasmodium falciparum erythrocyte membrane protein 1 (PfEMP1) on *P. falciparum* parasites binds to the Cμ4 domain of IgM, leading to erythrocyte rosetting and malaria disease [64]. Moreover, hyperacute transplant rejection is mediated by nIgM Abs against blood group Ags, both between mismatched individuals as well as between species [65]. Indeed, nIgM represents a considerable hurdle to xenotransplantation, an otherwise promising solution to the donor organ shortage problem. Given the immunopathogenic liabilities of nIgM, it is critical to consider all facets of nIgM activity before manipulating its levels for therapeutic purposes.

1.2 B-cell development

Lymphocytes have long been associated with Ab production, but it was not until the mid-1960s that the developmental origins of lymphocytes mediating humoral and cellular immunity were distinguished [66, 67]. Using Chickens as a model animal, Cooper and colleagues were able to remove either one or both of the main lymphocyte sources (in mice, lymphopoiesis occurs primarily in the bone marrow, which cannot be

surgically removed): the bursa of Fabricius (a lymphoid organ in the hindgut) and the thymus. Chickens lacking a bursa were unable to mount Ab responses, while those having undergone thymectomy retained this capacity. Following the conclusion that only those lymphocytes originating in the bursa give rise to Ab-producing cells, the cells of this subset were termed "B lymphocytes" or "B cells" [68].

B cells are now defined by Ig expression. Though B cells have many functions, their principal and most fundamental role is the production of Ab following terminal differentiation. Indeed, the survival of patients suffering from genetic B-cell deficiencies can be greatly enhanced through infusions of Ig [69]. In addition to a secreted form, Ig is also expressed as a membrane-bound complex on the B cell surface, and is thus used as a B cell marker [70]. Membrane-bound Ig serves as the B cell Ag-receptor (BCR), where it both alerts B cells to the presence of pathogens and transmits essential tonic survival signals [71]. The generation and assembly of the BCR is the process around which B-cell development revolves. Like other immune cells, B cells develop from hematopoietic stem cells (HSCs), first in the fetal liver, and later in the bone marrow (BM) of the adult. Throughout ontogeny, however, the basic pattern of B-cell development is fundamentally the same, and consists of B lineage commitment, creation of the Ig repertoire, and positive and negative selection [72].

1.2.1 Immunoglobulin genes

Each B cell expresses a single type of Ig, that is, only one paratope. As the number of different Ig specificities is seemingly limitless, it follows that the number of individual Ig genes required to encode all Igs would have to be similarly large - on the order of billions. Clearly this is not possible, as there are only about 30,000 genes in both human and mouse [73, 74]. This mystery was solved by Tonegawa and his colleagues, who discovered that a finite number of Ig gene segments recombine stochastically within each B cell, forming a pool of B cells collectively carrying a virtually unlimited number of Ag receptors [75]. He was awarded the Nobel Prize in 1987 for his work. This ingenious genetic system gives the powerful advantage of allowing individual organisms to adapt almost without limit to environmental changes over space and time, as they are not restricted to a few fixed specificities [76].

1.2.1.1 Organization

Ig proteins are encoded by three separate gene clusters comprising both V and C regions, two for LC (called λ and κ), and one for HC. Each locus contains multiple segments, called variable (V), diversity (D), and joining (J) segments, that are recombined to form a unique V region that is transcribed together with the C region (Figure 3). The V region of the LC is formed from two of these segments called V_λ and J_λ or V_κ and J_κ, whereas the HC V region is made up of three DNA fragments, V_H, D_H, and J_H [77]. Mice carry two V_λ and three functional J_λ segments,

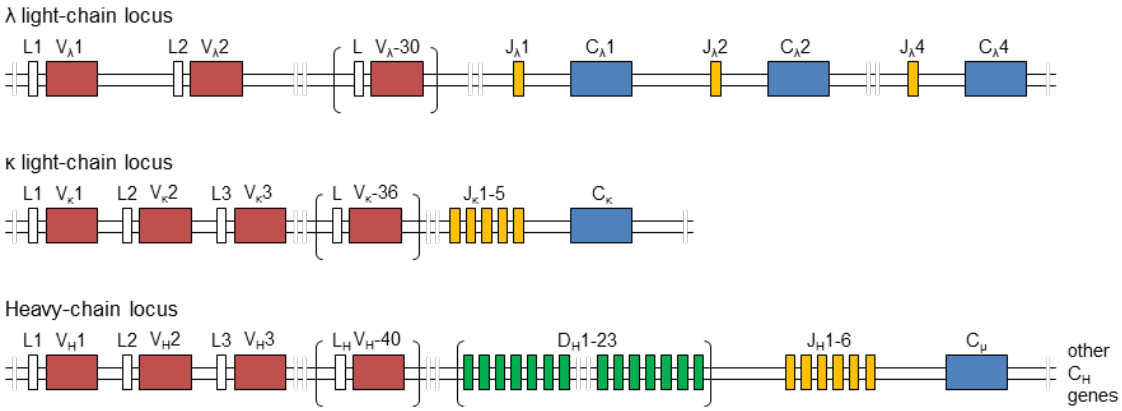

Figure 3: Germline immunoglobulin gene organization in humans

Diagram of the germline human Ig loci, showing V (red), D (green), J (yellow), and C (blue) segments. λ and κ loci contain V, J, and C segments, whereas the HC locus has V, D, J, and C segments. Each V-gene segment is downstream from a leader (L) sequence (white), which encodes a peptide that directs the ER trafficking of each nascent Ig chain. Designed after Janeway's immunobiology [8].

about 75 V_κ and four functional J_κ segments, and about 100 functional V_H, 14 active D_H, and four J_H gene segments. In humans there are about 30 functional V_λ and four J_λ segments, about 40 active V_κ and five active J_κ segments, and 39 functional V_H, 23 D_H, and six J_H gene segments [9, 76, 78, 79].

Within each V region are subregions of high sequence variability that are largely responsible for the Ag specificity of the encoded Ig. These intervals are called complementarity-determining regions (CDRs), and occur across the V-region sequence between more constant stretches of DNA known as framework regions. Each Ig chain has three CDRs, the last of which falls at the V-J or V-D-J junction of the LC and HC, respectively. The D_H segment, which constitutes the center of HC CDR3, is highly variable in both sequence and length, encoding 6-17 amino acids, and thus further amplifies Ig diversity [9, 76].

C-region genes are encoded downstream of the V-region gene segments. In mouse, there are two functional C_λ segments, one C_κ segment, and eight C_H segments distinguished by Greek letters and arranged 5′ to 3′ in the following order: μ, δ, γ3, γ1, γ2b, γ2a, ε, and α [76, 80]. These correspond to the Ig isotypes and subtypes of IgM, IgD, IgG, IgE, and IgA. Humans carry four C_λ segments, one C_κ segment, and nine C_H genes (μ, δ, γ3, γ1, α1, γ2, γ4, ε, and α2), in that order [76, 79, 81].

1.2.1.2 Rearrangement

Functional Ig genes are formed through somatic recombination of V_L and J_L or V_H, D_H, and J_H gene segments (collectively referred to as V(D)J recombination), which creates a contiguous V region just 5′ of the C region (Figure 4A) [82]. Though the gene segments used during each fusion event appears to be random, conserved sequences flanking each V, D, and J segment direct the recombination machinery where to cut the DNA, such that it does not split a gene segment, combine like segments with one another, or in the case of the HC, remove all D segments through direct fusion of V_H and J_H segments [76]. This is possible because two distinct recombination signal sequences (RSSs) are used. Both contain a nonamer and heptamer, but each conserved sequence is separated by either 12 or 23 base pairs (bp) of less conserved sequence (Figure 4B). V_λ segments have downstream 23-bp spacers, whereas J_λ segments have upstream 12-bp spacers. V_κ and J_κ segments exhibit the inverse. V_H and J_H segments are adjacent to 23-bp spacers, while D_H segments are flanked on both sides by 12-bp spacers (Figure 4C). Since only gene segments carrying disparate RSSs are recombined, rearrangement is restricted to V-J joining at LC loci, and V-D and D-J recombinations at the HC locus. This elegant mechanism, termed the "12/23" rule, was proposed by Early and colleagues in 1980 [77].

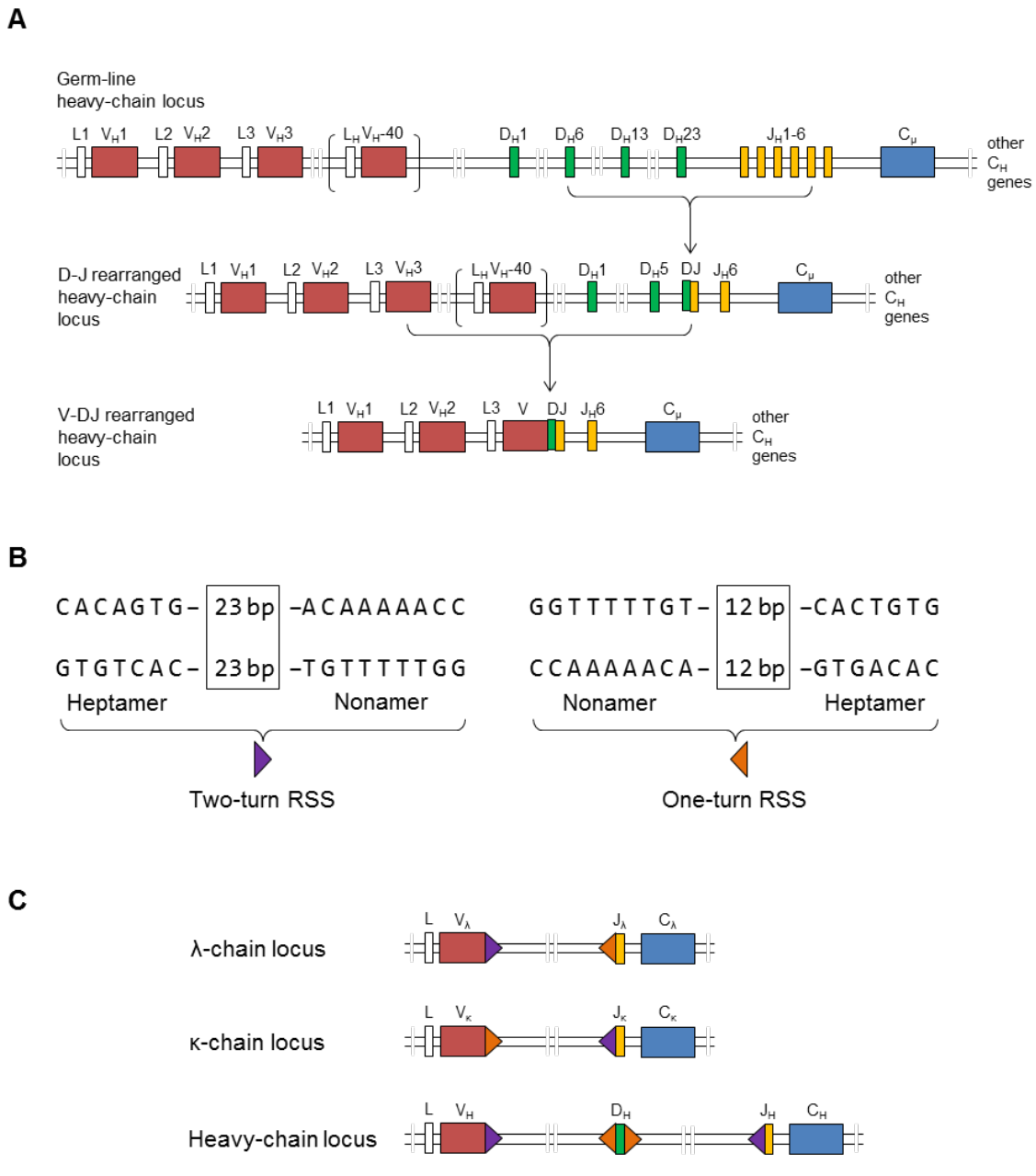

Figure 4: Immunoglobulin gene rearrangement

(Figure 4, continued) (**A**) Diagram showing the rearrangement of a D (green) to a J_H (yellow) Ig gene segment, with deletion of the intervening sequence, followed by a second deletion step joining a V segment (red) to the fused DJ sequence. Upstream leader (L) sequences (white) and downstream C segments (blue) are also shown. (**B**) Schematic of the two RSS types, both containing conserved nonamers and heptamers, but one separated by 23 bp that correspond to two turns of the DNA helix (left), and the other separated by a single-turn 12 bp sequence (right). (**C**) 23 bp-spaced RSSs (purple) are adjacent to V_λ, J_κ, V_H, and J_H segments. 12 bp-spaced RSSs (orange) are adjacent to J_λ and V_κ, and flank D segments on both sides. L sequences (white) and C segments (blue) are shown. Designed after Kuby immunology [79].

The actual cutting of the DNA helix is mediated by a complex of two recombination-activating gene (RAG) proteins, RAG1 and RAG2 [83]. Indeed, in the absence of either RAG gene, V(D)J recombination does not occur and B-cell development is halted [84, 85]. During RAG-mediated deletion of the intervening DNA segment, each of the two free ends of the split chromosome form hairpin loops [76]. Endonucleases nick each hairpin structure at random sites, resulting in single strand overhangs that are then filled in to form palindromic extensions referred to as P nucleotides [86]. An enzyme called terminal deoxynucleotidyl transferase (TdT) can then append a random small number of non-templated (N) nucleotides [87]. These combined processes are responsible for the incredible variety of CDR3s. Following these steps, the break is resolved through a common DNA repair pathway used by all cells called non-homologous end-joining [9].

Thus, three mechanisms together create the vast V-region diversity observed among newly generated B cells: combinatorial diversity of randomly rearranged V, (D), and J gene segments, flexibility at the junctions of fused segments, and combinatorial association of LCs and HCs into heterodimeric Ig molecules. Together, these mechanisms are estimated to have the potential to produce an astounding 10^{16} distinct Ig molecules [9].

As mentioned previously, each B cell expresses only one type of Ig, and thus only one HC allele and one LC allele (either λ or κ). This phenomenon is called "allelic

exclusion", and ensures that each B cell responds to only a single Ag determinant. It is thought that this restriction is a result of continued rearrangement until a functional V region is created, at which point recombination is halted. In this way, only one active V gene is created and thus expressed [76].

1.2.2 Stages of B-cell development

As BCR formation is the defining characteristic of B cells, B-cell developmental stages are delineated by the status of Ig-gene rearrangement and expression (Figure 5). The rigid sequence of events which brings about the production of a functional BCR is determined by the precisely controlled expression of RAG genes [88]. Prior to these events, however, B-cell lineage commitment takes place. B cells derive from an increasingly restricted set of precursors arising from multipotent HSCs in the BM. The first of these, the common lymphoid progenitor (CLP), has the capacity to form any of the three lymphocyte classes – B cells, T cells, and natural killer cells [89]. CLPs in turn give rise to the earliest B-lineage restricted cell type, pre-pro B cells. These cells are defined by their exclusive B-cell differentiation potential but lack of Ig rearrangement, and can be identified as $B220^{+}CD19^{-}$ [90, 91]. Throughout the course of B-cell development, B-cell lineage restriction is enforced by the transcription factor paired box 5 (PAX-5) [72].

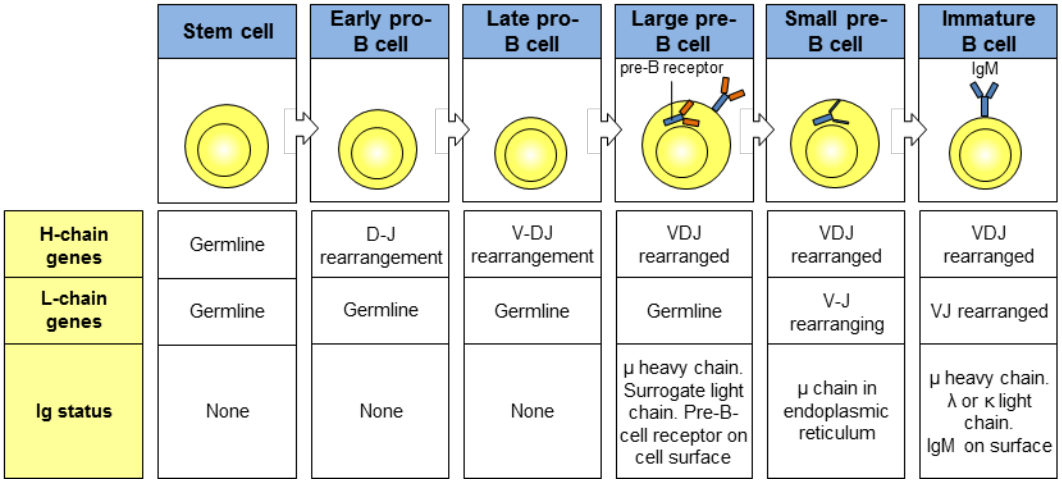

Figure 5: Stages of B-cell development

Diagram of B cell developmental stages, from HSC to immature B cell. Each column represents a stage, and describes the state of HC and LC rearrangement, as well as the Ig expression status at that point. Designed after Janeway's immunobiology [8].

1.2.2.1 BCR formation

Once a committed B-cell precursor begins to rearrange the HC, it is termed a progenitor (pro) B cell [88]. In this stage, both RAGs are upregulated and together mediate two sequential recombination events to produce a fully formed HC V-region. D and J gene segments are fused first (early pro-B), followed by joining of a V segment to the DJ rearrangement (late pro-B). The complete HC gene is then expressed as a μ chain (μHC), because it is transcribed with the IgM (μ) C-region segment, the most 5′ C-region in germline conformation.

The newly formed HC is then tested for its ability to combine successfully with LC to form a functional BCR. This occurs through association with a makeshift LC called the "surrogate" LC (SLC). As all B cells employ the same SLC proteins, λ5 and VpreB, a standardized screen of all HC rearrangements is accomplished [92]. Should HC and SLC assemble into a functional "pre-BCR", they associate with the Ig signaling molecules Igα and Igβ at the cell surface, which triggers a burst of proliferation. In this way, a successful HC rearrangement is positively selected and propagated to many individual cells, which proceed to form their own unique BCRs through association with distinct LC rearrangements [93, 94].

Following successful pre-BCR formation and entry into cell cycle, μHC expression is downregulated. This marks the next phase of B-cell development, the precursor B cell (pre-B cell) stage [95]. Two sub-stages distinguish those pre-B cells

which are undergoing pre-BCR-induced proliferation (large pre-B cells), and those which have ceased dividing (small pre-B cells). At this juncture, RAG is re-expressed and rearrangement of the *bona fide* LC begins [96]. It appears that V_{κ} genes are rearranged prior to attempts at the V_{λ} locus [97].

1.2.2.2 B-cell tolerance and maturation

Surface expression of the fully-formed BCR indicates that a developing B cell has reached the immature stage. This is a critical point in B-cell development, as the inherently random process of V(D)J rearrangement inevitably produces BCRs that are reactive with both foreign- and self-determinants [96]. Indeed, as many as 50% of newly generated BCRs bind self-Ag with potentially pathogenic affinity. Nevertheless, the incidence of autoimmune disease is less than 8%, due in part to a negative-selection process termed central tolerance. Should the BCR of an immature B cell bind self-Ag above a threshold affinity, three mechanisms prevent the continued maturation of the cell in its current state. First, the BCR is internalized and RAG expression continued, promoting the rearrangement of an alternative LC. This process is referred to as "receptor editing". Should the BCR still bind self-Ag with forbidden affinity, the cell will die (clonal deletion) or become hypo-responsive to BCR engagement (anergy) [98]. In this way, the collective BCR repertoire of Ag-responsive immature B cells exiting the BM exhibits nearly exclusive foreign reactivity.

Immature B cells not eliminated by central tolerance mechanisms begin to express surface IgD in addition to IgM by alternative splicing of a single transcript [99]. At this stage, B cells exit the BM and migrate to the spleen to mature through several transitional stages [100]. Here, B cells become mature follicular (MF) or marginal zone (MZ) B cells, which are further described as "naïve" since they have not yet encountered their cognate Ag, that is, the Ag to which their BCR binds. Mature B cell subsets congregate in distinct sub-anatomical sites in secondary lymphoid tissues such as spleen, lymph nodes (LNs), tonsils, and Peyer's patches [96]. Though they continuously circulate through the body by way of the blood and lymph, follicular B cells form what are called B cell follicles as they pass through secondary lymphoid organs. MZ B cells cease migrating and accumulate in the splenic MZs, allowing them to monitor the circulation and respond rapidly to blood-borne pathogens [101]. Survival of both mature B cell types requires tonic, low-level BCR signaling as well as recognition of the cytokine B cell-activator of the tumor necrosis factor family (BAFF) through BAFF receptor [102].

1.2.2.3 Distinct features of early B lymphopoiesis

Though the basic pattern of B-cell development remains the same throughout the life of an individual, several processes differ between the fetus and adult such that divergent BCR repertoires are formed during these periods. In contrast to adult B lymphopoiesis (outlined in the preceding sections), which occurs in the BM, fetal B cells form primarily in the liver. Among the chief peculiarities of fetal B-cell development are

a lack of N-nucleotide additions, positive selection for HC rearrangements that poorly assemble pre-BCR, and positive selection of self-reactive clones.

As fetal pro-B cells fail to express high levels of TdT during HC rearrangement, few or no N-nucleotides are added to V-D and D-J junctions [103]. The absence of such randomized reading-frame shifts leads to selection for V-gene rearrangements that are distinct from those preferred in the adult [72]. As in adult BM, expression of the rearranged HC is followed by pre-BCR-mediated selection; however, in the fetus such selection appears to be for HCs that poorly associate with SLC rather than those which form functional pre-BCR on the cell surface. Indeed, enforced expression of pre-BCR-forming HC rearrangements inhibits the proliferation of fetal pro-B cells [104]. This irregularity further directs the fetal B-cell repertoire toward V-genes that are rarely found among B cells formed in the adult, such as V_H11 and V_H12 [105, 106]. In addition, and perhaps most strikingly, immature B cells expressing self-reactive BCRs are positively selected in the fetus, whereas non-self-reactive B cells appear to be excluded [107, 108].

The unique repertoire generated during fetal B-cell development is retained in the adult through self-renewal of fetus-derived B cells [109]. Such B cells were first identified by expression of both CD19 and Ly-1 (now known as CD5), and were thus termed "Ly-1^+" B cells. However, it was later discovered that $CD5^-$ B cells are also produced early in ontogeny, and CD5 expression can be induced on B cells formed in

the adult. Thus, the term "B1" B cells has been employed to refer to fetal-lineage B cells, while "B2" references adult BM-derived B cells [72].

B1 cells, while rare in secondary lymphoid organs of the adult, are highly enriched in the peritoneal and pleural cavities [110]. Here they are poised to respond rapidly to foreign material [111]. The polyreactivity and autoreactivity of B1 cells allows them to broadly recognize pathogens as well as apoptotic cells. Indeed, the fetal B-cell lineage has long been closely associated with nIgM. However, $CD5^+$ B1 cells (also called B1a cells) have also been found to produce self-reactive IgG and exacerbate autoimmune disease in models of SLE [112-114].

1.3 The humoral immune response

Though the mature B cell pool is collectively capable of recognizing a virtually unlimited array of Ags, the number of individual B cells that are specific for a particular Ag is relatively small. Thus, in order to boost the probability of cognate Ag encounter, most B cells continuously circulate through the blood and lymph, making brief stops in each secondary lymphoid tissue (where Ags collect), forming B cell follicles. Others, such as MZ B cells and B1 cells, lie in wait at sites of heightened Ag exposure or blood flow. In this way, rare specific B cells readily encounter and are activated by their corresponding Ag. Following Ag recognition, B cells divide and eventually differentiate into Ab-producing cells, their ultimate fate. Indeed, the effector element and principal end of B-cell immunity is the Ab molecule.

1.3.1 B-cell activation

Following activation, a B cell can go down a number of different paths. Though these paths eventually converge at Ab production, each engenders qualitatively and temporally distinct outcomes. Factors that influence this arc include the mode, strength, and conditions under which activation occurs. Two principal mechanisms for B-cell activation exist, and are distinguished by their reliance on T-cell assistance.

1.3.1.1 T-dependent activation

As a second level of control against the development of autoimmunity, most Ags only activate B cells in the context of T-cell interaction. Thymus-derived lymphocytes (T cells) are the second lymphocyte lineage distinguished through the experiments of Cooper *et al.* [67]. Like B cells, T cells bear heterodimeric Ag receptors which are formed through V(D)J rearrangement and subjected to tolerizing negative selection [79]. There is a very low chance that a B cell and T cell reactive to the same self-Ag would both escape central tolerance. In contrast to BCRs, however, T-cell receptors (TCRs) only recognize peptide Ags, and only those that have been processed and displayed on the surface of a cell bound within the major histocompatability complex (MHC) [115]. The subset of T cells which recognizes peptide-loaded MHC class II (pMHCII) and promotes B-cell activation is defined by expression of the co-receptor molecule CD4.

As with B cells, T cells specific for a particular Ag are relatively infrequent in the body at any given time, and thus also congregate in lymphoid tissues (forming T cell

zones). Dendritic cells (DCs) play the critical role of sentinel, and are stationed throughout the body to take-up Ag and carry it to local lymphoid tissues to present to T cells. As professional Ag-presenting cells, DCs specialize in capturing, processing, and presenting Ag [116]. Though they do not express rearranged Ag-receptors, DCs are able to sense infectious particles through germline-encoded receptors called pattern recognition receptors (PRRs), which recognize conserved molecular motifs on pathogens [117]. PRR engagement induces DCs to upregulate cytokines and co-stimulatory molecules that are required, along with pMHCII, to activate $CD4^+$ T cells [116, 118]. Activated $CD4^+$ T cells then divide and differentiate into "helper" T cells (T_H), which express the B-cell activating molecule CD154 (CD40 ligand) and secrete different cytokines depending on the conditions under which they were activated [118].

Encounter with cognate Ag crosslinks BCR, sending an activation signal to the B cell. As B cells are also professional Ag-presenting cells, the BCR:Ag complex is endocytosed and the Ag processed and presented on the surface of the cell in MHCII. Through pMHCII:TCR interactions, the B cell then joins with one of the now numerous T_H cells that are specific for the same Ag [119]. During this engagement, T_H cells provide the second signal required for B-cell activation - CD40 engagement through CD154. Finally, cytokines secreted by the T_H cell instruct the B cell which class of Ig to produce, thus completing the propagation of information from initial insult to DC to T cell to B cell to Ab [118]. Most MF B cells recognize TD Ags, and respond by rapidly dividing.

This process, during which the number of B cells that target an Ag is greatly increased, is referred to as "clonal expansion". These B cells then go on to refine their effector capabilities in a structure known as the "germinal center" (GC), discussed below in section 1.3.2.1.

1.3.1.2 T-independent activation

In contrast to the majority of Ags, which can activate B cells only with the help of T cells, certain Ags are able to directly stimulate the proliferation and differentiation of B cells. Such Ags are termed thymus-independent (T-independent, or TI) because they were first identified by immunizing athymic nude mice [120]. TI Ags are able to activate B cells independent of MHCII-restricted T-cell help because they possess one of two special characteristics, which split them into two classes: TI type 1 (TI-1) and TI-2. TI-1 Ags are B-cell mitogens (cell-cycle stimulants), such as PRR ligands, that happen to also be bound by certain BCRs [79]. In this way, two activating signals are received even in the absence of CD40:CD154 interaction. The most well-characterized TI-1 Ag is lipopolysaccharide (LPS), a bacterial cell membrane component. TI-2 Ags are large polymers exhibiting a simple repeating structure [121]. These two characteristics, size and repetition, allow TI-2 Ags to extensively crosslink cognate BCR and activate B cells, once again bypassing T cell help [120]. B cells that recognize TI Ags are most commonly found among MZ and B1 B cells, and generally respond rapidly with short-lived IgM production, but no long-term protection [120-122].

1.3.2 Ig affinity maturation and class-switching

1.3.2.1 The germinal center reaction

V(D)J recombination equips the B-cell pool to recognize virtually any foreign Ag, but not necessarily with high affinity. To increase the strength and specificity of an Ab response, clonally expanded B cells develop additional variability through somatic mutations, which are then selected to produce a large population of B-cell clones with very high affinity for the target Ag. This phenomenon, called "affinity maturation", was discovered when serum taken at different times after immunization was found to contain Abs with escalating affinity [123]. Importantly, the lower the quantity of Ag injected, the more dramatic the rise. A few years later in 1970, Weigert and colleagues made the observation that these late, strong-binding Abs carried high numbers of mutations [124].

It was not until 1991 that Jacob *et al.* made the connection between affinity maturation and special structures in secondary lymphoid tissues called GCs [125]. GCs are foci of rapidly dividing B cells which form in B cell follicles a week or so following immunization with a TD Ag. Each GC is divided into two functional "zones". The dark zone (DZ) is so named because it is the site of clonal expansion, and thus appears dark under the microscope due to the numerous closely packed nuclei [126]. Mutation also occurs in the dark zone, with about one mutation introduced per cell division by an enzyme called activation-induced cytidine deaminase (AID) [118, 126, 127]. DZ B cells (called centroblasts) mutate at an astonishing rate that is about 10^6-fold higher than the

rate of spontaneous mutation [128]. Most mutations are single bp substitutions in the V-regions, though rare insertions and deletions do occur as well [118].

Following mutation, B cells are selected in the light zone (LZ) according to the new affinity of their BCRs [126]. Higher-affinity B cells gather larger amounts of Ag from non-hematopoietic LZ cells called follicular dendritic cells (FDCs) [128]. FDCs capture and retain Ab:Ag complexes on their surface for long periods primarily through complement receptors, but also through Fcγ receptors [128, 129]. LZ B cells (called centrocytes) thus display different densities of pMHCII on their surface in proportion to the affinity of their BCR. This allows centrocytes to compete for costimulatory help from a limiting number of GC T_H cells, called follicular T_H cells (T_{FH}); higher affinity centrocytes receive T-cell help and are activated, while lower affinity cells do not and are eliminated by apoptosis [128]. T cells are required for affinity maturation, as in the absence of T cells or CD154-mediated help, GCs disappear [130-132]. Activated centrocytes then migrate back to the DZ to proliferate and mutate. These new mutations again alter the affinity of each centroblast's BCR, which are then selected in a second round of LZ competition. Through such reiterations of mutation and selection, the average affinity of B cells in a GC quickly rises, with each individual GC producing B cells with the highest relative BCR affinity possible [118].

1.3.2.2 Class-switch recombination

In order for a B cell to produce Ab of an isotype other than IgM, it must first undergo a second Ig gene rearrangement event called "class-switch recombination" (CSR). During CSR, a downstream C_H segment is joined with the V-region by deletion of the intervening DNA (Figure 6). The process of CSR begins when AID deaminates cytosines within Ig switch (S) regions, sequences just 5′ to each C_H segment (with the exception of C_δ) comprising short tandem repeats. The resulting uracil residues are then repaired by a mechanism that introduces single-strand breaks into the DNA, which are then converted into double-strand breaks. The broken chromosome ends are fused through a type of end-joining distinct from the non-homologous recombination mechanism employed in V(D)J recombination [99].

As AID acts selectively on actively transcribed S regions, switching can be directed to a particular isotype by regulating DNA accessibility. Through the production of cytokines, T_H cells instruct B cells to activate different S regions [99]. Switching to IgG1 is induced by interleukin 4 (IL-4), which also drives second-step recombination to IgE. IgG2a and IgG3 are produced in response to interferon γ (IFNγ), whereas transforming growth factor β (TGFβ) stimulation can lead to either IgG2b or IgA. As each isotype has distinct functional attributes, the humoral immune response is thus tuned to most effectively defend the host from different types of attack [8, 118].

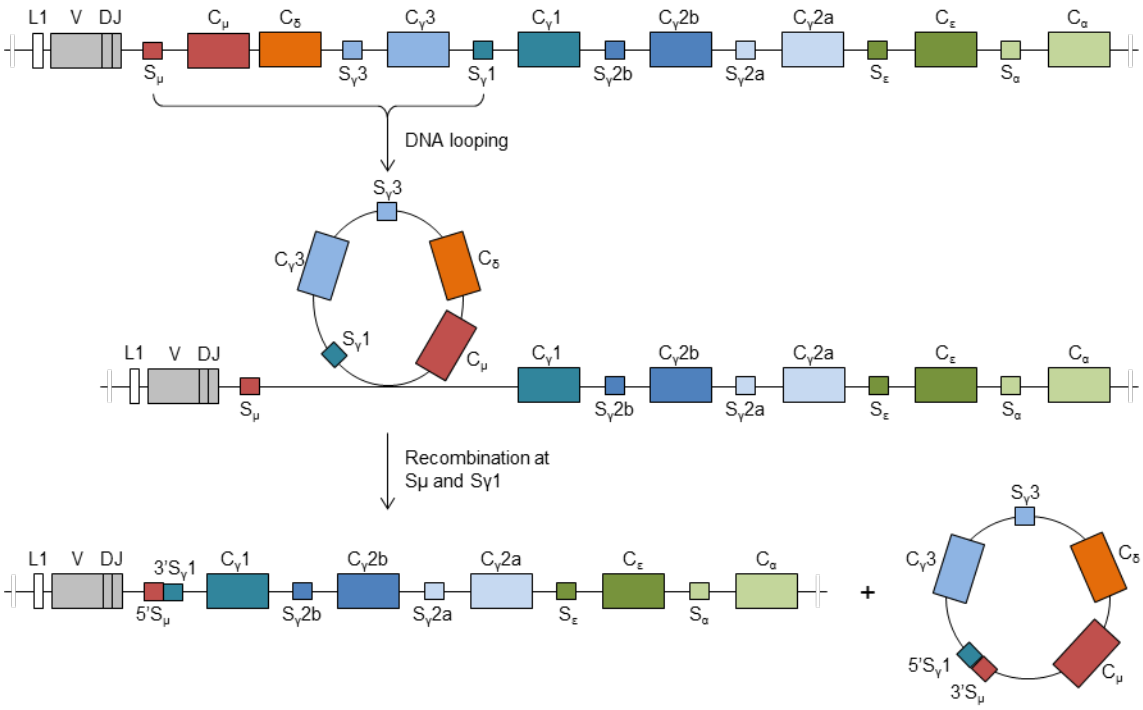

Figure 6: Class-switch recombination

Diagram of an Ig HC locus switching from Cμ (IgM, red) to Cγ1 (IgG1, turquoise). DNA looping brings the S regions physically close, and recombination deletes the invervening sequence (circle at bottom right). Designed after Kuby immunology [79].

Though CSR is induced most strongly in the GC, where AID levels are high, switching can occur just after Ag encounter, before the GC has yet formed or even in cells that never enter the GC at all [99].

1.3.3 Effector B-cell formation

As mentioned at the beginning of this introduction, the ability of the immune system to defend more quickly and strongly against a secondary pathogen exposure is the defining characteristic of adaptive immunity, that is, immune responses mediated by B and T lymphocytes [118]. The humoral branch of such immune "memory" is mediated by two types of cells that form following B-cell activation: memory B cells and Ab-secreting cells, called plasma cells (PCs). Memory B cells serve as a reservoir of affinity matured, class-switched B cells that can be rapidly activated to boost PC numbers and Ab levels, which form the immediate, direct line of defense against reinfection [133].

1.3.3.1 Memory B cells

Most memory B cells develop in the GC in response to TD Ags, though GC-independent pathways exist and TI memory has been reported in the B1 lineage [118, 134-136]. As no master transcriptional regulator of memory B-cell differentiation has been discovered, it is thought that memory B cells form in and exit the GC on a stochastic basis [133]. Two major types of memory B cell appear following TD activation: unswitched (IgM^+) and class-switched (mostly IgG^+) [134]. Each plays a distinct role in

the recall response, which is characterized by speed, strength, and specificity - the more rapid production of a larger amount of higher affinity Ab [133].

High-affinity Ab responses occur much more rapidly against previously encountered Ag for three main reasons. The first is prior clonal expansion, which increased the number of circulating B cells (and T cells) specific for that Ag, and thus the speed with which the Ag is encountered the second time. Secondly, these clonally expanded B cells have already undergone affinity maturation and thus do not need to enter the GC. Finally, IgG^+ memory B cells maintain a transcriptional program intermediate between GC B cells and PCs, allowing them to differentiate much more quickly [137]. In order to fine tune the memory response, reactivated IgM^+ memory B cells preferentially proliferate and reenter the GC where they undergo further affinity maturation, class-switching, and the formation of a new set of memory B cells [138].

Recall responses are possible because memory B cells persist in the circulation long after the instigating pathogen has been cleared. Such survival does not require BCR:Ag interaction, though tonic BCR signals seem to play a role in the maintenance of IgG^+ memory B cells through induction of the anti-apoptotic molecule B-cell lymphoma 2 (Bcl-2) [133, 139, 140]. Though BAFF is dispensable for switched memory B-cell survival, it is required for the persistence of IgM^+ memory B cells [133]. In contrast to studies that suggest IgM^+ memory B cells live much longer than their switched counterparts, strain-specific IgG^+ memory B cells have been recovered from the

circulation of humans who survived the 1918 influenza pandemic 90 years before [141, 142].

1.3.3.2 Antibody-secreting cells

The driving force behind B cell-mediated immune memory is high-affinity Ab produced long-term. However, such Ab is not produced until the GC is well under way and begins to release dividing PC precursors, called plasmablasts (PBs), about 2 weeks following the initial insult [143]. In order to protect the host during the first few days of infection, unmutated IgM-secreting PBs are formed early in the response [122, 144, 145]. As these early PBs migrate out of the B-cell zones into the red pulp of the spleen, they are called "extrafollicular". Extrafollicular PBs are short-lived, dying by apoptosis within a week to make way for the more robust GC-derived humoral response [118, 146]. High-affinity, class-switched PBs appear to leave the GC relatively early, within 3-5 days of GC formation [147]. These cells then go on to maintain the high titers of potent Ab that protect against subsequent infection. PCs are thus powerful immune effector cells, and are discussed in detail below in section 1.4.

1.4 Plasma cells

The hypothesis that Ab is the product of PCs was first put forward by Bjorneboe and colleagues in 1947 [148]. They observed that while adipose tissue in rabbits did not normally contain hematopoietic cells, certain fat deposits, such as renal sinus fat tissue, became infiltrated almost exclusively with PCs following immunization, while others,

such as retroperitoneal fat tissue, did not. Analysis of extracts of these two tissues revealed that Ab accumulated in the former but not the latter. The authors of this study concluded, therefore, that PCs are the source of secreted Ig.

Though PCs are now defined by their Ab-secreting function, PCs had long been previously identified by their unique morphology. In contrast to the generally round shape of other hematopoietic cells, PCs are elongated with a large cytoplasm and offset nucleus. Large quantities of rough endoplasmic reticulum (ER) and secretory granules can be seen filling the cytosol [149]. More recently, however, several surface molecules have become associated with PCs, and are now used in their identification and isolation. Foremost among these is syndecan-1, also called CD138, a heparin sulfate proteoglycan that binds to matrix proteins such as collagen and fibronectin [150, 151]. This receptor mediates B cell adhesion in a stage-specific manner, as it is expressed on pre-B and immature B cells in the BM, is lost upon maturation and release into the periphery, and then re-expressed during differentiation into PCs [152]. Other changes in surface molecule expression associated with PC differentiation include upregulation of CXCR4 and CD43, and downregulation of B220, CD19, CD23, CXCR5, MHCII, CD79, CD86, CD21, and surface Ig [143, 146].

1.4.1 Plasma-cell differentiation

The terminal differentiation of B cells into PCs brings about a fundamental shift in the gene expression program, as well as a massive increase in protein synthesis, and

finally cell cycle arrest. These dramatic changes are coordinated by B lymphocyte induced maturation protein 1 (Blimp-1), a transcription factor that is expressed by all antibody-secreting cells (ASCs), and is at its highest level in ASCs that have ceased dividing (PCs) [153]. The central role of Blimp-1 in PC formation is evidenced by the fact that ectopic Blimp-1 expression in B cells is sufficient to drive their differentiation [154]. Furthermore, removal of Blimp-1 by knockout of the encoding prdm1 gene prevents the development of ASCs and the accumulation of serum Ig of all isotypes both at rest and in response to immunization [153, 155].

To effect the global changes in gene expression necessary for PC differentiation, Blimp-1 targets the master transcriptional regulators of mature B cell and GC B cell gene programs, PAX5 and B-cell lymphoma 6 (Bcl6), respectively [122]. This is because PAX5 and Bcl6 directly antagonize the expression of genes involved in PC differentiation, function, and survival, and must thus be suppressed to permit the formation of ASCs. The mutual negative regulation of Blimp-1 and PAX5/Bcl6 may represent a mechanism by which ASC differentiation is restrained following B-cell activation until the proper time, such as upon achieving sufficient affinity maturation, or formation and reactivation of memory B cells during a secondary response [143].

The secretion of vast quantities of Ab puts strain on the secretory machinery of PCs as unfolded and misfolded proteins build up to toxic levels in the ER lumen. To prevent a subsequent halt in protein synthesis and/or initiation of apoptosis, PCs

upregulate X box-binding protein 1 (XBP1), a transcription factor that induces the expression of molecular chaperones able to aid in the proper folding of proteins [122]. Upregulation of XBP1 requires Blimp-1 expression, as its promoter is strongly suppressed by PAX5 [156]. Indeed, Blimp-1-deficient B cells fail to properly induce XBP1 expression following activation, and deletion of Blimp-1 in fully-formed PCs causes them to die by apoptosis [143, 155]. Concurrent with the enhanced expression of the XBP1 gene, XBP1 messenger RNA (mRNA) is spliced in such a way that a frameshift is formed that adds a transactivation domain to the encoded protein. This domain enables the efficient upregulation of factors that then counter the build-up of unfolded and misfolded proteins in the ER, and allow normal Ig production and secretion [157, 158].

Cell cycle exit is not only a hallmark of PC terminal differentiation, but also appears to be essential for the establishment of persistent PC populations. Knockout of p18(INK4c), an inhibitor of cyclin-dependent kinase, in B cells not only prevents them from becoming quiescent, it also hinders their ability to mount substantial Ab responses following immunization, GC formation, and initial PB differentiation [159]. Blasting ASCs exit the cell cycle due to Blimp-1 suppression of c-myc, a transcriptional activator of cell division [143, 160].

Before Blimp-1 can mediate the aforementioned processes, it must be upregulated by another transcription factor, interleukin regulatory factor 4 (IRF4) [153]. As an upstream mediator of PC differentiation, IRF4 directly induces the expression of

Blimp-1. Not surprisingly, IRF4 is also highly expressed by and essential for initiating the differentiation of all PCs, with IRF4-deficient mice lacking serum Ig at rest and failing to mount Ab responses following immunization [143].

1.4.2 Plasma-cell localization

In response to modifications in chemokine receptor expression, differentiating PBs migrate to several sites throughout the body. For example, ASCs forming in spleen and LN follicles downregulate both C-X-C chemokine receptor type 5 (CXCR5), which controls retention in B cell areas, and C-C chemokine receptor type 7 (CCR7), which directs T-zone homing [161]. Elimination of these GC-trafficking molecules allows PBs to egress and migrate to locations near or, via the circulation, quite distal, depending on which chemokine receptors are coordinately upregulated [1].

Expression of CCR9 and CCR10 are frequently induced in mucosal immune responses, and draw PBs into distinct mucosal tissues. The CCR9 ligand CCL25 is expressed almost exclusively in small intestine, whereas CCL28 is produced in many mucosal sites, and attracts CCR10-expressing cells. CXCR3 expression is a mark of PCs residing in inflamed tissue, and is induced by IFNγ, as are CXCR3 ligands in the inflamed tissue itself [1, 162]. Indeed, PCs are not uncommon in the kidneys of (NZB x NZW)F_1 mice and SLE patients, as well as the synovia of RA patients [162].

However, the most important and widely studied PC chemokine receptor is CXCR4. This molecule is upregulated by Blimp-1 and renders PBs sensitive to CXCL12,

the sole ligand of CXCR4 that is expressed in the splenic red pulp, the LN medullary chords, and most significantly the BM stroma [122, 143, 153, 161, 162]. Indeed, PCs can be seen closely associated with $CXCL12^{+}$ BM stromal cells [1]. The importance of CXCR4 to the efficient homing of PCs to the BM has been demonstrated in mice with B cells lacking CXCR4. Following immunization, PCs fail to accumulate in the BM of these mice, but instead remain in the blood [122, 161].

The BM is the principal destination for newly generated PCs, especially those generated in the GC [146, 163, 164]. Indeed, it is thought that only those PCs generated during T-dependent responses accumulate in the BM, though cells secreting IgM, IgG, IgA, and IgE can all be found there [162, 163]. This is not surprising, as the BM microenvironment is well-known for its role in the development, differentiation, and maintenance of a variety of hematopoietic cells, frequently mediated by BM stroma-derived signals [122].

1.4.3 Maintenance of plasma-cell populations

Incredibly, Ag-specific Abs can be found in the blood years, even decades following initial exposure. Indeed, the half-life of serum Ab against non-replicating protein Ags such as tetanus or diphtheria toxoids is estimated to be 10-20 years, while those of Abs raised in response to live viruses such as measles, mumps, or vaccinia are thought to be hundreds to thousands of years [165]. Long-lasting serum Ab, also called "humoral memory", is a vital component of immune memory, as it makes it possible to

be protected against rarely encountered pathogens, or perhaps now even more importantly, shielded as an adult from those infections against which one was vaccinated as a child. Nevertheless, the half-life of circulating Ab molecules is only on the scale of days [166]. How then does the presence of Ag-specific Abs continue throughout life?

1.4.3.1 Hypotheses to explain humoral memory

To explain the dramatic disparity between the half-life of Ab molecules in the serum and the length of time Ag-specific Ab titers can be detected, two key models have been proposed. Though not mutually exclusive, these possibilities rest on fundamentally distinct views of PC biology. In the first, PCs are thought to be short-lived and continuously generated from memory B cells stimulated by re-exposure or persistent Ag. In the second, PCs are long-lived "memory" cells distinct from memory B cells, and survive indefinitely in specialized niches [162].

Several lines of evidence have ruled out the first of these models, namely the steady replacement of short-lived PCs by memory B-cell differentiation, as a major mechanism by which humoral memory is maintained. First, it is clear that chronic infection or intermittent re-exposure are dispensable for the maintenance of long-term humoral immunity. This is because the Ab responses induced by vaccination with the non-replicating Ags tetanus toxoid or diphtheria toxoid can be detected for over a decade, as mentioned above [167]. In contradiction to the argument that Ag may

nevertheless persist in these individuals, long-term Ag-specific Ab titers can be detected in Ag-free mice receiving memory B cell-depleted BM cells from ovalbumin-immunized animals [168]. A number of B-cell depletion experiments provide further direct evidence against a role for continuous memory B-cell differentiation in the long-term maintenance of Ab titers [164, 169].

The hypothesis that long-lived PCs (LLPCs) are the basis of humoral memory was first proposed in 1998 by Slifka and Ahmed, even though LLPCs had first been documented over 30 years before [167]. Transfer studies have demonstrated that a subpopulation of Ag-specific PCs can survive for the lifespan of the host in the absence of detectable Ag or replenishment by memory B cells. The half-life of these PCs was estimated by distinct methods to be 100 or 138 days [164]. Bromodeoxyuridine (BrdU) labeling experiments revealed that these PCs are not simply self-renewing, but persist without proliferation [170]. Together, these studies led to the current paradigm wherein long-term, high-affinity Ab titers are maintained by LLPCs in the BM.

1.4.3.2 Plasma-cell survival niches

Despite reports of LLPCs *in vivo* and their ability to produce Ab for decades, PCs die rapidly upon isolation, even when taken from the BM [171, 172]. This is because PCs require continual external signals to stave off ER stress-induced apoptosis. These molecular signals and the cells that produce them are what make up the PC survival

niche. Such niches exist primarily in BM, but also in secondary lymphoid organs and inflamed tissue [1, 162].

Several survival factors for IgG-producing PCs have been identified through both *in vitro* and *in vivo* studies, which together have suggested a model in which synergy and redundancy ensure an uninterrupted stream of strong anti-apoptotic stimulation. The most potent survival signals yet identified are IL-6 and members of the tumor necrosis factor (TNF) family, a proliferation-inducing ligand (APRIL) and BAFF, though CXCL12, TNFα, IL-5 and crosslinked CD44 and CD28 have also been found to enhance the survival of IgG PCs to varying extents [162, 171]. IL-6 strongly promotes IgG PC persistence *in vitro*, and is one of the chief soluble survival signals produced in the BM; however, it is not vital to PC longevity *in vivo* [171]. Nevertheless, IL-6 is often associated with PC malignancies [1]. APRIL and BAFF appear to play redundant roles in the support of PCs, which they bind via B-cell maturation antigen (BCMA), though APRIL may be the predominant of the two signals [1, 173, 174]. In contrast to IL-6 deficiency, lack of BCMA results in a dearth of Ag-specific IgG ASCs in the BM of immunized mice [175]. It is likely that IL-6, APRIL, and BAFF work in concert to maximally promote PC survival [1, 175]. These factors support PC longevity by inducing the upregulation of the anti-apoptotic protein myeloid cell leukemia protein 1 (Mcl-1), which is required for normal maintenance of PCs and serum Ig [1, 175, 176].

Several cell types in the BM produce IL-6 and APRIL, and together form a second level of redundancy in the support the long-term PC survival, as none of these cells is independently essential for all IgG PCs to persist in the BM [1]. The positioning of niche cells appears to be random, with PCs exhibiting no clear sub-anatomical preference [122]. This may be due to the fact that their location is dictated by association with stromal cells. BM stromal cells express CXCL12, vascular-cell adhesion molecule 1 (VCAM-1), and intercellular adhesion molecule 1 (ICAM-1), thereby attracting and retaining PBs that express the respective ligands CXCR4, very late antigen 4 (VLA-4), and lymphocyte function-associated antigen 1 (LFA-1) [1, 169, 177]. In addition to retaining PCs in the BM, stromal cells also directly promote PC survival through the production of IL-6 and APRIL [172, 174]. Once ensconced among stromal cells, PCs are further supported by a variety of hematopoietic cells, including megakaryocytes, macrophages, and eosinophils, which provide support by secreting IL-6 and APRIL [1, 122, 178]. Eosinophils, however, are the primary source of these cytokines, with some 50% of IgG PCs in close association with eosinophils *in situ*. Indeed, eosinophils are required for the normal maintenance of Ag-specific IgG ASCs in the BM following immunization [177]. Other cell types support small numbers of LLPCs in the spleen (DCs, macrophages, and basophils), LNs (macrophages and neutrophils), and mucosa-associated lymphoid tissues (neutrophils) [1, 122].

Because the survival of PCs is dependent on extrinsic signals, and a finite number of supportive niche cells exist, it follows that only so many LLPCs can be maintained in an individual at any given time. It has been estimated that the BM can support at most about 10^6 PCs in mice and 10^9 in humans. As the number of tetanus toxoid (TT)-specific LLPCs estimated to take up residence in human BM following immunization is about 10^6, it is thought that human humoral memory has a capacity of about 10^3 specificities. In light of these observations, Radbruch and colleagues put forth a model in which newly formed PBs migrate to BM niches and compete with LLPCs already established there [162]. Indeed, within a week of tetanus vaccination, TT-specific PBs are detected in the blood along with non-TT-reactive PCs that were presumably displaced from the BM. As predicted, the frequency of mobilized PCs specific for other Ags each is around 0.1% of total blood PCs (1 in 10^3) [162].

1.4.4 Natural antibody-producing cells

In contrast to the clear picture that has emerged regarding PBs and PCs formed during immune responses, the identity and nature of nIgM-producing cells have remained controversial areas of study. Initial studies linking fetal B cells, particularly $CD5^+$ B1a cells, with the presence of serum IgM under naïve conditions led to the widespread assumption that B1a cells are the source of nIgM [179]. Forster and Rajewsky first showed in 1987 that transfer of total peritoneal cavity (PerC) cells into allotype-mismatched neonates selectively supplied a substantial proportion of both

$CD5^+$ PerC B cells and circulating IgM [109]. A link between $CD5^+$ PerC B cells in transfer recipients was again observed by Lalor and colleages a few years later [180]. Similar experiments by Baumgarth *et al.* further demonstrated that the majority of IgM circulating in naïve mice is derived from B1 cells, and even showed that this nIgM is a critical component of innate immune protection against influenza virus [31, 181, 182].

These initial correlation studies convincingly established the connection between fetal-lineage B cells and nIgM. However, subsequent work clouded the issue by conflating nIgM with induced "immune" IgM. Like MZ B cells, B1 cells respond rapidly to infection by differentiating into Ag-specific IgM PBs/PCs [183]. Indeed, immunization of mice with LPS or carbohydrate Ag induces the migration of PerC B1a cells to the spleen and their differentiation into PBs/PCs that express both CD138 and high levels of Blimp-1 [184-186]. These studies are often cited erroneously as evidence that nIgM is produced B1a cells in the spleen.

Even so, researchers attempting to study "true" nIgM ASCs in the absence of exogenous stimulation disagree in their conclusions. Though several reports showed that PerC cells do not spontaneously produce IgM, Rothstein's group insisted for a number of years that PerC B1a cells are the source of nIgM and spontaneously secrete Ab without differentiation into PCs (no expression of CD138, Blimp-1, or XBP1) [186-188]. However, they later found that PerC B1a cells do not themselves supply serum IgM, as they continued to detect IgM ASCs among PerC B1a cells taken from $Irf4^{-/-}$ mice,

which lack serum IgM [189]. They concluded that nIgM is supplied by splenic B1a cells, which failed to produce IgM in the absence of Irf4$^{-/-}$ and thus correlated with the absence of serum IgM. Nevertheless, the authors failed to determine if splenic B1a cells in fact made up the majority splenic IgM ASCs either in this or a later publication, likely because they made the assumption that nIgM must be derived from B1a-phenotype cells [190]. Similarly, Choi and colleagues recently claimed that nIgM is produced by BM B1a cells that also fail to exhibit canonical characteristics of ASCs, such as CD138 expression and PC morphology [191]. Like Holodick *et al.*, Baumgarth's group detected spontaneous IgM expression among a population of B1a cells, which they then claimed produce most circulating nIgM, though they did not perform the experiments required to come to this conclusion. Indeed, calculations based on their data suggest that the cells they describe constitute at most 5% of all IgM ASCs in the BM alone; it is, therefore, very unlikely that these B1a cells are responsible for supplying more than a small fraction of serum IgM [191]. Though these studies show that different cells in multiple tissues produce IgM in naïve mice, it has been fallaciously concluded that because cells in a particular population secrete some amount of IgM, those cells must be a major source of nIgM. Therefore, the identity and characteristics of the cell population that directly produces most circulating nIgM remained obscure.

1.5 Thesis prospectus

The critical role of nIgM in preventing both infectious and autoimmune diseases is well-established [24, 192]. Studies in the late 1980s and '90s found a strong correlation between PerC B cells and serum IgM in naïve animals, leading to the assumption that B1a cells are the source of nIgM [31, 109, 179-182]. Several studies went on to identify populations of B1a cells in the PerC, spleen, and BM which spontaneously produce IgM, though the controversial production of IgM by PerC cells was later found to be inconsequential [188-191]. Splenic and BM B1a cells are thus the currently accepted sources of serum nIgM, though no study has yet demonstrated that B1a cells in any organ contribute significantly to nIgM levels, and it is doubtful that BM B1a cells contribute much at all [191]. Furthermore, though B1a cells are claimed to produce large amounts of nIgM, they do not exhibit typical phenotypic, morphologic, or genetic features of PCs, characteristics that are directly linked to their capacity to secrete massive quantities of Ab protein. It was, therefore, likely that the cell population largely responsible for maintaining high titers of circulating nIgM had not yet been discovered, and thus remained uncharacterized.

1.5.1 Specific Aim I: To identify the immediate cellular source of nIgM

IgM-secreting cells have been found in multiple tissues. To determine which organs contained the bulk of nIgM ASCs, I performed enzyme-linked immunosorbent spot (ELISPOT) assay analysis of PerC, LN, spleen, and BM cells, and established that

the spleen and BM contain essentially all IgM secreting cells in the mouse, as LN and PerC contained negligible numbers. By extrapolating the number of IgM ASCs I counted in the tibiae and femurs to total marrow, I found that the BM contains roughly 80% of nIgM ASCs. To determine the phenotype of BM IgM ASCs, I stained BM cells for cytoplasmic IgM (cIgM) and other B cell markers. Cells expressing high levels of cIgM produced IgM in ELISPOT, and were also membrane-bound IgM^+ (mIgM) $CD138^+$ IgD^- $CD5^-$ $B220^{lo/-}$ and large in size. When spun onto slides, this cell population appeared identical to class-switched PCs. By comparing the number of $mIgM^+CD138^+B220^{lo/-}FSC^{hi}$ cells to the number of IgM ASCs identified by ELISPOT assay, I established that virtually all IgM ASCs in the BM exhibit this phenotype.

Having identified the primary source of nIgM, I performed transfer experiments which showed that BM nIgM ASCs differentiate from PerC B cells that are neither B1a, B1b, nor B2. Nevertheless, sequencing of the nIgM PC Ig HC genes and examination of B1-8i knockin mice indicated that this population is fetal-derived. BrdU uptake was slow in the $B220^-$ fraction of the compartment, demonstrating that these cells represent LLPCs. Finally, I demonstrated that nIgM PCs are supported by a survival niche distinct from that of IgG PCs. Through this study, I have defined the source of nIgM for the first time, and established the new paradigm that nIgM is maintained by LLPCs, not undifferentiated B1a cells.

1.5.2 Specific Aim II: To define the BM survival niche of nIgM PCs

Ag-specific Ab titers are maintained long-term by long-lived IgG PCs in the BM, which require specialized survival niches to persist. My data showed that constitutive production of nIgM is also maintained by BM-resident PCs, and that these nIgM PCs do not share the survival niche occupied by IgG PCs. Instead, survival of IgM PCs is greatly enhanced by IL-5. To identify the cellular source of IL-5 in the BM, I examined mice lacking the canonical sources of IL-5: T cells, type 2 innate lymphoid cells (ILC2s), and MCs. I determined that none of these hematopoietic populations was responsible for supporting nIgM PCs; however, I found that IgM PCs strongly associate with IL-5 expressing BM stromal cells, which support their survival *in vitro* when stimulated. To determine if IL-5 is required for nIgM PC survival, I depleted IL-5 in normal mice by injecting neutralizing Ab. *In vivo* neutralization of IL-5 revealed that, like individual survival factors for IgG PCs, IL-5 is not the sole supporter of IgM PCs *in vivo*, but is likely one of several redundant molecules that together ensure uninterrupted signaling. My results provide a foundational understanding of the mechanisms by which the nIgM PC survival niche operates, and offer the potential to discriminately modulate distinct LLPC populations.

1.5.3 Specific Aim III: To define the precursor of nIgM PCs

Several reports have demonstrated a strong correlation between $CD5^+$ B1 cells and nIgM. However, I found that purified B1a cells inefficiently reconstitute nIgM PCs

when transferred into Rag1-deficient mice. To identify the PerC B cell that gives rise to nIgM PCs, I transferred PerC cells fractionated by expression of CD19, CD5, and CD11b. I found that only the $CD19^{+}CD5^{+}CD11b^{-}$ compartment contained cells capable of differentiating into nIgM PCs. However, not all $CD19^{+}$, $CD19^{+}CD5^{+}$, or $CD19^{+}CD5^{+}CD11b^{-}$ cell transfers resulted in the recovery of serum IgM, though PerC B1a cell numbers were fully restored in virtually all recipients. These data demonstrate that B1a cells are insufficient to supply nIgM. Furthermore, they indicate that the precursor of nIgM PCs is a rare cell. By transferring decreasing numbers of unfractionated PerC cells into Rag1 knockouts, I found a striking decrease in the rate, but not occurrence, of serum IgM reconstitution between stochastically sampled pools of 10^{6} and $3x10^{5}$ PerC cells. I conclude that the $CD19^{+}CD5^{+}CD11b^{-}$ compartment comprises two cell types, one the more abundant precursor of B1a cells, and the other rarer subset, either the direct precursor of nIgM PCs or an inducer cell required for B1a cells to differentiate into nIgM PCs. By transferring neonatal liver (NL) cells, I determined that the development of nIgM PC precursors is dependent on the early hematopoietic environment. Finally, I found that PerC B cells in mice carrying an inversion of the upstream transcriptional regulatory elements of the cKit gene are incompetent to form nIgM PCs. This study provides new insight into the generation of nIgM, as well as the roles of different B1-cell subsets.

2. Materials and Methods

2.1 Mice

C57BL/6, BALB/c, B6.SJL-Ptprc^{a} Pepc^{b}/Boy (CD45.1), B6.129S2-Cd40lgtm1Imx (CD154$^{-/-}$), B6.129S7-Rag1tm1Mom (Rag1$^{-/-}$), B6.129P2(C)-Ightm2Cgn (B1-8i), C.129S1(B6)-Gata1tm6Sho (ΔdblGATA), and B6.Cg-Kit$^{W\text{-}sh}$ mice (Sash) were purchased from the Jackson Laboratory and maintained under specific pathogen-free conditions at the Duke University Animal Care Facility. Lat$^{-/-}$ mice were kindly provided by Dr. Weiguo Zhang, B6.129-MyD88^{tm1Aki} (MyD88$^{-/-}$) mice by Dr. Yiping Yang, and B6.C3Fea/a-Rora^{sg} (ROR$\alpha^{-/-}$) mice by Dr. Anton Jetten. Mice used in experiments were female and 8-12 weeks of age, except for transfer recipients, which received cells at 8-12 weeks of age, and were analyzed 10 weeks later. All experiments involving animals were approved by the Duke University Institutional Animal Care and Use Committee.

2.2 ELISPOT assay

Numbers of ASCs were determined by standard ELISPOT assay. Briefly, 96-well ELISPOT plates were coated with goat anti-mouse Igκ and anti-mouse Igλ polyclonal antibodies (SouthernBiotech) in carbonate buffer overnight at 4°C. After blocking plates with phosphate-buffered saline (PBS) containing 0.5% bovine serum albumin (BSA) (Affymetrix) for 2 hours at room temperature, serially diluted cell suspensions of mouse organs or hybridomas producing monoclonal mouse IgM (B1-8) or IgG (H33γ1) were added to each well and incubated at 37°C for 3 hours. After washing with distilled

water, plates were blocked overnight at 4°C. Alkaline phosphatase (AP)-labeled polyclonal goat anti-mouse IgM, goat anti-mouse IgG, or goat anti-mouse IgA (SouthernBiotech) was then added, and plates were incubated at room temperature for 1 hour. After washing, bound AP activity was visualized by adding a solution of SIGMAFAST BCIP/NBT tablets (Sigma-Aldrich) dissolved in distilled water for 20 minutes at room temperature, followed by washing with distilled water. Membranes were air-dried overnight before spots were counted manually under a dissecting microscope.

2.3 Antibodies and flow cytometry

The following monoclonal antibodies specific for mouse surface Ags were used for flow cytometry and fluorescence-activated cell sorting (FACS). Anti-mouse CD11b PE (M1/70), IgD APC-Cy7 (clone: 11-26c.2a), CD28 FITC (E18), Thy1.2 PE-Cy7 (30-H12), I-A/I-E FITC (M5/114.15.2), IFNγ purified (XMG1.2), mouse IgG2b isotype control FITC (MPC-11), rat IgG2b isotype control FITC (RTK4530), and rat IgG1 isotype control Alexa Fluor488 (RTK2071) were purchased from BioLegend (San Diego, CA, USA). Anti-mouse cKit APC (2B8), FcεR1 PE (MAR-1), CD45.1 eFluor 450 (A20), CD34 FITC (RAM34), Sca-1 PE (D7), CD8α PE (53-6.7), CD11c PE (N418), Gr-1 PE (RB6-8C5), TER-119 PE (TER-119), IgM PE-Cy7 (II/41), IgM FITC (II/41), CD45R APC (RA3-6B2), CD5 APC (53-7.3), IgD FITC (11-26c), CD5 PE (53-7.3), CD11b APC-eFluor780 (M1/70), CD23 Biotin (B3B4), BrdU FITC (Bu20a), IL-5 purified (TRFK5), CD3ε purified (145-2C11),

Thy1.2 purified (30-H12), rat IgG2a isotype control APC (eBR2a), rat IgG2bκ isotype control purified (eB149/10H5), and rat IgG1κ isotype control purified (eBRG1) were purchased from eBioscience (San Diego, CA, USA). Anti-mouse CD4 PE (GK1.5), TCRβ PE (H57-597), CD138 PE (281-2), CD43 APC (S7), CD125 Alexa Fluor488 (T21), CD45R PE-CF594 (RA3-6B2), CD28 purified (37.51), Streptavidin PE-Texas Red, and rat IgG1 isotype control FITC (R3-34) were purchased from BD Biosciences (San Jose, CA, USA). Anti-mouse Ly-6B PE (7/4) was purchased from AbD Serotec (Raleigh, NC, USA).

Both analysis of cell phenotypes and cell isolation were performed by flow cytometry. Briefly, cells were labeled with fluorochrome-conjugated monoclonal antibodies specific for mouse surface Ags (listed above) in Iscove's Modified Dulbecco's Medium (IMDM) (Gibco) containing 2% fetal bovine serum (FBS) (HyClone), and kept in this media (FACS) or resuspended in PBS (Gibco) containing 2% FBS (flow cytometry) prior to analysis. Bound biotin-conjugated antibodies were revealed by fluorochrome-labeled streptavidin. Dead cells in unfixed samples were labeled by adding propidium iodide (Sigma Aldrich) prior to sample analysis. To label intracellular IgM, cells were stained for surface Ags and dead cells (with 7-Aminoactinomycin D, 7-AAD; BD Pharmingen), washed twice, and then fixed and permeabilized with fixation/permeabilization solution (eBiosciences), according to the manufacturer's instructions, and finally stained for intracellular IgM. Labeled cells were analyzed on a BD LSR II or sorted on a BD FACSAria, with Diva software (BD Biosciences). Doublets

were excluded from analysis and cell sorting by combination(s) of forward scatter (FSC)-A vs. FSC-H, FSC-H vs. FSC-W, and side scatter (SSC)-H vs. SSC-W gatings. Propidium Iodide$^+$ or 7-AAD$^+$ cells (dead cells) were also excluded from my analysis. Flow cytometric data were analyzed using FlowJo software (Treestar).

2.4 Cytospin

Sorted cells were spun onto slides using a Cytospin III (Shandon) and stained with the Protocol Hema3 system (Fisher Scientific) according to the manufacturer's instructions (PCs), or fixed for 15 minutes with Carnoy's solution and stained with Toluidine blue for 10 minutes (MCs). Cells were photographed at room temperature on an Olympus BX-60 microscope with a 40x/0.85 objective lens using a Spot camera and Spot software (Diagnostic Instruments).

2.5 Quantitative PCR

Levels of mouse V_H11, V_H1, IL-5, and Lin28b mRNA were determined by quantitative polymerase chain reaction (PCR). Briefly, total RNA was extracted from cells using TRIzol LS Reagent (Invitrogen) and treated with DNase I (Invitrogen). Complementary DNA (cDNA) was synthesized from the RNA using Superscript III reverse transcriptase (Invitrogen). V_H11 and V_H1 cDNA was amplified in primary PCR reactions using the following primer sequences: V_H11, 5'-GAAGTGCAGCTGTTGGAGAC-3'; V_H1, 5'-CAGGTCCAACTGCAGCAGCC-3'; J_HOut, 5'-CTYACCTGAGGAGACDGTGA- 3'. PCR conditions were 95°C for 7 min, followed

by 20 cycles of 95°C for 30 s, 58°C for 20 s, and 72°C for 45 s, and finally 72°C for 5 min. For V_H11 and V_H1, the products of the primary reactions were used for quantitative PCR, and relative gene expression was calculated by the comparative threshold method relative to Igβ transcript levels, as previously described [193]. For IL-5 and Lin28b, cDNA was analyzed directly by quantitative PCR to determine gene expression relative to β-actin transcript levels. PCR conditions were 95°C for 30 s, followed by 40 cycles of 95°C for 5 s and 60°C for 30 s. Primer sequences used: V_H11, 5′-GAAGTGCAGCTGTTGGAGAC-3′; V_H1, 5′-CAGGTCCAACTGCAGCAGCC-3′; J_HIn_1, 5′-GTGGTCCCTGCGCCCCAG-3′; J_HIn_2, 5′-GGTBCCTTGGCCCCAGTA-3′; Igβ_F, 5′-GTCATGGGATTCAGCACCTT-3′; Igβ_R, 5′-AGCCTTGCTGTCATCCTTGT-3′; IL-5_F, 5′-TCACCGAGCTCTGTTGACAA-3′; IL-5_R, 5′-CCACACTTCTCTTTTTGGCG-3′; Lin28b_F, 5′-TTGTGCCTGTGTGATCTGTGACCT-3′; Lin28b_R, 5′-AGGTAGTCGGTGCCATCATTTCCA-3′; β-actin_F, 5′-GGGAATGGGTCAGAAGGACT-3′; β-actin_R, 5′-GGGGTGTTGAAGGTCTCAAA-3′.

2.6 Cell transfer

PerC cells from several mice were pooled after isolation by lavage with 5 ml PBS containing 2% FBS. LN cells were obtained from pooled axial and inguinal LNs taken from the same donor mice. NL cells were obtained by pooling livers from pups born within 24 hours of harvest. Whole tissue suspensions or sorted cell populations were injected in 200 μl sterile PBS intraperitoneally (i.p.).

2.7 ELISA

Total serum IgM and IgG levels were determined by comparison to monoclonal IgM (B1-8) or IgG (H33γ1) Ab standards, respectively, in a sandwich enzyme-linked immunosorbent assay (ELISA). Briefly, 96-well ELISA plates were coated with goat anti-mouse Igκ and anti-mouse Igλ polyclonal antibodies (SouthernBiotech) in carbonate buffer overnight at 4°C. After blocking plates with PBS containing 0.5% BSA for 2 hours at room temperature, serially diluted sera or monoclonal standard antibodies were added to wells and incubated at room temperature for 1 hour. After washing, horseradish peroxidase (HRP)-labeled polyclonal goat anti-mouse IgM or goat anti-mouse IgG (SouthernBiotech) was added and incubated at room temperature for 1 hour. After washing, bound HRP activity was visualized using a TMB peroxidase kit (BioLegend), and optical densities (OD) were determined at 450 nm. ChoP-binding serum IgM was measured in a similar manner, with ChoP-conjugated BSA (Biosearch Technologies) and BSA coated plates. End-point titer (EPT) was defined as the highest dilution at which the 450 nm OD reading was at least 2-fold greater than the OD reading of the same sample at the same dilution on BSA coated plates.

2.8 Sequence analysis

Ig heavy chain sequences were obtained from single BM PB/PCs sorted into 96-well PCR plates containing lysis buffer (proprietary, Atreca Inc., San Carlos, CA), which were frozen on dry ice, and shipped to Atreca Inc. for sequencing by their proprietary

Immune Repertoire Capture™ method. VDJ rearrangements, point mutations, and N nucleotide additions were identified with IMGT/V-QUEST (http://www.imgt.org). Sequences were deposited in the public database GenBank (http://www.ncbi.nlm.nih.gov/genbank) under accession numbers KP053417 – KP053609.

2.9 BrdU assay

C57BL/6 mice were fed BrdU (Sigma-Aldrich) in their drinking water at a concentration of 0.8 mg/ml. Fresh BrdU water was given every 2-3 days. Mice were sacrificed 7, 14, 21, or 28 days following treatment initiation, and BrdU incorporation was evaluated by flow cytometry using the BD Biosciences BrdU FITC kit, according to the manufacturer's instructions.

2.10 Immunofluorescence

C57BL/6 femurs were prepared for sectioning by submerging in 1% paraformaldehyde (Alfa Aesar) overnight at 4°C. Femurs were then soaked in PBS containing 10% sucrose (Amresco) at 4°C for 2 hours, followed by 20% sucrose for 2 hours, 30% sucrose for 2 hours, and then fresh 30% sucrose overnight. Femurs were then embedded in O.C.T. compound (Tissue Tek) and frozen in liquid nitrogen. 5 μm thick sections were cut on a Leica CM3050 cryostat, and stored at -20°C.

Femur sections were stained at room temperature. Briefly, slides were first blocked for 15 minutes with PBS containing 0.5% BSA, 0.1% Tween-20 (Sigma), 1% Fc

block (BD Biosciences), and 5% Rat IgG (Sigma-Aldrich). Sections were then incubated with 1 μg/ml anti-mouse IgM FITC (BD Biosciences) or 2 μg/ml polyclonal goat anti-mouse IgG FITC (SouthernBiotech) for 3 hours, washed, blocked for 15 minutes, stained with 5 μg/ml anti-FITC Alexa Fluor488 (Invitrogen) for 1 hour, washed, stained with 0.8 μg/ml anti-Siglec-F PE (BD Biosciences) or anti-TCRβ PE (eBioscience) for 3 hours, washed, and stained with 40 ng/ml 4',6-diamidino-2-phenylindole (DAPI) (KPL) for 5 minutes. Images were acquired at room temperature on a Zeiss Axiovert 200M microscope with a 20x/0.75 objective lens, using a Zeiss AxioCam MRm camera, and Axiovision software.

To assess the *in situ* association of FITC-IgG$^+$ or FITC-IgM$^+$ ASCs with PE-Siglec-F$^+$ eosinophils or PE-TCRβ$^+$ T cells in a blinded fashion, sections were first scanned for FITC-positive cells. After photographing in the FITC channel, PE-positive cells and DAPI were photographed in the same field of view. Photographs were later examined to compare the total number of FITC$^+$ cells to the number of FITC$^+$ cells in direct contact with PE$^+$ cells. DAPI was used to ensure that FITC-staining cells contained a nucleus, and were thus in fact cells and not non-specific, brightly staining debris.

2.11 Cell culture

T_H2-skewed splenic CD4$^+$ T cells were obtained by culturing sorted cells with recombinant mouse IL-2 (R&D Systems), recombinant mouse IL-4 (PeproTech), and anti-

IFNγ (BioLegend) for 3 days at 37°C in 24-well plates pre-coated with anti-CD3 at 5 μg/ml and anti-CD28 at 2 μg/ml at 37°C for 4 hours.

Total BM was fractionated according to plastic adherence by plating suspended BM cells on a 10 cm dish in 10 ml IMDM containing 2% FBS at 37°C for 2 hours. Non-adherent (N-Ad) cells were gently collected by pipetting, and the plate gently washed with PBS. 5 ml PBS with 2 mM EDTA (Ambion) were added to the plate, and incubated at 37°C for 10 minutes. After tapping the plate, dislodged adherent (Ad) cells were collected by pipetting. 10 ml IMDM with 2% FBS were used to wash the plate and collect remaining cells.

The survival of BM ASCs under different conditions was compared in cell culture. BM PB/PCs were sorted into a 96-well culture plate at 200 cells/well, and cultured in triplicate in media alone or on a layer of N-Ad or Ad BM cells, with or without recombinant mouse IL-6 or recombinant mouse IL-5 (PeproTech) at 20 ng/ml, or LPS (Sigma) at 0.5 μg/ml. The input number of ASCs was determined by ELISPOT. After 2 days, the number of ASCs in each well was enumerated by ELISPOT. Survival rate was determined by comparing ASC numbers obtained on day 2 to the input ASC number.

2.12 Antibody treatment

Thy1.2^{+} cells were depleted from mice by i.p. injection of functional grade purified anti-Thy1.2 (eBioscience) or isotype control Rat IgG2bκ (eBioscience) at 200

μg/injection every 3 days for a total of 5 injections. Mice were analyzed 1 day following the final injection.

IL-5 was neutralized *in vivo* by intravenous (i.v.) injection of anti-IL-5 (eBioscience) or isotype control Rat IgG1κ (eBioscience) at 100 μg/injection every 3 days for 2 or 4 injections. Mice were analyzed 3 days following the final injection.

2.13 Statistical analysis

Statistical significance (*, $p < 0.05$; **, $p < 0.01$; ***, $p < 0.001$, ****, $p < 0.0001$) in paired data was determined by two-tailed Student's t test.

3. Identification and characterization of natural IgM-producing cells

In this chapter, I identify the source of nIgM to be $CD138^{+}IgM^{+}IgD^{-}B220^{lo/-}CD5^{-}FSC^{hi}$ PBs and PCs in the BM. The following text was modified from the original manuscript, "Natural IgM is produced by $CD5^{-}$ plasma cells that occupy a distinct survival niche in bone marrow", published in volume 194 of the Journal of Immunology, 2015 [194].

3.1 Introduction

nIgM is a critical mediator of innate immune protection. In contrast to Ag-driven Ab production, nIgM is constitutively secreted to forestall the early dissemination of infectious particles. Indeed, IgM Abs against viruses, bacteria, and fungi are readily detectable in the circulation of unimmunized mice, and are highly efficient in activating complement and sequestering Ag in secondary lymphoid organs [24, 31, 195-197]. These functions not only control the early spread of pathogens directly, but also promote the initiation of T-dependent humoral responses [31, 195].

The importance of circulating nIgM in controlling infection has been demonstrated in mice lacking secreted IgM. Such mice have higher mortality rates following cecal ligation and puncture, and are highly susceptible to infection with *Streptococcus pneumoniae*, influenza virus, and *Pneumocystis murina* [29, 31, 195, 198]. nIgM also plays a major role in maintaining tissue homeostasis by promoting the

phagocytic clearance of apoptotic cells [25, 40, 41, 45, 196], and suppressing inflammatory cytokine production by dendritic cells and macrophages [45, 192]. Mice deficient in secreted IgM spontaneously develop dsDNA-reactive IgG with age, and autoimmune disease when on an MRL/lpr background [46, 47]. Conversely, nIgM lessens disease severity in models of atherosclerosis and inflammatory autoimmune arthritis [45, 53, 199], and in humans appears to ameliorate the disease symptoms of SLE and to protect against cardiovascular disease [19, 54]. Thus, nIgM plays a major role in preventing both infectious and autoimmune diseases.

Despite this significant role, the source of nIgM is poorly understood. Although $CD5^+$ B1a cells have long been associated with nIgM [25, 31, 109, 181, 199-201], their role in the production of nIgM is unclear. B1a cells, enriched in the PerC, arise during fetal development and persist in the adult by self-renewal [109-111]. PerC B1a cells, however, while found by some to spontaneously produce very low levels of IgM [188, 189], do not contribute significantly to serum IgM levels [189]. Rather, nIgM has been proposed to be produced by splenic B1a cells [111, 187, 189], as LPS induces PerC B1a cells to migrate to the spleen and differentiate into IgM ASCs [184, 202]. Alternatively, nIgM production has been attributed to a population of BM-resident B1a cells that, surprisingly, lack the characteristics of PCs and constitute only a small fraction (<5%) of IgM ASCs in the BM [191]. Although both models are consistent with reports of constitutive IgM ASCs in spleen and BM [17, 203], the contribution of B1a cells to serum IgM levels has not been

determined. Thus, while B1a cells (and their progeny) secrete IgM, the identity and characteristics of the cells responsible for maintaining high levels of nIgM in the serum remain obscure.

Here, I show that CD5$^-$ BM PBs and PCs are responsible for the production of >80% of serum IgM in naive mice, and trace the immediate precursor of these ASCs to a PerC resident population that is neither B1a, B1b, nor B2 in phenotype. Most BM IgM ASCs are LLPCs that occupy a distinct survival niche; comparison of factors that promote the survival of BM IgM and IgG PCs revealed that while IgG PCs require IL-6 [1, 162, 171], IgM PCs are supported by IL-5. My study demonstrates that the primary source of nIgM is a non-differentiated, B-lineage precursor that matures into long-lived BM PCs, even in the absence of CD154-mediated signals. In the BM, this PC population occupies a novel survival niche that sustains the secretion of copious amounts of IgM encoded by V(D)J rearrangements characteristic of fetal-lineage B cells. In mice, nIgM in the serum is the product of a novel population of fetal-derived, innate PCs and PBs.

3.2 Results

3.2.1 The majority of nIgM-producing cells is CD5$^-$ BM PB/PCs

To identify the source of nIgM, I first enumerated IgM ASCs in several lymphoid organs in naïve mice. Consistent with previous reports [186, 191, 204], PerC and LNs contained relatively few IgM ASCs; however, I observed substantial numbers of IgM ASCs in spleen and BM (Figure 7A). After normalizing the numbers of IgM ASCs

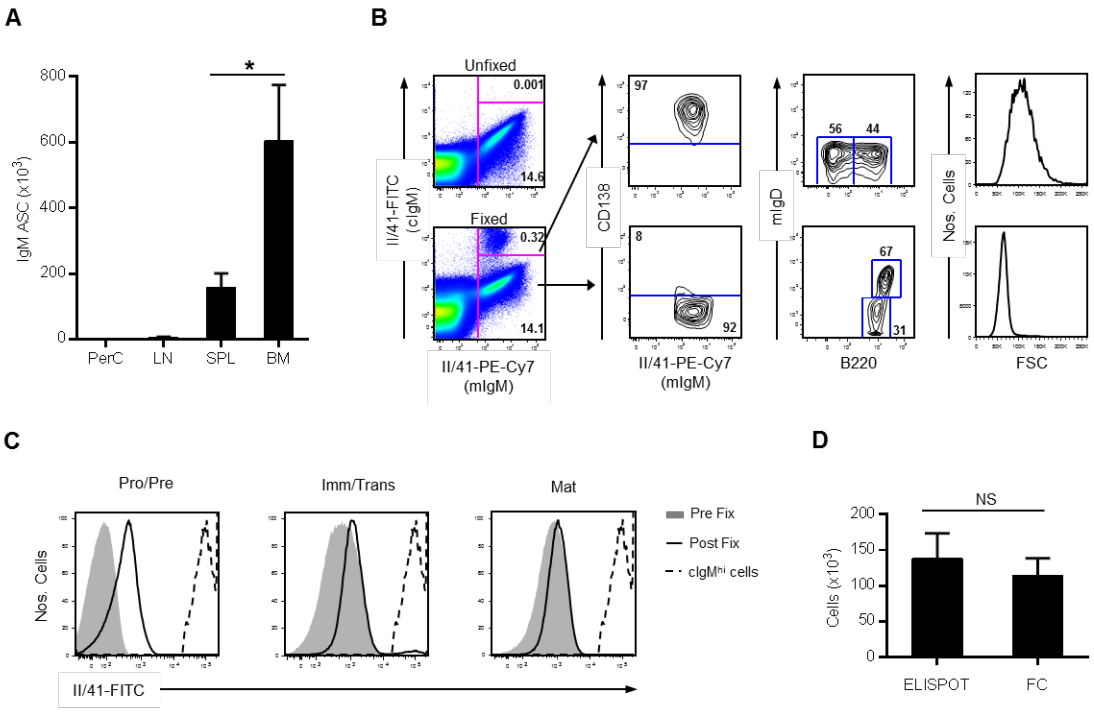

Figure 7: The majority of nIgM-producing cells is large CD138⁺ BM cells

(Figure 7, continued) (**A**) Number of IgM ELISPOTs in the PerC, total LNs, spleen, and total BM of B6 mice. Number of IgM ASCs counted in both axial and inguinal LNs was multiplied by 12.5 to estimate the total number in all LNs combined. Total BM number extrapolated from the number obtained in the femurs and tibiae multiplied by 5.52 (39), on the assumption that ASCs are uniformly distributed in all marrow-containing bones. Data represent mean ± SEM of nine mice. (**B**) BM cells that were fixed following staining (Unfixed) were stained for surface antigens (including II/41-PE-Cy7), washed, stained for II/41-FITC, and then fixed and permeabilized. BM cells that were fixed prior to the second IgM stain (Fixed) were first stained for surface antigens (including II/41-PE-Cy7), washed, fixed and permeabilized, and then stained for intracellular IgM (II/41-FITC). Flow plots depict BM cells pre-gated on live lymphocytes (*far left*), $cIgM^{hi}$ cells (*right, top row*), or $cIgM^{lo}$ cells (*right, bottom row*). Data are representative of two independent experiments. cIgM, cytoplasmic IgM; mIgM, membrane-bound IgM; mIgD, membrane-bound IgD; forward scatter, FSC. (**C**) Representative flow plots showing FITC II/41 labeling of surface stained pro/pre (Pro/Pre), immature/transitional (Imm/Trans), and mature (Mat) BM B cells stained with FITC II/41 before (Pre Fix, filled gray histogram) or after (Post Fix, solid black line) permeabilization. For comparison, each plot includes the cells in the $cIgM^{hi}$ gate in (B) (dotted black line). Data are representative of two independent experiments. (**D**) Total number of IgM ASCs in femurs and tibiae determined by ELISPOT and flow cytometry (gated on live $mIgM^{+}CD138^{+}B220^{lo/-}FSC^{hi}$ lymphocytes). Data are representative of a total of nine mice, and show mean ± SEM. FC, flow cytometry; NS, not significant.

in femurs and tibiae to account for all marrow present in the skeletal system [205], it was clear that BM comprises a significantly larger reservoir of IgM ASCs than spleen, containing some 80% of all IgM ASCs (Figure 7A).

PBs and PCs contain high, diagnostic levels of cytoplasmic Ig. I used, therefore, intracellular IgM staining to identify and characterize IgM PB/PCs in the BM by flow cytometry. Cytoplasmic IgM (cIgM) and surface, membrane-bound IgM (mIgM) were distinguished by staining sequentially with the anti-IgM mAb II/41 conjugated with distinct fluorophores. First, BM cells were reacted with fluorescently labeled mAbs against IgM (II/41-PE-Cy7), CD138, IgD, and B220; after washing, the surface-labeled cells were fixed and permeabilized, and then exposed to II/41-FITC. This labeling strategy revealed a population of $mIgM^{+}$ cells that were brightly stained by II/41-FITC ($cIgM^{hi}$), but required the fixation and permeabilization step (Figure 7B).

Virtually all $cIgM^{hi}$ BM cells expressed CD138, a marker of PB/PCs [152], and mIgM, but did not express mIgD (Figure 7B). The $cIgM^{hi}mIgM^{+}CD138^{+}mIgD^{-}$ compartment was divided by B220 expression, with approximately 60% of cells $B220^{-}$ and 40% $B220^{lo}$; all $cIgM^{hi}mIgM^{+}CD138^{+}mIgD^{-}$ cells exhibited high FSC (Figure 7B). In contrast, the great majority of $cIgM^{lo}mIgM^{+}$ BM cells (>90%) were $CD138^{-}$ and exhibited patterns of B220 and mIgD expression consistent with immature/transitional ($cIgM^{lo}mIgM^{+}CD138^{-}IgD^{-}B220^{lo}$) and mature ($cIgM^{lo}mIgM^{+}CD138^{-}IgD^{+}B220^{hi}$) B cells. All $cIgM^{lo}mIgM^{+}$ cells exhibited low FSC (Figure 7B). The MFI for cIgM in the $cIgM^{hi}mIgM^{+}$

cell compartment was >100-fold higher than that in cells expressing the phenotypes of pro-/pre-B, immature/transitional, and mature B cells (Figure. 7C). Significantly, the numbers of mIgM^{+}CD138^{+}B220$^{lo/-}$FSC^{hi} BM cells were approximately equal to the numbers of BM IgM ASCs detected by ELISPOT (Figure 7D). I conclude that essentially all IgM ASCs in the BM are mIgM^{+}CD138^{+}B220$^{lo/-}$FSC^{hi} PB/PCs.

To confirm the capacity of mIgM^{+}CD138^{+} BM cells to secrete Ab, I sorted this population, dividing it by FSC and B220 expression into mIgM^{+}CD138^{+}B220^{-}FSC^{hi}, mIgM^{+}CD138^{+}B220^{lo}FSC^{hi}, and mIgM^{+}CD138^{+}B220$^{hi/lo}$FSC^{lo} compartments (Figure 8A). For comparison, I also recovered mIgM^{-}CD138^{+}B220^{-}FSC^{hi} BM cells as class-switched controls (Figure 8A). All populations were then characterized by microscopy and ELISPOT. As expected, the mIgM^{-}CD138^{+}B220^{-}FSC^{hi} compartment (R1 gate; Figure 8A) was composed of cells with a PB/PC morphology, as were the mIgM^{+}CD138^{+}B220^{-}FSC^{hi} (R2 gate) and mIgM^{+}CD138^{+}B220^{lo}FSC^{hi} (R3 gate) compartments (Figure 8A). In contrast, mIgM^{+}CD138^{+}B220$^{hi/lo}$FSC^{lo} cells (R4 gate) were exclusively small lymphocytes (Figure 8A). By ELISPOT, mIgM^{-}CD138^{+}B220^{-}FSC^{hi} (R1 gate) PB/PCs secreted IgM (7%), IgG (42%), or IgA (35%) (Figure 8A). Whereas both the B220^{-} (R2 gate) and B220^{lo} (R3 gate) fractions of mIgM^{+}CD138^{+}FSC^{hi} cells secreted Ab, they secreted IgM only (R2, 82%; R3, 58%). The small lymphocytes in the mIgM^{+}CD138^{+}B220$^{hi/lo}$FSC^{lo} compartment (R4 gate) did not secrete IgM, IgG, or IgA (Figure 8A).

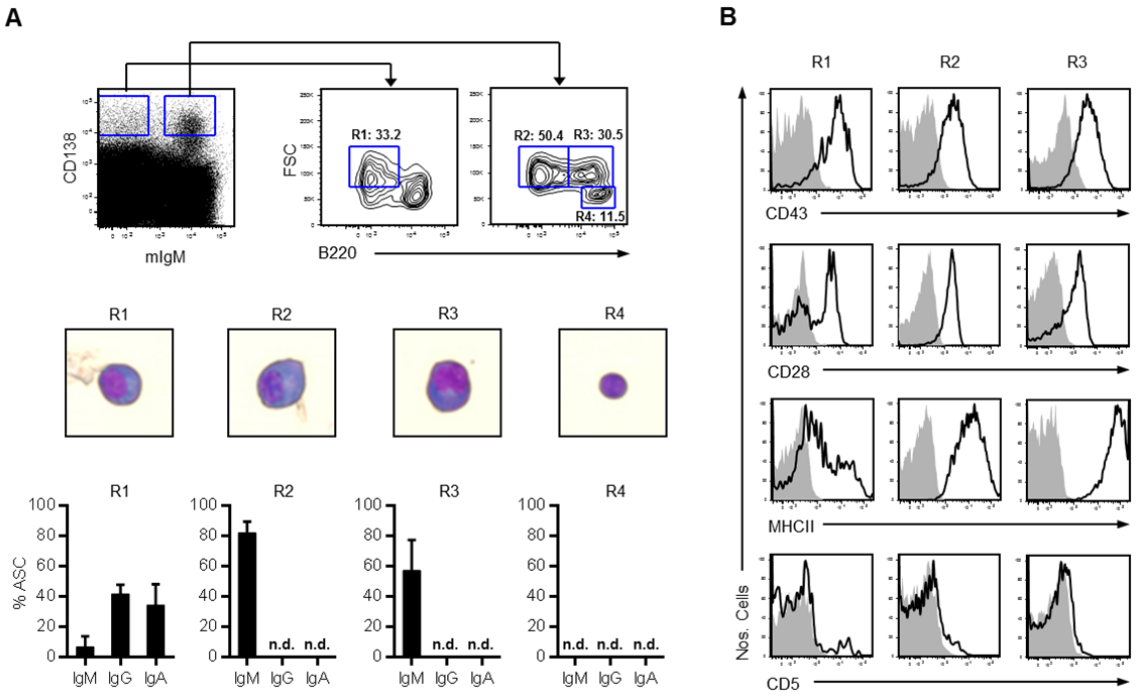

Figure 8: nIgM-producing cells are CD5$^-$ PBs/PCs

(**A**) mIgM$^+$ and mIgM$^-$ subsets of CD138$^+$ BM cells (pre-gated on live lymphocytes) were FACS sorted based on size and expression of B220, and analyzed by microscopy and ELISPOT. Data are representative of at least two independent experiments. n.d., not detected. (**B**) Flow plots showing surface expression of CD43, CD28, MHCII, and CD5 on mIgM$^-$CD138$^+$B220$^-$FSC^{hi} (R1), mIgM$^+$CD138$^+$B220$^-$FSC^{hi} (R2), and mIgM$^+$CD138$^+$B220^{lo}FSC^{hi} (R3) BM cells. Data are representative of two independent experiments.

Additional characterization of surface molecules on mIgM^{-}CD138^{+}B220^{-}FSC^{hi} (R1), mIgM^{+}CD138^{+}B220^{-}FSC^{hi} (R2), and mIgM^{+}CD138^{+}B220^{lo}FSC^{hi} (R3) BM PB/PCs revealed that all types expressed comparably elevated levels of CD43 and CD28 (Figure 8B), molecules previously associated with ASCs [206, 207]. As expected, mIgM^{-} CD138^{+}B220^{-}FSC^{hi} PCs displayed a bimodal pattern of MHCII expression [206], whereas both IgM-producing populations (R2, R3) uniformly expressed high levels of MHCII, with expression highest in the B220^{lo} (R3) compartment (Figure 8B). None of these ASC populations expressed significant levels of CD5, a defining marker of B1a cells.

3.2.2 BM nIgM PB/PCs differentiate from a non-B1a peritoneal precursor

While B1a cells *per se* are not the source of nIgM (Figures 7 and 8), the two have long been closely associated [25, 31, 109, 181, 199-201]. Transfer experiments have demonstrated that cells from the PerC, a population enriched for B1a cells, efficiently reconstitute serum IgM in B cell-depleted mice, while conventional B2 cells do not [109]. I determined, therefore, whether BM IgM ASCs differentiate from PerC B cells or conventional, B2 cells by injecting 3x10^{6} unfractionated PerC or LN cells into the PerC of congenic, Rag1-deficient mice. I used LNs as a source of B2 cells because LNs, unlike spleen and BM, are essentially devoid of B1a cells [208]. Both PerC and LN B cells survived transfer; after 10 weeks the numbers of B cells recovered from the PerC, spleen, and BM of recipients given PerC cells increased [1.9 (±0.5) x 10^{6}; 134%] over the number of injected B cells, and fell somewhat in LN recipients [7.5 (±5.2) x 10^{5}; 64%] (Table 1).

Analysis of serum IgM concentrations in recipient mice revealed that PerC cells were far more effective in restoring IgM levels. Ten weeks after transfer, serum IgM in LN cell recipients averaged only 122 (±32) μg/ml; in contrast, serum IgM in mice receiving PerC cells matched normal controls by 4 weeks [758 (±305) μg/ml], and subsequently increased to 1038 (±727) μg/ml by week 10 (Figure 9A). Three major B-cell populations have been described in the PerC: B1a, B1b, and B2 [209]. To determine whether one of these populations was responsible for restoring serum IgM, I transferred $5x10^5$ PerC B1a ($IgM^{hi}IgD^{lo}B220^{lo/-}CD11b^{+}CD23^{-}CD5^{+}$), B1b ($IgM^{hi}IgD^{lo}B220^{lo/-}CD11b^{+}CD23^{-}CD5^{-}$), or B2 ($IgM^{lo}IgD^{hi}B220^{hi}CD11b^{-}CD23^{+}CD5^{-}$) cells into the PerC of Rag1-deficient mice [209]. The number of transferred B cells ($5x10^5$) approximates the number of each B-cell type in ($3x10^6$) unfractionated PerC cells. At 10 weeks post-transfer, I observed B-cell expansion (B1a) or survival (B1b and B2) in all recipients (Table 1); however, none of the transferred populations efficiently reconstituted serum IgM in recipient animals (Figure 9A). Against expectation, serum IgM levels in recipients of B1a cells rose slowly and at 10 weeks reached a maximum [236 (±415) μg/ml] that was only 23% of that generated by PerC cell transfer (Figure 9A). Reconstitution of serum IgM was even less efficient in B1b and B2 recipients, with serum

Table 1: B cell reconstitution in Rag1$^{-/-}$ recipient mice

Transferred Population	PerC			SPL	BM	Total B cells Recovered
	B1a	B1b	B2	IgM$^+$	IgM$^+$	
PerC[a]	193.7 ± 64.7[c]	198.0 ± 62.3	51.0 ± 32.3	1230.7 ± 310.4	252.1 ± 184.1	1925.5 ± 506.4
LN[a]	15.8 ± 4.7	78.2 ± 36.4	51.6 ± 36.6	573.6 ± 518.5	31.0 ± 10.2	750.3 ± 522.0
B1a[b]	567.0 ± 363.1	64.8 ± 24.8	0.8 ± 1.4	267.6 ± 409.6	348.3 ± 547.7	1248.5 ± 1076.3
B1b[b]	6.7 ± 4.5	70.0 ± 6.1	0.0 ± 0.0	110.9 ± 39.0	93.5 ± 80.6	281.1 ± 43.2
B2[b]	4.7 ± 2.2	89.8 ± 58.7	6.5 ± 6.2	112.0 ± 89.0	47.5 ± 33.2	260.5 ± 184.9

[a] $3x10^6$ total cells; approximately $1.44x10^6$ (48% of PerC) or $1.17x10^6$ (39% of LN) B cells

[b] $5x10^5$ cells sorted from PerC

[c] Mean recovered cell number ± SD ($x10^3$)

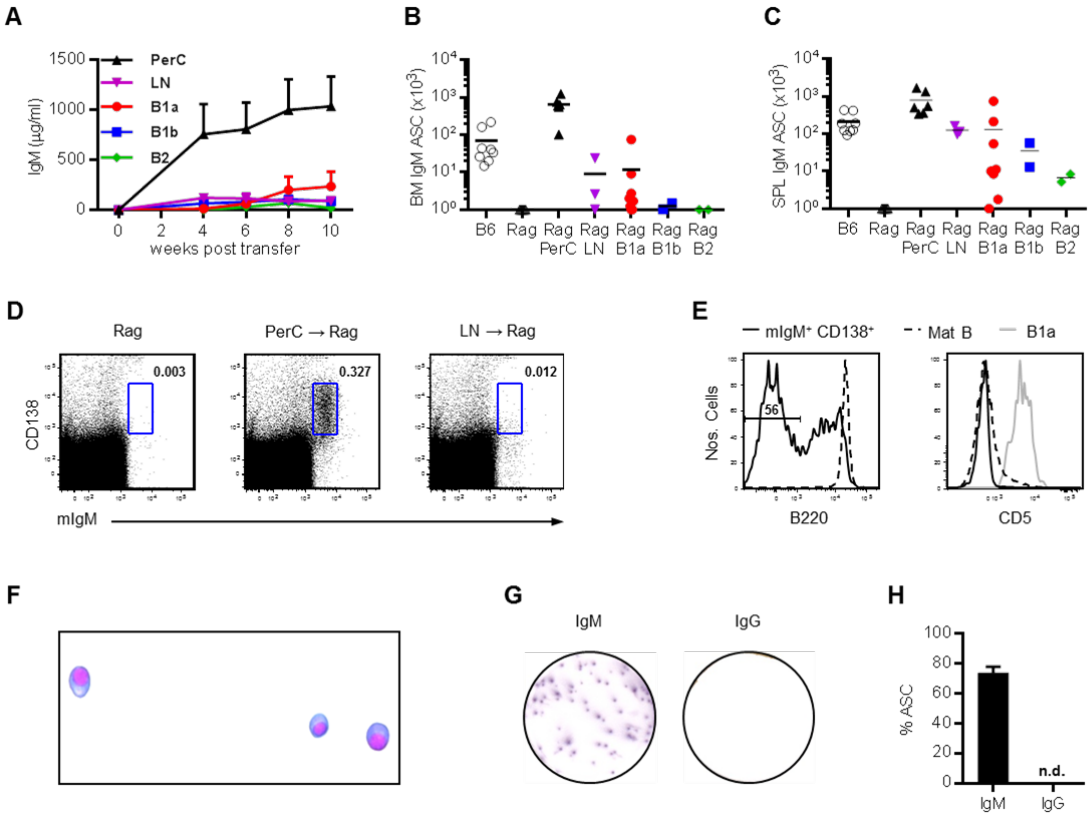

Figure 9: Peritoneal cavity cell transfer restores IgM PB/PCs in the bone marrow of Rag1$^{-/-}$ mice

(Figure 9, continued) $3x10^6$ unfractionated PerC washout cells or LN cells, or $5x10^5$ FACS sorted PerC B1a, B1b, or B2 cells from B6 mice were injected i.p. into $Rag1^{-/-}$ mice. (**A**) Serum IgM concentration after transfer, mean ± SEM. PerC, PerC cell-recipient $Rag1^{-/-}$ mice; LN, LN cell-recipient $Rag1^{-/-}$ mice; B1a, B1b, and B2, sorted B cell-recipient $Rag1^{-/-}$ mice. Numbers of IgM ELISPOTs from the BM (femurs and tibiae) (**B**) and spleen (**C**) of control and recipient mice analyzed 10 weeks after transfer. Each symbol represents one mouse, lines represent means. (**D**) Representative flow plots of BM from control and recipient mice 10 weeks after transfer (pre-gated on live lymphocytes). (**E**) Expression of B220 and CD5 on $mIgM^+CD138^+FSC^{hi}$ BM cells in PerC cell-recipient mice 10 weeks after transfer, compared to mature BM B cells or PerC B1a cells from untreated B6 controls. Micrograph (**F**) and ELISPOTs (**G** and **H**) of $mIgM^+CD138^+B220^{lo/-}FSC^{hi}$ cells sorted from the BM of PerC cell-recipient mice 10 weeks after transfer. (G) Scans of ELISPOT membranes, seeded with 100 sorted cells per well. (H) n.d., not detected. Data in (A) and (H) show mean ± SEM. Recipient mouse n = 6 (PerC), 3 (LN), 8 (B1a), 2 (B1b), and 2 (B2) from two to four independent transfer experiments.

IgM concentrations at 10 weeks reaching only 89 (±34) μg/ml and 21 (±8) μg/ml, respectively (Figure 9A).

Consistent with their recoveries of serum IgM, PerC cell recipients had very high numbers of BM IgM ASCs [65.4 (±36.8) x 10^4] at 10 weeks post-transfer, higher even than C57BL/6 (B6) controls [7.0 (±7.7) x 10^4; $p < 0.001$]. Consistent with their absent or poor recoveries of serum IgM, BM IgM ASC numbers were 70- to 55-fold lower in LN cell [0.9 (±1.3) x 10^4] and B1a recipients [1.2 (±2.6) x 10^4], and virtually undetectable in mice reconstituted with B1b [0.1 (±0.08) x 10^4] or B2 cells [0.01 (±0.01) x 10^4] (Figure 9B).

In contrast to their substantial differences in BM IgM ASC numbers, splenic IgM ASC numbers in mice reconstituted with PerC cells [80 (±57) x 10^4], LN cells [13 (±3.5) x 10^4], or B1a cells [13 (±26) x 10^4] were comparable (Figure 9C). Indeed, even mice receiving B1b or B2 cells had detectable, albeit lower, numbers of splenic IgM ASCs, [3.5 (±3.1) x 10^4] and [0.7 (±0.2) x 10^4], respectively (Figure 9C).

Transfer of PerC cells, but not LN, B1a, B1b, or B2 cells, efficiently reconstituted the serum IgM and BM IgM ASCs of Rag1-deficient mice (Figure 9A and B). To determine whether transfer of unfractionated PerC cells reconstitutes the $mIgM^+CD138^+B220^{lo/-}FSC^{hi}CD5^-$ PB/PC compartment in the BM (Figures 7 and 8), I examined the BM of PerC and LN cell recipients by flow cytometry (Figure 9D). Consistent with my ELISPOT data (Figure 9B), I observed a large population of $mIgM^+CD138^+FSC^{hi}$ cells in the BM of PerC cell but not LN cell recipients 10 weeks after

transfer (Figure 9D and data not shown). Just over half of these cells were $B220^{-}$, and the rest $B220^{lo}$; none expressed CD5 (Figure 9E). To confirm that these $mIgM^{+}CD138^{+}B220^{lo/-}FSC^{hi}$ cells secreted IgM, I isolated them at 10 weeks post-transfer and evaluated them by microscopy and ELISPOT. The sorted $mIgM^{+}CD138^{+}B220^{lo/-}FSC^{hi}$ cells were PB/PCs by morphology (Figure 9F), and some 75% secreted IgM in ELISPOT assay, while none secreted IgG (Figure 9G and H).

3.2.3 BM IgM PB/PCs descend from fetal B cells

3.2.3.1 VDJ rearrangements used by BM IgM PB/PCs exhibit hallmarks of fetal-lineage B cells and natural antibody

The PerC is enriched for fetal-lineage B lymphocytes which exhibit preferential use of the V_H11 and V_H12 gene segments, low frequencies of V(D)J mutations, and few or no N-nucleotide additions due to the absence of TdT expression in fetal-lineage precursors [103, 105, 106, 210, 211]. To determine whether IgM PB/PCs in the BM of naïve adult mice display these traits of fetal-lineage B cells, I sequenced the Ig HC genes from IgM [$mIgM^{+}CD138^{+}B220^{lo/-}FSC^{hi}$ (Figure 8A, R2 and R3 gates)] and non-IgM [$mIgM^{-}CD138^{+}B220^{-}FSC^{hi}$ (Figure 8A, R1 gate)] BM PB/PCs. While both compartments exhibited diverse V_H gene usage, V_H11 family segments were far more prevalent (18.4% vs. 0%) in IgM^{+} than IgM^{-} PB/PCs; similarly VDJ rearrangements containing V_H12 gene segments were detected only in IgM^{+} PB/PCs (Fig. 11A) [105]. VDJ rearrangements utilizing V_H11 segments are associated with phosphatidylcholine reactivity and are characteristic of the natural Ab repertoire [105, 210, 212].

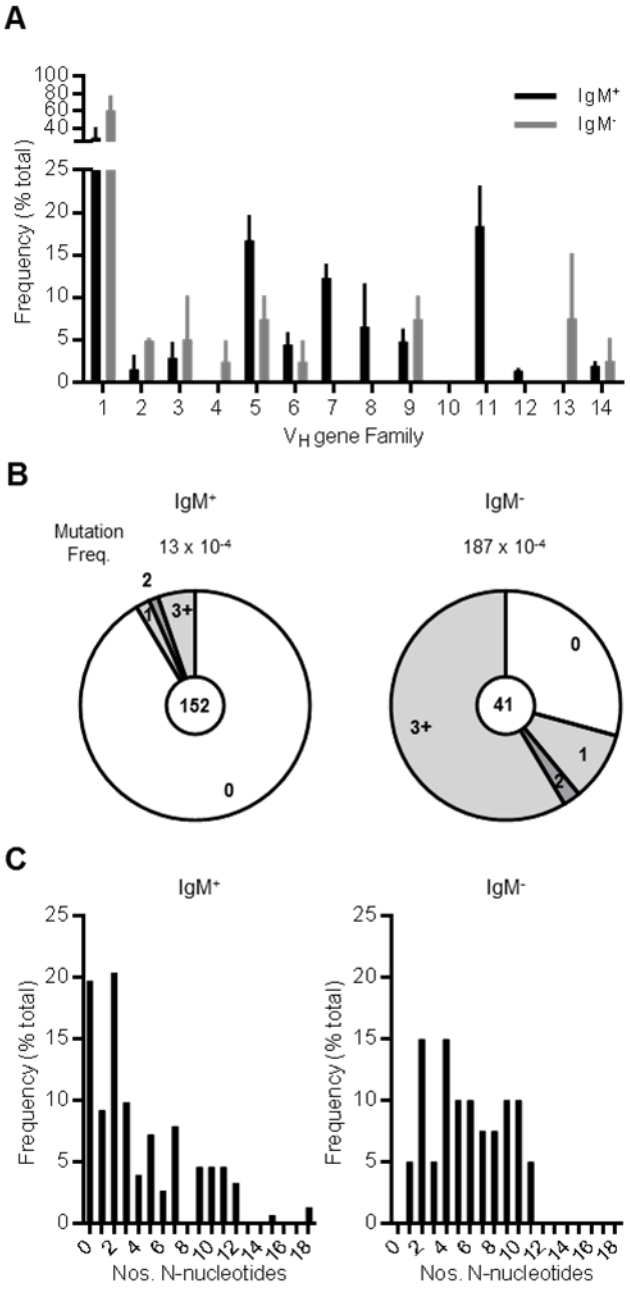

Figure 10: VDJ rearrangements used by bone marrow IgM PB/PCs exhibit hallmarks of fetal-lineage B cells and natural antibody

(Figure 10, continued) IgH genes from IgM-producing mIgM^{+}CD138^{+}B220$^{lo/-}$FSC^{hi} (IgM^{+}) and IgG-producing mIgM^{-}CD138^{+}B220^{-}FSC^{hi} (IgM^{-}) BM cells from naïve B6 mice were sequenced. (**A**) Proportion of sequences using each V_H gene family, showing mean ± SEM of results from two individual mice. (**B**) Proportion of V_H gene sequences carrying 0, 1, 2, or 3 or more mutations. Numbers of sequences analyzed are indicated inside pie charts. (**C**) Proportion of sequences carrying different numbers of N-nucleotide additions. Data represent a total of 152 IgM sequences and 41 IgG sequences from the BM of two mice.

VDJ sequence analysis revealed that <9% (13/152) of IgM PB/PCs carried ≥1 V_H mutations and <6% (8/152) had ≥3 V_H mutations. In contrast, 71% (29/41) of VDJ rearrangements recovered from non-IgM PB/PCs contained V_H genes with ≥1 mutation, and 59% (24/41) had ≥3 mutations (Fig. 11B). I also found that the distribution of N-nucleotide additions was different between the IgM^+ and IgM^- PB/PC compartments, with strong skewing toward absent or short N sequences (0-2 nucleotides, 49%) in IgM^+ PB/PCs and longer insertions (≥3, 80%) in IgM^- PB/PCs (Fig. 11C). Indeed, while 20% of IgM^+ PB/PCs had no identifiable N-sequence addition, all IgM^- PB/PCs carried at least 1 untemplated HCDR3 nucleotide (Fig. 11C). I conclude that the IgM^+ BM PB/PCs reconstituted by unfractionated PerC cells differentiate from fetal-lineage precursors, distinct from differentiated B1a and B1b cells, and that the pattern of VDJ rearrangements in this IgM^+ PB/PC compartment is consistent with the natural Ab repertoire.

3.2.3.2 BM IgM PB/PCs are absent in B1-8i VDJ knockin mice

The development of fetal-lineage B cells appears to be promoted by the frequent self-reactivity of B1 BCRs [107, 213, 214]. Conversely, B1-cell development is disfavored in knockin mice expressing VDJ rearrangements from mature B2 cells, perhaps because they have been purged for autoreactivity [214, 215]. Given that the VDJ rearrangements recovered from $mIgM^+CD138^+B220^{lo/-}FSC^{hi}$ BM cells are consistent with a fetal-lineage origin (Figure 10), I analyzed mice homozygous for the B1-8i VDJ knockin allele [216].

This VDJ knockin supports normal B-cell development in the BM and, with $V_\lambda 1$, confers reactivity to the hapten (4-hydroxy-3-nitrophenyl) acetyl (NP) [216]. I observed in B1-8i mice a virtually complete (99%) loss of PerC B1a cells and a 76% reduction in B1b cell numbers; in contrast, the B2-cell compartment was fully intact (160%) (Figure 11A).

Serum IgM levels in naïve B1-8i mice were only 7% of B6 controls, whereas serum IgG levels rose well above (250%) those of B6 mice (Figure 11B). Along with the loss of PerC B1a cells and serum IgM and the substantial reduction of B1b cells, IgM ASC numbers in the BM of B1-8i mice were <10% of B6 controls (Figure 11C). This reduction was not due to a general effect on ASC differentiation, as BM IgG ASC numbers in B1-8i animals were higher (190%) than B6 controls (Figure 11C). The loss of IgM ASCs in the BM of B1-8i mice was reflected in comparable reductions in $mIgM^+CD138^+$, but not $mIgM^-CD138^+$ cell frequencies (Figure 11D). Indeed, numbers of $mIgM^+CD138^+B220^{lo/-}FSC^{hi}$ BM PB/PCs in B1-8i mice were only 18% of controls, but $mIgM^-CD138^+B220^-FSC^{hi}$ PB/PC numbers were higher (162%) than those in B6 mice (Figure 11E). Collectively, these data show that B1-8i VDJ knockin mice preferentially support the development of B2 cells, $mIgM^-CD138^+B220^-FSC^{hi}$ PB/PCs, and serum IgG over PerC B1a and B1b cells, $mIgM^+CD138^+B220^{lo/-}FSC^{hi}$ BM PB/PCs and serum IgM (Figure 11). I conclude that in general these two cellular and humoral axes are independent of one another.

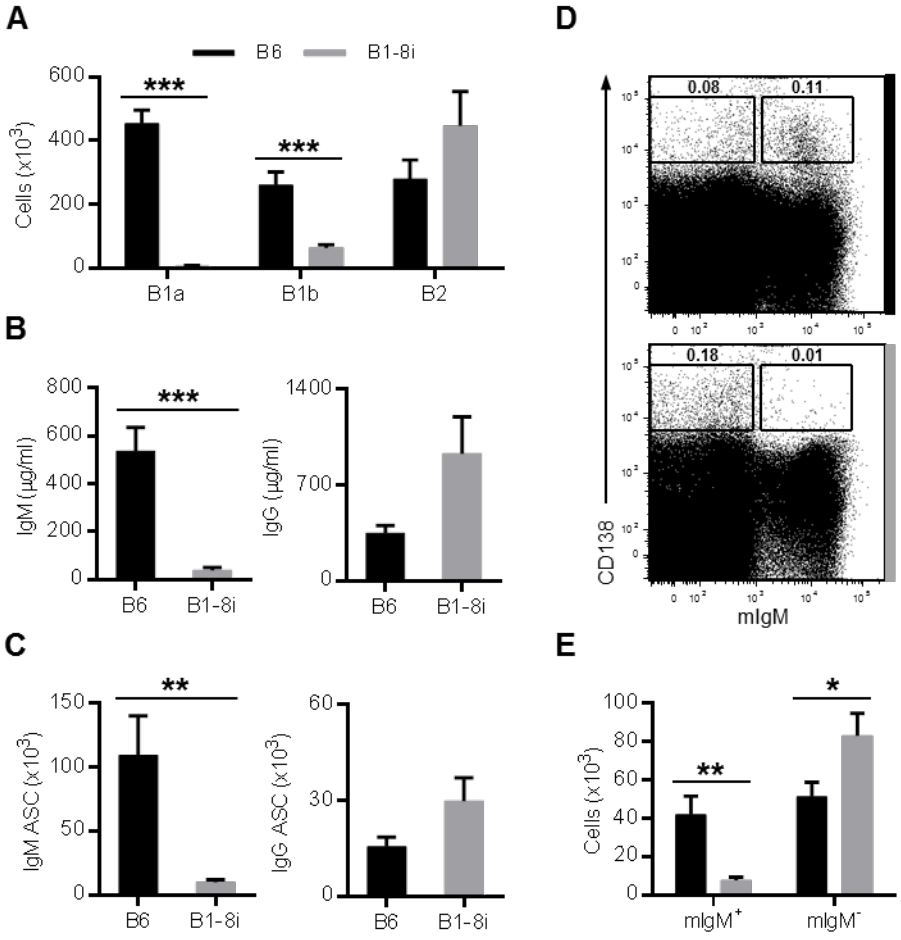

Figure 11: Bone marrow IgM PB/PCs are absent in B1-8i VDJ knockin mice

Naïve B6 (black bars) and B1-8i homozygous knockin mice (gray bars) were analyzed. (**A**) Number of B1a, B1b, and B2 cells in the PerC determined by flow cytometry. (**B**) Concentration of serum IgM and IgG. (**C**) Number of IgM and IgG ELISPOTs in the BM (femurs and tibiae). (**D**) Representative flow plots of B6 (*upper panel, black bar*) and B1-8i knockin (*lower panel, gray bar*) BM (pre-gated on live lymphocytes). (**E**) Number of $mIgM^{+}CD138^{+}B220^{lo/-}FSC^{hi}$ ($mIgM^{+}$) and $mIgM^{-}CD138^{+}B220^{-}FSC^{hi}$ ($mIgM^{-}$) cells in the BM. Data represent a total of nine mice of each genotype from three independent experiments, and show mean ± SEM.

3.2.4 IgM PB/PCs in the BM do not require CD154

nIgM is constitutively present in the serum, even absent CD154-CD40 interactions [132]. To determine whether the $mIgM^{+}CD138^{+}B220^{lo/-}FSC^{hi}$ PB/PC compartment in the BM is sensitive to the absence of CD154 expression, I quantified serum IgM and IgG and enumerated IgM and IgG ELISPOTs in the BM of B6 and congenic $CD154^{-/-}$ mice. As expected [132], serum IgM levels were indistinguishable in $CD154^{-/-}$ and B6 mice, while IgG levels were reduced >90% in knockout animals (Table 2). Similarly, IgM ASC numbers in the BM of $CD154^{-/-}$ mice were unchanged from those in B6 mice, while BM IgG ASC numbers were reduced 80% in knockout animals (Table 2). The stability of the IgM ASC compartment in the BM of $CD154^{-/-}$ mice was mirrored by the maintenance of normal numbers of $mIgM^{+}CD138^{+}B220^{lo/-}FSC^{hi}$ PB/PCs, while $mIgM^{-}CD138^{+}B220^{-}FSC^{hi}$ PB/PC numbers were significantly reduced (Table 2).

Interestingly, both IgM and IgG ASC numbers were reduced in the spleens of $CD154^{-/-}$ mice, by 43% and 96%, respectively (Table 2), indicating that a substantial fraction of splenic IgM ASCs require T:B collaboration. The significant reduction in splenic IgM ASC numbers in $CD154^{-/-}$ mice was not, however, correlated with lower serum IgM levels (Table 2). Assuming constant rates of IgM secretion, the absence of quantitative linkage between serum IgM and splenic IgM ASC numbers supports the notion that nIgM and the $mIgM^{+}CD138^{+}B220^{lo/-}FSC^{hi}$ PB/PC compartment of the BM

Table 2: IgM ASC numbers are reduced in the spleen but not the BM of CD154$^{-/-}$ mice

	Serum Ig (μg/ml)		BM ASCs (x10^3)[a]		BM PB/PCs (x10^3)[b]		Spleen ASCs (x10^3)[a]	
	IgM	IgG	IgM	IgG	IgM$^+$	IgM$^-$	IgM	IgG
C57BL/6	273 ± 319[c]	309 ± 63.8	18.5 ± 10.0	5.9 ± 3.7	18.0 ± 11.0	10.4 ± 3.6	128 ± 47.3	13.7 ± 13.4
CD154$^{-/-}$	339 ± 358	28.8 ± 38.2[d]	13.4 ± 9.8	1.2 ± 1.0[e]	17.7 ± 12.7	3.1 ± 1.0[e]	72.9 ± 22.3[e]	0.53 ± 0.44

[a] Determined by ELISPOT

[b] Determined by flow cytometry; IgM$^+$, mIgM$^+$CD138$^+$B220$^{lo/-}$FSC^{hi}; IgM$^-$, mIgM$^-$CD138$^+$B220$^-$FSC^{hi}

[c] Mean ± SD of five mice

[d] $p < 0.001$

[e] $p < 0.05$

comprise an innate humoral axis that is isolated from classical, Ag-driven humoral responses.

If serum IgM and mIgM^{+}CD138^{+}B220$^{lo/-}$FSC^{hi} PB/PCs in the BM represent an innate humoral compartment, the repertoire of BM IgM PB/PCs should not change in the absence of cognate T-cell help. I determined, therefore, whether the overrepresentation of V_H11 rearrangements in mIgM^{+}CD138^{+}B220$^{lo/-}$FSC^{hi} BM PB/PCs in B6 mice (Figure 10) is retained in the absence of CD154. To do this, I used quantitative PCR to determine the relative quantities of V_H11 and V_H1 VDJ transcripts in sorted mIgM^{-}CD138^{+}B220^{-}FSC^{hi} and mIgM^{+}CD138^{+}B220$^{lo/-}$FSC^{hi} PB/PCs from the BM of B6 and CD154-deficient congenics; V_H11 expression was then normalized to V_H1 usage. As expected (Figure 10A and [105]), the V_H11/V_H1 ratio in mIgM^{-} PB/PCs from B6 mice was 6.1 x 10^{-3}, while in mIgM^{+} PB/PCs the ratio was 3.2 x 10^{0}, or >500-fold higher (Figure 12A). The high ratio of V_H11/V_H1 was essentially unchanged in CD154 knockout mice at 6.9 x 10^{0} (Figure 12A), indicating that the skewed V_H gene segment usage, and presumably repertoire, of mIgM^{+}CD138^{+}B220$^{lo/-}$FSC^{hi} BM PB/PCs is unaffected by the absence of T:B collaboration.

I then determined whether the specificity of nIgM in the serum of B6 and CD154$^{-/-}$ mice differed. In both strains, titers of IgM specific for ChoP, a common target of nIgM [19], did not differ (Figure 12B). Thus, the specificity of mIgM^{+} PB/PCs in mouse BM is independent of CD154:CD40 signaling.

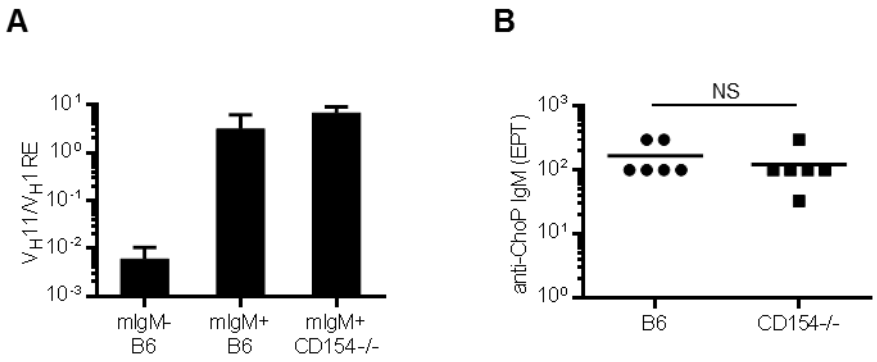

Figure 12: The repertoire of nIgM PCs and nIgM is unaltered in the absence of CD154

(**A**) Ratio of V_H11 to V_H1 expression relative to Igβ in sorted $mIgM^-CD138^+B220^-FSC^{hi}$ or $mIgM^+CD138^+B220^{lo/-}FSC^{hi}$ BM cells, measured by quantitative real-time PCR as described in "Materials and Methods". Data are from two independent experiments, and show mean ± SEM. RE, relative expression. (**B**) End-point titer (EPT) of serum IgM binding to ChoP in ELISA; ChoP binding by the NP-reactive, negative control IgM Ab B1-8 was undetectable (not shown). Each symbol represents one mouse, lines represent means. anti-ChoP, anti-phosphorylcholine.

3.2.5 Most nIgM-producing BM cells are long-lived

A fraction of high-affinity, class-switched B cells leave GCs and differentiate into LLPCs in the BM where they are maintained with little or no cell division in a specific survival niche [122, 164, 170, 217]. To determine whether mIgM$^+$ PB/PCs in the BM are also long-lived, I provided mice with drinking water containing BrdU for 4 weeks and analyzed BrdU uptake by mIgM$^-$CD138$^+$B220$^-$FSC^{hi}, mIgM$^+$CD138$^+$B220$^-$FSC^{hi}, mIgM$^+$CD138$^+$B220^{lo}FSC^{hi} BM PB/PCs at 1 week intervals (Figure 13). Controls for BrdU uptake included immature and mature BM B cells. As reported [218], by 1 week, >95% of immature B cells were labeled, while <10% of mature B cells became BrdU$^+$ (Figure 13). After 4 weeks of continuous labeling, only 12.5 (±2.2)% of mature B cells had incorporated BrdU, indicating little or no mitosis in this compartment. As expected [219], 36.8 (±9.9)% of mIgM$^-$CD138$^+$B220$^-$FSC^{hi} cells were BrdU$^+$ at 1 week; labeling increased more gradually later, to a maximum of 63.0 (±8.7)% and 66.3 (±13.6)% BrdU$^+$ at weeks 3 and 4 (Figure 13). The kinetics of BrdU-labeling of mIgM$^+$CD138$^+$B220^{lo}FSC^{hi} BM cells were similar, with about 48.7 (±14.4)% becoming BrdU$^+$ in 1 week and 62.5 (±15.0)% and 77.2 (±8.3)% of cells labeled at weeks 3 and 4 (Figure 13). BrdU uptake by mIgM$^+$CD138$^+$B220$^-$FSC^{hi} PB/PCs was noticeably slower, with <12% labeled at 1 week and then increasing monotonically to 46.9 (±10.5)% BrdU$^+$ cells at week 4 (Figure 13). These results indicate that mIgM$^+$CD138$^+$B220^{lo}FSC^{hi} cell compartment comprises cycling

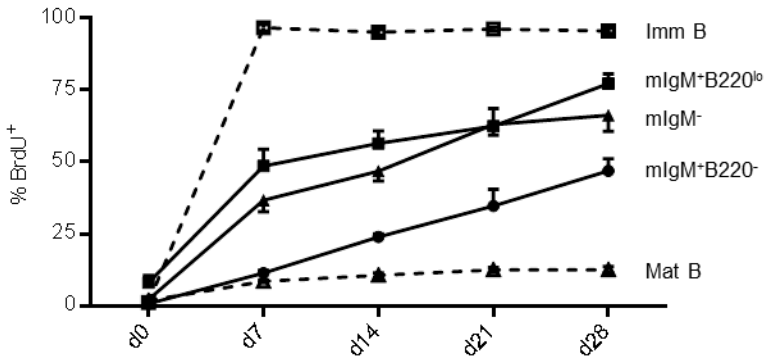

Figure 13: BrdU incorporation by PB/PC populations in the bone marrow

Naïve B6 mice were given 0.8 mg/ml BrdU in drinking water for 4 weeks. Plot shows the percent of $BrdU^+$ $B220^{lo}CD93^+IgM^{lo}IgD^-$ immature B cells (Imm B), $B220^{hi}CD93^-IgM^{lo}IgD^{hi}$ mature B cells (Mat B), $mIgM^+CD138^+B220^-FSC^{hi}$ ($mIgM^+B220^-$), $mIgM^+CD138^+B220^{lo}FSC^{hi}$ ($mIgM^+B220^{lo}$), and $mIgM^-CD138^+B220^-FSC^{hi}$ ($mIgM^-$) cells in the bone marrow at each timepoint. Data show the mean ± SEM of four to six mice at each timepoint from two or three independent experiments.

PBs, while mIgM^{+}CD138^{+}B220^{-}FSC^{hi} cells are predominantly non-cycling, long-lived BM PCs.

3.2.6 BM survival niches for IgM and IgG PCs are distinct

IgG BM PCs are not intrinsically long-lived [171, 172]. If not prompted by survival cues to initiate the unfolded protein response, PCs die from ER stress-induced apoptosis [162]. IgG PCs persist in the BM within niches that supply survival factors produced by adjacent cells [122]. My labeling experiments demonstrated low division rates and persistence by mIgM^{+}CD138^{+}B220^{-}FSC^{hi} PCs (Figure 13), and I sought to determine whether this CD154-independent PC compartment of the BM occupies the survival niche that supports IgG-secreting PCs [122].

IL-6, a survival factor that defines the BM survival niche of IgG PCs, is secreted by eosinophils that are in frequent and direct contact with IgG PCs [177]. I examined, therefore, histologic sections of BM by immunofluorescence to determine whether eosinophils were also in frequent contact with IgM PCs (Figure 14A). As reported [177], nearly 40% of IgG PCs were in direct contact with Siglec-F^{+} eosinophils, a value significantly higher than the 21.5% background frequency that would occur by chance (Figure 14B). In contrast, the frequency of IgM PCs contacting Siglec-F^{+} cells (21%) was no different than the expected background, demonstrating that IgM PCs are not co-distributed with eosinophils in the BM.

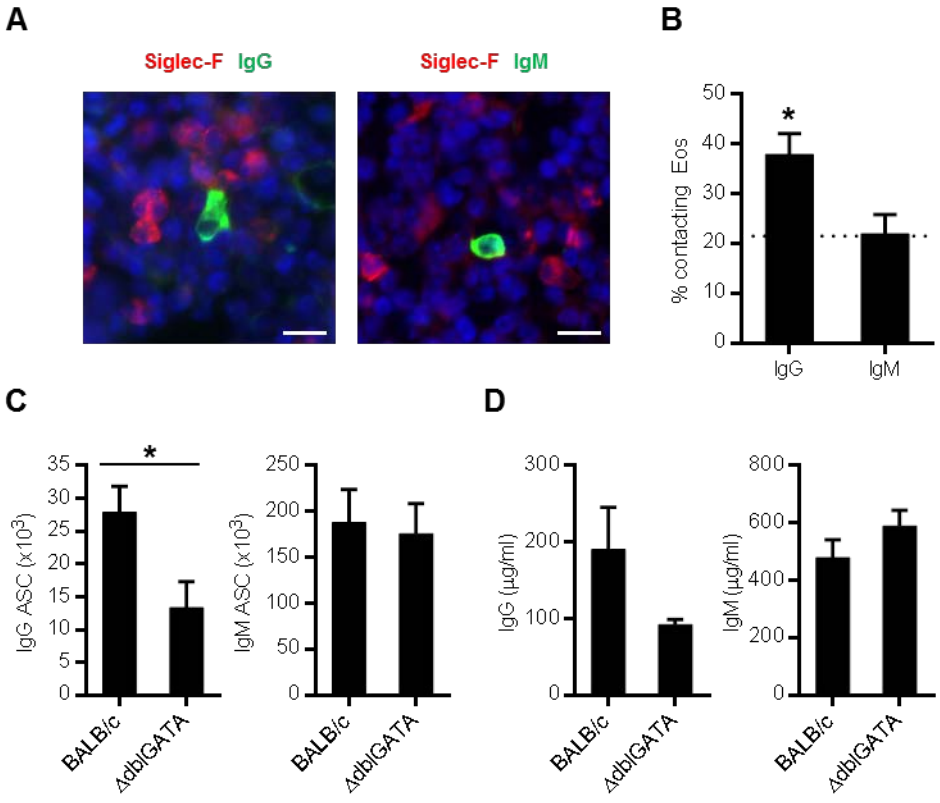

Figure 14: Maintenance of IgM PCs in the bone marrow is independent of eosinophils

(**A**) Representative immunofluorescence micrographs of femur sections from naïve B6 mice stained with DAPI, PE anti-Siglec-F, and either FITC anti-IgG (*left panel*) or FITC anti-IgM (*right panel*). Scale bar represents 10 µm. (**B**) Frequency of IgG$^+$ or IgM$^+$ PCs in contact with Siglec-F$^+$ eosinophils in femur sections. Dotted line indicates the frequency of randomly selected DAPI$^+$ nuclei that were adjacent to Siglec-F$^+$ cells. A total of at least 110 IgG and IgM PCs each was photographed from femur sections from six different mice. Number of IgG and IgM ELISPOTs in the BM (femurs and tibiae) (**C**) and concentration of IgG and IgM in the serum (**D**) of eosinophil-deficient ΔdblGATA mice and BALB/c controls. Data represent a total of nine mice of each genotype from three independent experiments, and show mean ± SEM.

Eosinophil-deficient, ΔdblGATA mice [220] exhibit significantly lower numbers of BM IgG ASCs than their congenic controls [177]. To determine whether IgM ASC numbers in the BM also change in the absence eosinophils, I compared ΔdblGATA mice to normal BALB/c controls, and found a 52% reduction ($p = 0.0196$) in BM IgG ASC numbers but no change ($p = 0.809$) in the numbers of IgM ASCs (Figure 14C). I observed a comparable (52%) but non-significant ($p = 0.095$) reduction in serum IgG, whereas serum IgM levels remained stable ($p = 0.198$) in mice lacking eosinophils (Figure 14D). Thus, eosinophils are dispensable for the maintenance of BM IgM ASCs and serum IgM.

To identify survival factors that support the survival of BM mIgM$^+$ PB/PCs, I cultured mIgM$^+$CD138$^+$ or mIgM$^-$CD138$^+$ BM cells in media alone or in media supplemented with IL-6 or IL-5; after 48 hrs in culture, IgM and IgG ASCs were enumerated by ELISPOT [171]. In media alone, IgM and IgG ASC numbers were reduced by >94% and >90% , respectively, suggesting that IgM ASCs, like IgG ASCs, are not intrinsically long-lived but require survival factors to persist in the BM (Figure 15A). Addition of IL-6, a key survival factor for IgG PC survival in the BM [1, 162, 171], had no effect ($p = 0.061$) on IgM ASC survival but increased the recovery of IgG ASCs nearly 6-fold ($p = 0.001$) (Figure 15A). Supplementation by IL-5, a survival factor for fetal-lineage B cells [221, 222], produced reciprocal effects; IgM ASC numbers were increased >4-fold

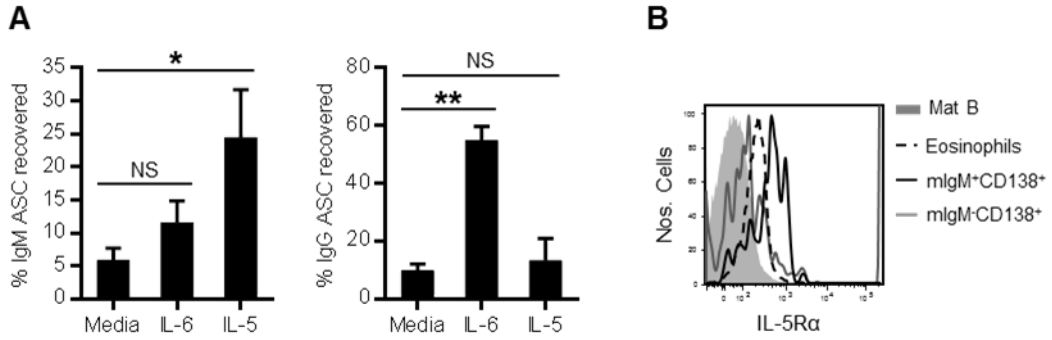

Figure 15: Distinct cytokines mediate the survival of IgM and IgG bone marrow PCs

(**A**) mIgM^{+}CD138^{+} (*left panel*) or mIgM^{-}CD138^{+} (*right panel*) BM cells were cultured for 2 days in media alone, or in media supplemented with 20 ng/ml IL-6 or 20 ng/ml IL-5. IgG and IgM ASC input number was determined by ELISPOT of sorted cells at day 0 and was compared to the number of ASC detected in wells on day 2. Data show mean ± SEM. (**B**) Representative flow plot of IL-5Rα expression on B220^{+}IgM^{lo}IgD^{hi} mature BM B cells (Mat B), Ly-6B^{-}SSC^{hi} BM eosinophils (Eosinophils), and mIgM^{+}CD138^{+}B220$^{lo/-}$FSC^{hi} (mIgM^{+}CD138^{+}) and mIgM^{-}CD138^{+}B220^{-}FSC^{hi} (mIgM^{-}CD138^{+}) BM cells. Data represent two independent experiments.

($p = 0.021$) over medium alone but provided no significant ($p = 0.691$) advantage to IgG ASCs (Figure 15A).

To support these *in vitro* observations, I analyzed $mIgM^{+}CD138^{+}B220^{lo/-}FSC^{hi}$ and $IgM^{-}CD138^{+}B220^{-}FSC^{hi}$ BM cells by flow cytometry for expression of IL-5 receptor α subunit (IL-5Rα). Remarkably, $mIgM^{+}CD138^{+}B220^{lo/-}FSC^{hi}$ cells expressed higher levels of IL-5Rα than even eosinophils, cells known to depend on IL-5 for their generation and activity [223]. In contrast, $mIgM^{-}CD138^{+}B220^{-}FSC^{hi}$ PB/PCs and mature B cells, populations known not to require IL-5 [171, 223], expressed much lower levels of IL-5Rα (Figure 15B). Collectively, these data demonstrate that the cellular and molecular factors that mediate the survival of nIgM PB/PCs in the BM are distinct from those that sustain long-lived IgG PC populations.

3.3 Discussion

nIgM is constitutively present in the serum, and provides a first line of defense against invading pathogens. nIgM also promotes the phagocytic clearance of apoptotic cells, aiding in the maintenance of tissue homeostasis [25, 40, 41, 45, 196]. Indeed, mice lacking secreted IgM are highly susceptible to infection by bacteria, viruses, and fungi [29, 31, 195, 198] and less able to control autoimmune disease [45, 53, 199]. However, despite widespread recognition that nIgM plays a crucial role in the prevention of infectious and autoimmune diseases, the source of nIgM has remained elusive. Current models for the origin of nIgM hold that B1a cells in the BM and spleen spontaneously

generate the high levels of this serum component [111, 187]. Nonetheless, while fetal-lineage B cells have long been associated with nIgM [25, 31, 109, 181, 199-201], B1 cells *per se* have never been shown to supply the serum IgM of naïve mice.

Here, I identify in the BM a discrete population of IgM-secreting PBs and PCs that fully reconstitutes serum IgM in naïve, Rag1-deficient mice. Enumeration of IgM ASCs in various lymphoid tissues indicated that ≈80% of all IgM ASCs in the mouse reside in the BM (Figure 7A). By flow cytometry, I identified BM cells containing high levels of cytoplasmic IgM that were uniquely distinguished by a $mIgM^{+}CD138^{+}B220^{lo/-}FSC^{hi}$ phenotype (Figure 7B). Purified $mIgM^{+}CD138^{+}B220^{-}FSC^{hi}$ BM cells were >80% IgM ASCs by ELISPOT and exhibited a PC morphology (Figure 8A). Additional surface phenotyping revealed that $mIgM^{+}CD138^{+}B220^{lo/-}FSC^{hi}$ BM PB/PCs express CD43, CD28, and MHCII, but do not express CD5 (Figure 8B). The numbers of $mIgM^{+}CD138^{+}B220^{lo/-}FSC^{hi}$ cells present in the BM were virtually identical to the numbers of BM IgM ASCs (Figure 7D); thus, all or the great majority of IgM ASCs in the BM of naïve mice are $mIgM^{+}CD138^{+}B220^{lo/-}FSC^{hi}CD5^{-}$ PB/PCs.

Adoptive transfer of PerC cells into Rag-1 deficient congenics fully restored the $mIgM^{+}CD138^{+}B220^{lo/-}FSC^{hi}$ PB/PC compartment in the BM and normal levels of serum IgM (Figure 9). In contrast, transfer of LN cells reconstituted neither IgM ASCs in the BM nor serum IgM. Splenic IgM ASC numbers, however, were fully restored both by PerC and LN cell transfer, demonstrating that the high levels of nIgM in serum are

maintained by BM, not splenic, IgM ASCs. I conclude that BM and splenic IgM ASCs have separate origins, as splenic IgM ASCs were reconstituted by both PerC and LN cells, whereas BM IgM ASCs were generated only by the transfer of PerC cells.

The PerC contains at least three populations of differentiated B cells: B1a, B1b, and B2 [209]. To determine whether one of these populations was responsible for the reconstitution of IgM ASCs and serum IgM, I transferred each B-cell population separately. In contrast to unfractionated PerC cells, purified B1a, B1b, or B2 cells were very ineffective at reconstituting serum IgM and IgM ASCs in the BM (Figure 9A and B). Transferred B1a, B1b and B2 cells or their progeny were readily recovered 10 weeks after transfer, demonstrating their viability (Table 1). These results indicate that nIgM ASCs in the BM differentiate from precursors in the PerC that are neither B1a, B1b, nor B2 cells.

The VDJ rearrangements present in mIgM^{+}CD138^{+}B220$^{lo/-}$FSC^{hi} BM PB/PCs display features typical of fetal-linage B cells (Figure 10), including overrepresentation of the V_H11 and V_H12 gene families, no or few mutations, and little or no N-nucleotide addition [105, 106, 210, 211]. I directly tested the origins of mIgM^{+}CD138^{+}B220$^{lo/-}$FSC^{hi} BM cells by examining B1-8i knockin mice, in which B2-cell development is intact [216] but B1a and most B1b cells are absent (Figure 11A). In B1-8i mice, I observed a dramatic loss of serum IgM in naive animals (Figure 11B) and the virtual absence of IgM PB/PCs in the BM, both by ELISPOT (Figure 11C) and flow cytometry (Figure 11D and E). Thus,

the nIgM produced by mIgM^{+}CD138^{+}B220$^{lo/-}$FSC^{hi} PB/PCs are not products of conventional, B2-cell development and differentiation. My observations support an earlier study by Hayakawa *et al.* [213] demonstrating that transgenic mice expressing a B1a cell-derived, autoreactive BCR exhibited a maturational block in B2-cell development, but supported the development of B1 cells and autoreactive serum IgM. My experiment with B1-8i mice is reciprocal to that of Hayakawa and colleagues [213]; I noted normal B2-cell development with no or few B1a or B1b cells and no serum IgM (Figure 11). These complementary studies emphasize my conclusion that these two cellular and humoral axes are distinct and independent.

The presence of nIgM in serum does not require CD154:CD40 interaction [132]. If mIgM^{+}CD138^{+}B220$^{lo/-}$FSC^{hi} BM PB/PCs are the source of nIgM, their presence must also be independent of CD154. Examination of CD154$^{-/-}$ mice revealed normal quantities of both serum IgM and mIgM^{+}CD138^{+}B220$^{lo/-}$FSC^{hi} PB/PCs in the BM (Table 2). The quality of nIgM and the IgM PB/PC repertoire was also little or unchanged in the absence of cognate T-cell help; CD154$^{-/-}$ and their congenic controls had indistinguishable titers of ChoP-binding serum IgM, as well as similar ratios of V_H11/V_H1 transcripts in the mIgM^{+}CD138^{+}B220$^{lo/-}$FSC^{hi} BM PB/PC compartment. (Figure 12).

The short half-life of serum Ig in mice requires continual production for steady levels to be maintained [166]. Indeed, the half-life of mouse serum IgG is only 7 days, and that of IgM is shorter still at 2 days [166]. Therefore, to maintain serum Ig levels,

PCs must either be long-lived or constantly replaced by differentiating precursors [162]. While it is well-established that BM IgG PCs generated by infection or immunization are long-lived [164, 170], it is generally thought that IgM-producing cells are transient [122]. To determine whether IgM ASCs in the BM are long-lived or rapidly replaced, I performed a BrdU labeling experiment and found that most mIgM^{+}CD138^{+}B220$^{lo/-}$FSC^{hi} BM cells are LLPCs, slowly replaced at a constant rate by dividing PBs (Figure 13).

PCs are not intrinsically long-lived [171, 172], however, but require survival signals to prevent apoptotic death [1, 162]. For IgG PCs, survival signals are provided by neighboring cells that define a specialized "survival niche" [122]. Eosinophils are a major component of this IgG PC niche [177], and produce both IL-6 and APRIL, cytokines that act synergistically to promote survival in IgG PCs [1, 162, 171, 172, 175]. As mIgM^{+}CD138^{+}B220^{-}FSC^{hi} BM PCs are also long-lived (Figure 13), but die rapidly when isolated from the BM (Figure 15A), I examined whether nIgM PB/PCs in the BM are maintained by the survival niche of IgG PCs. I found that whereas IgG PCs in the BM preferentially co-localize with eosinophils [177], IgM PB/PCs do not (Figure 14B). Furthermore, mice deficient in eosinophils had reduced levels of serum IgG (Figure 14D) and significantly lower numbers of BM IgG ASCs (Figure 14C). In contrast, serum IgM levels and numbers of BM IgM ASCs were normal in mice lacking eosinophils (Figure 14C and D), indicating that eosinophils are dispensable for IgM- but not IgG PCs. Thus,

long-lived IgM- and IgG PCs in the BM occupy and depend upon distinct survival niches.

Indeed, while IL-6 promoted the survival of BM IgG ASCs *in vitro* [171], it provided no survival benefit for IgM ASCs (Figure 15A). This result fits well with the great increases of serum IgG1, but not IgM, in IL-6 transgenic mice [224]. Conversely, IL-5, a survival factor for fetal-lineage B cells [221, 222], significantly increased the number of IgM ASCs recovered after culture (Figure 15A). My observations are consistent with reports that IL-5Rα-deficient mice have reduced levels of serum IgM but not IgG1 [222], and IL-5 transgenic mice have elevated levels of serum IgM, but unchanged IgG levels [225]. These correlations could reflect IL-5-mediated changes in the survival of IgM PB/PCs in the BM and/or the numbers of fetal-lineage precursor cells.

My findings do not support a recent claim by Choi *et al*. [191] that $CD5^+$ B1a cells in the BM are a significant source of nIgM. This report concludes that $CD5^+$ B1a cells in the BM, a small population that neither resembled differentiated PB/PCs nor comprised substantial numbers of IgM ASCs (average <0.9% of BM B1a cells) [191], "significantly" contributes to steady-state serum IgM levels. Given that these $CD5^+$ B1a ASCs constitute <5% of IgM ASCs in the BM [191], it is difficult for me to understand this line of argument; by definition, 95% of serum IgM could not be derived from this B1a compartment.

Similarly, Holodick and colleagues [189] conclude that "the genesis of natural serum IgM" lies with splenic B1a cells, but do not demonstrate by experiment a direct connection between these two compartments. In contrast to both Choi *et al*. [191] and Holodick *et al*. [189], I have shown that nIgM in the serum is invariably linked to the presence of a CD154-independent population of $CD5^{-}mIgM^{+}CD138^{+}B220^{lo/-}FSC^{hi}$ PB/PCs in the BM (Figures 9 and 11; Table 2). This population comprises virtually all of the IgM ASCs in the BM, which constitute about 80% of all IgM ASCs (Figures 7 and 8).

Although it is plausible that BM B1a cells might downregulate CD5 expression and differentiate into IgM ASCs, I demonstrate that B1a cells [$IgM^{hi}IgD^{lo}B220^{lo/-}CD11b^{+}CD23^{-}CD5^{+}$ [209]] are not a significant source of natural serum IgM. Adoptive transfer of B1a cells into $Rag1^{-/-}$ mice fully restored B1a cell numbers in the PerC, but not serum IgM or BM IgM ASCs (Table 1; Figure 9A and B). Instead, nIgM and nIgM PBs and PCs are derived from a population of PerC cells that is neither B1a, B1b, nor B2 (Figure 9A and B). Earlier studies that transferred enriched, but not purified, B1a cells likely failed to differentiate the true PerC precursors from B1a cells, leading to the misconception that B1a cells [$IgM^{hi}IgD^{lo}B220^{lo/-}CD11b^{+}CD23^{-}CD5^{+}$ [209]] are the source of nIgM [25, 180]. Alternatively, no single PerC B-cell type may be able to generate nIgM PB/PCs in the BM, but rather some form of cooperation between different cell types might be necessary.

Another intriguing possibility is that a PerC precursor cell might produce both B1a cells and the nIgM PB/PCs in the BM via independent differentiation pathways. This hypothetical precursor could maintain a stable, continuing source of nIgM and B1a cells little affected by exposure to Ag. In this way, the innate repertoire of both nIgM and the pool of B1a cells might be buffered against Ag-driven clonal expansions and contractions.

The brisk incorporation of BrdU by $mIgM^{+}CD138^{+}B220^{lo}FSC^{hi}$ PBs is followed by slower transfer of label into the $mIgM^{+}CD138^{+}B220^{-}FSC^{hi}$ PC pool (Figure 13). This relationship suggests that nIgM PCs are replaced by (continuously generated) natural PB emigrants, but only when the unique IgM PC survival niche is not replete. In this way, natural serum IgM would be maintained at a level defined by the carrying capacity of the BM survival niche.

In summary, I have identified the primary source of the nIgM circulating in naïve mice: CD154-independent, $CD5^{-}$ IgM PBs and PCs in the BM. These natural PCs differentiate from a fetal-lineage precursor in the PerC and occupy a distinct survival niche in the BM associated with IL-5 signaling. These IgM PCs, their BM survival niche, and nIgM constitute an innate cellular and humoral axis that may point to the origins of Ab-mediated protection.

Finally, my results inform the development of therapies to target different BM PC compartments. For example, they open the possibility of eliminating high-affinity,

autoreactive IgG-producing cells, while leaving protective nIgM ASCs intact. Conversely, as nIgM restricts the engraftment of xenotransplants [226], selective depletion of BM nIgM ASCs may help prepare patients to receive grafts, while preserving protective IgG PC memory formed by immunization and infection.

4. The bone marrow survival niche of natural IgM PCs

In the previous chapter, I demonstrated that most circulating nIgM is produced by a discrete population of nIgM PCs in the BM that are long-lived and occupy a unique survival niche characterized by IL-5. In this chapter, I sought to describe the cellular components of the nIgM PC survival niche. The work described here is under preparation for publication.

4.1 Introduction

High titers of both natural and immune Ab are critical to host defense [24, 227]. Virtually all current vaccines are based on the induction of Ab, to protect against pathogens that may be encountered in the future. Such humoral immune memory is possible because titers of specific Abs remain high enough to reliably neutralize infectious particles long after the vaccine has been given. Indeed, levels of vaccine-induced serum Ab against tetanus and diphtheria toxoids remain sufficiently robust for 10-20 years, while those induced by live pathogens are thought to have half-lives on the order of centuries [165]. However, Ab molecules in the circulation have half-lives of only about one week, depending on the isotype [166]. Though the stimulation of memory B cells during re-exposure induces the generation of replacement PCs, this process is not thought to account for the disparity in Ab titer and molecule half-lives [164, 167-169]. It is, however, well established that long-term Ab titers are maintained by LLPCs that

persist in the BM where they continuously produce Abs until replaced by newly generated PBs [162, 164, 167, 170].

Long life is not an inherent property of PCs, however, as they rapidly die by ER-stress induced apoptosis when isolated [171, 172]. Instead, external signals promote PC longevity by inducing the upregulation of anti-apoptotic proteins [1, 175]. Extensive research has revealed that IgG PCs receive such survival signals in specialized niches, primarily in the BM [1, 162]. IL-6, APRIL, and BAFF are among the most potent survival factors for IgG PCs, and appear to work in concert to best support their persistence [162, 171]. Indeed, removal of any one of these molecules fails to deplete IgG PCs from the BM, suggesting that their redundancy safeguards the continuous strong anti-apoptotic stimulation vital to PC survival [1, 171, 173-175]. To best receive survival signals, IgG PCs are anchored in the BM by chemokine and adhesion molecule-expressing BM stromal cells [1, 169, 177]. Nearby, eosinophils and megakaryocytes produce IL-6 and APRIL, forming a second level of redundancy; though eosinophils are the primary producers of both cytokines in the BM, IgG PCs are not fully lost in eosinophil-deficient mice [1, 177].

High levels of IgM are also maintained in the circulation throughout life. Most of this IgM is present independently of external Ag exposure, and is thus described as natural IgM [17, 18]. The quantity and unique binding pattern of nIgM remains relatively constant throughout life, though levels can vary more than 100-fold between

individuals [20-22]. nIgM broadly recognizes pathogens through conserved molecular structures, thereby acting as an innate-like, first-line defense against invading microorganisms [24, 29, 30]. Mice lacking circulating IgM show an increased susceptibility to infection by viruses, bacteria, fungi, and parasites [31-36]. In addition to its critical role in blocking pathogen dissemination, nIgM also targets determinants exposed on apoptotic cells, and promotes their phagocytic destruction via C1q binding [19, 25, 26, 38]. Indeed, nIgM is a critical mediator of apoptotic cell clearance, and prevents the development of autoimmune disease and atherosclerosis in mice [40-42, 46, 47]. In humans, inverse correlations have been identified between nIgM titers and the incidence and severity of SLE [26, 48-51].

In chapter 3, I showed that nIgM levels in the serum are maintained by a discrete population of $CD138^{+}IgM^{+}CD5^{-}$ PCs residing in the BM (Figures 7 and 8). Like BM IgG PCs, nIgM PCs are long-lived but slowly replaced at a constant rate by newly generated PBs (Figure 13). Also, nIgM PCs die rapidly when cultured in isolation (Figure 15). However, in contrast to IgG PCs, nIgM PCs are not supported by IL-6 or eosinophils (Figure 14) [177]; instead, IL-5 significantly increases their survival *in vitro* (Figure 15). I thus concluded that a distinct nIgM survival niche exists in the BM, and that it is driven at least in part by IL-5.

Here, I show that nIgM PCs are not supported by the primary hematopoietic sources of IL-5: T cells, ILC2s, or MCs. I found instead that nIgM PCs associate with BM

stromal cells, which produce IL-5 and support the *in vitro* survival of nIgM PCs when stimulated with LPS. *In vivo* neutralization of IL-5 revealed that IL-5 is not the sole supporter of IgM PCs *in vivo*, but like individual IgG PC survival factors, is likely one of multiple cytokines that collectively ensure continual pro-survival signaling. In summary, I have determined that long-lived nIgM PCs are not supported by IL-5 producing hematopoietic cells, but associate with BM stromal cells to receive multiple redundant survival signals.

4.2 Results

4.2.1 T cells are not required for the maintenance of nIgM

T cells are the primary source of IL-5 in mice, and are present in the BM. Thus, to determine if IL-5 is supplied to nIgM BM PCs by adjacent T cells, I examined sections of BM by immunofluorescence (Figure 16A). In contrast to eosinophils, which are found in contact with approximately 40% of IgG PCs [194], the frequency of neither IgG (13%) nor IgM (16%) PCs adjacent to T cells was significantly higher than that expected to occur stochastically (13%) (Figure 16B). Thus, T cells are not preferentially located near IgM PCs in the BM.

To determine whether T cells are dispensable for the maintenance of nIgM PCs in the BM, I examined linker for activation of T cells (Lat)-deficient mice, which lack all mature T-cell populations, as T-cell development is arrested at the double-negative stage [228]. While these mice had 48% fewer BM IgG ASCs compared to B6 controls,

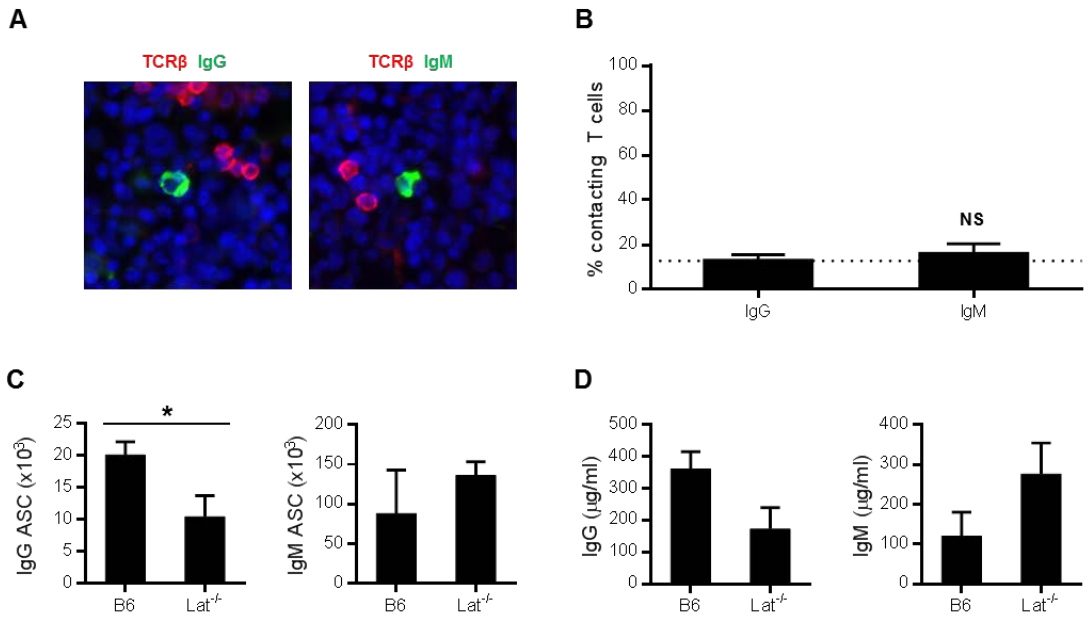

Figure 16: T cells are not required for the maintenance of nIgM

(**A**) Representative immunofluorescence micrographs of femur sections from naïve B6 mice stained with DAPI, PE anti-TCRβ, and either FITC anti-IgG (*left panel*) or FITC anti-IgM (*right panel*). (**B**) Frequency of IgG$^+$ or IgM$^+$ PCs in contact with TCRβ$^+$ T cells in femur sections. Dotted line indicates the frequency of randomly selected DAPI$^+$ nuclei that were adjacent to TCRβ$^+$ cells. (**C**) Number of IgG and IgM ASCs in the BM determined by ELISPOT. (**D**) Concentration of serum IgG and IgM measured by ELISA. Data represent a total of six mice from two independent experiments, and show mean ± SEM.

the numbers of IgM ASCs were elevated by 54% (Figure 16C). Similarly, whereas the concentration of serum IgG was reduced by 52% in Lat-deficient mice, I observed a 129% increase in the levels of circulating IgM (Figure 16D). Thus, T cells are not required for nIgM PCs to differentiate or survive in the BM.

4.2.2 Type 2 innate lymphoid cells are dispensable for the maintenance of nIgM

ILC2s have emerged as an important source of type 2 cytokines, including IL-5 [229]. These cells reside mainly at mucosal surfaces, but are also found in small numbers in the BM [229, 230]. I evaluated, therefore, whether ILC2s support BM-resident nIgM PCs.

I first employed a genetic ablation approach by examining mice lacking the transcription factor retinoic acid receptor-related orphan receptor α (RORα), which is required for the development of ILC2s [231]. These mice displayed a global disturbance of both IgM and IgG production, with IgM levels 4-fold and IgG 2-fold lower in serum from knockout animals than wild type (WT) littermates (Figure 17A). Accordingly, numbers of both IgM and IgG ASCs were reduced in both the BM (IgM, 2-fold; IgG, 1.5-fold) and spleen (IgM, 2-fold; IgG, 3-fold) of knockout compared to WT mice (Figure 17B and C). These results revealed a widespread defect in Ab production in the absence of RORα, and suggested that either RORα or ILC2s are required for the normal formation and/or maintenance of ASCs.

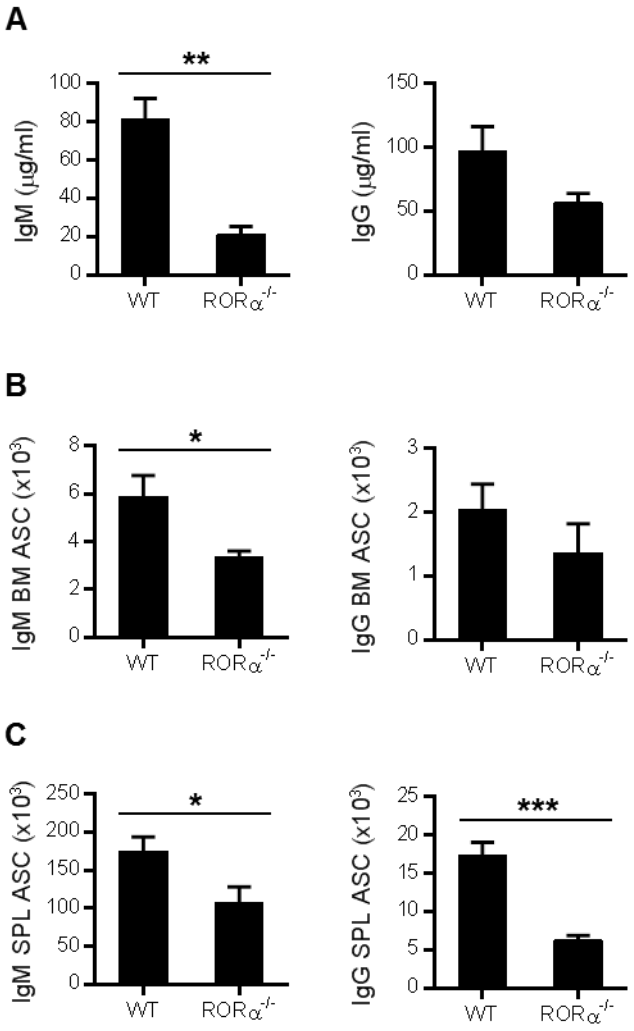

Figure 17: ROR$\alpha^{-/-}$ mice have a global defect in ASC development and Ab production

(**A**) Concentration of serum IgM and IgG measured by ELISA. (**B**) Number of IgM and IgG ASCs in the BM determined by ELISPOT. (**C**) Number of IgM- and IgG ASCs in the spleen determined by ELISPOT. Data represent a total of five WT littermates and four ROR$\alpha^{-/-}$ mice, and show mean ± SEM.

I next used, therefore, an Ab-depletion method to study the role of ILC2s in ASC maintenance while avoiding manipulation of B cells. ILC2s can be identified using a combination of surface markers that includes thymocyte differentiation antigen 1.2 (Thy1.2) [230, 232, 233]. Indeed, anti-Thy1.2 Ab treatment is frequently used to deplete mice of ILCs [234-236]. This method is used in the context of T cell-deficiency, to avoid conflation of the involvement of T cells and ILCs in a given process [234, 236]. Therefore, to examine the effect of ILC2 depletion on BM IgM PC survival, I first transferred $3x10^6$ unfractionated PerC cells from B6 mice into Rag1-deficient mice [194]. Six weeks later, I injected mice with anti-Thy1.2 monoclonal Ab or isotype control Ab every 3 days for 5 injections, and then sacrificed the animals 1 day following the final treatment.

Examination of the BM showed an 80- and 149-fold reduction in the number of $Thy1.2^+$ cells compared to untreated Rag1-deficient mice, or PerC cell-recipient mice treated with isotype control Ab, respectively; $Thy1.2^+$ cells were nearly undetectable in the BM of treated animals (Figure 18A). Nevertheless, levels of serum IgM remained essentially unchanged after treatment with either isotype control Ab [pre, 601 (±221) μg/ml; post, 559 (±278) μg/ml] or anti-Thy1.2 [pre, 934 (±126) μg/ml; post, 1148 (±543) μg/ml] (Figure 18B). The numbers of IgM ASCs in the BM of PerC cell-recipient mice were similarly stable, with no significant difference ($p = 0.346$) being observed between isotype control [27.8 (±27.6) x 10^4] and anti-Thy1.2 Ab-treated animals [47.7 (±16.6) x 10^4] (Figure 18C). Flow cytometric analysis reflected these results, with no

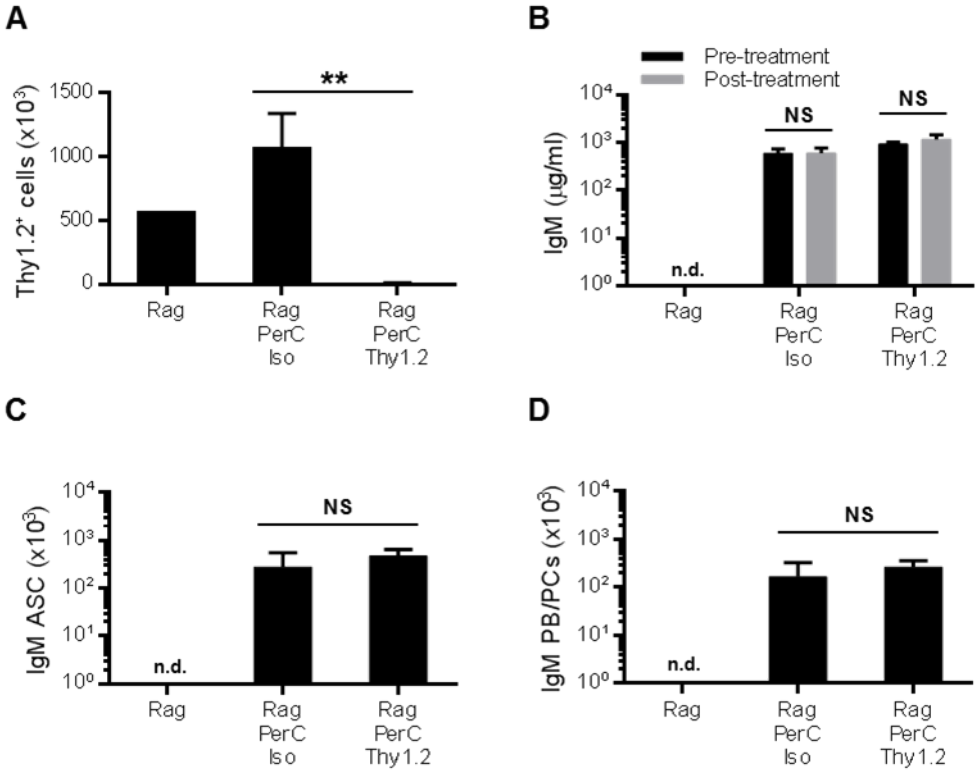

Figure 18: Depletion of Thy1.2$^+$ cells does not affect nIgM or nIgM PCs in Rag1$^{-/-}$ recipients of PerC cells

3x10^6 total PerC cells from B6 mice were injected i.p. into Rag1$^{-/-}$ mice. 6 weeks later, recipient mice were injected with either isotype control antibody or anti-Thy1.2 (200µg/injection) every 3 days for 5 injections. Mice were sacrificed 1 day after the final injection. Rag, untreated Rag1$^{-/-}$; Rag PerC Iso, PerC-recipient Rag1$^{-/-}$ mice treated with isotype control Ab; Rag PerC Thy1.2, PerC-recipient Rag1$^{-/-}$ mice treated with anti-Thy1.2 Ab. (**A**) Number of Thy1.2$^+$ cells in the BM determined by flow cytometry. (**B**) Concentration of serum IgM measured by ELISA. Pre-treatment serum was taken 1 day prior to initiation of injections, and post-treatment serum was taken at sacrifice. (**C**) Number of IgM ASCs in the BM determined by ELISPOT. (**D**) Number of mIgM$^+$CD138$^+$B220$^{lo/-}$FSC^{hi} cells in the BM determined by flow cytometry. Data represent a total of three mice of each treatment from one experiment, and show mean ± SEM.

significant difference found in the number of $CD138^{+}IgM^{+}B220^{lo/-}FSC^{hi}$ cells in the BM of isotype control or anti-Thy1.2 Ab-treated mice ($p = 0.419$) (Figure 18D). Collectively, these results indicate that ILC2s are dispensable for the maintenance of nIgM and the BM PCs that produce it, whereas RORα is critical for the normal formation of ASCs in general, either directly or indirectly.

4.2.3 Mast cells are not required for the maintenance of nIgM

4.2.3.1 Natural IgM production is disrupted in mast cell-deficient Sash mice

MCs are also a source of type 2 cytokines, producing IL-5 in detectable quantities following stimulation [237, 238]. Though MCs are primarily known for their role as first-responders to infection at exposed surfaces such as the skin and mucosae [237], I next tested whether MCs might also provide IL-5 to nIgM PCs in the BM. To do so, I utilized mice carrying an inversion of the upstream transcriptional regulatory elements of the cKit gene, called "Sash" mice [239]. These animals lack mature MCs in all organs, but have an otherwise intact immune system, as hematopoiesis is not disturbed [239]. Indeed, Sash mice are widely used to study the role of MCs in various contexts, such as infection and inflammation [240, 241].

Examination of the PerC of Sash mice confirmed that they lack MCs, as identified by high expression FcεR1 and cKit (Figure 19A) [239]. Measuring serum Ig concentrations revealed that Sash mice have a 90% reduction in circulating IgM, as well as a 66% loss of IgG (Figure 19B). A corresponding 83% reduction in

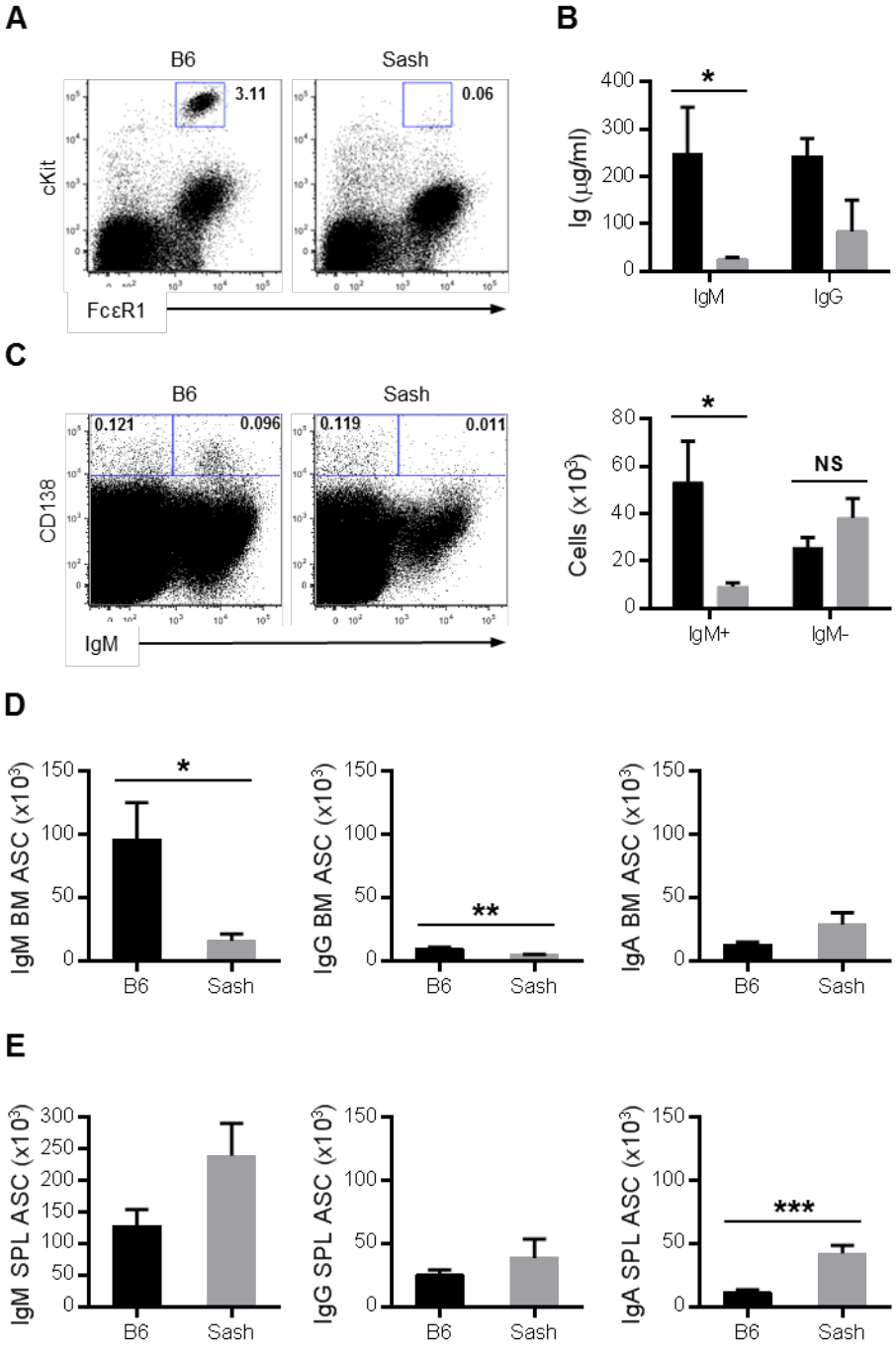

Figure 19: nIgM production is disrupted in Sash mice

(Figure 19, continued) (**A**) Representative flow plots of PerC cells, pre-gated on single live leukocytes. (**B**) Concentration of serum IgG and IgM measured by ELISA. (**C**) Representative flow plots of BM cells, pre-gated on single live leukocytes. Histograms summarize numbers of $mIgM^{+}CD138^{+}B220^{lo/-}FSC^{hi}$ and $mIgM^{-}CD138^{+}B220^{-}FSC^{hi}$ cells in the BM (**D**) Number of ASCs in the BM determined by ELISPOT. (**E**) Number of ASCs in the spleen determined by ELISPOT. Data represent a total of six mice of each genotype from two independent experiments, and show mean ± SEM.

$CD138^{+}IgM^{+}B220^{lo/-}FSC^{hi}$ IgM PB/PCs was found in the BM of Sash mice, whereas the numbers of class-switched $CD138^{+}IgM^{-}B220^{-}FSC^{hi}$ PCs were not significantly different (Figure 19C).

IgM ASC numbers were found also by ELISPOT to be reduced in the BM of Sash mice (84%) compared to B6 controls, as were IgG ASC numbers (51%), while IgA numbers were elevated (216%) (Figure 19D). Notably, the numbers of ASCs of all three isotypes were increased in the spleen of mutant animals compared to controls (Figure 19E). These data indicate that the maintenance of nIgM PCs in the BM, but not the spleen, of Sash mice is disrupted. I conclude that the Sash mutation specifically inhibits nIgM production by directly or indirectly altering either fetal B-cell development, PerC B-cell differentiation, or the survival of BM IgM PCs.

4.2.3.2 Restoration of PerC mast cells does not rescue natural IgM production in Sash mice

As mature MCs are absent from the PerC in Sash mice, I hypothesized that MC-derived cytokines are required for PerC B cells to differentiate into nIgM PCs, a process dependent upon IL-5 [221]. Indeed, i.p. injection of IL-5 elevates serum IgM levels 4-fold [222, 242]. I injected, therefore, Sash mice i.p. with 10^6 unfractionated PerC cells from Rag1-deficient mice, to restore MCs while avoiding transfer of donor B cells, or with PBS as an injection control.

Ten weeks later, MCs did not appear in the PerC of PBS injected Sash mice, but accumulated in donor cell-recipient mice to numbers lower, but not significantly

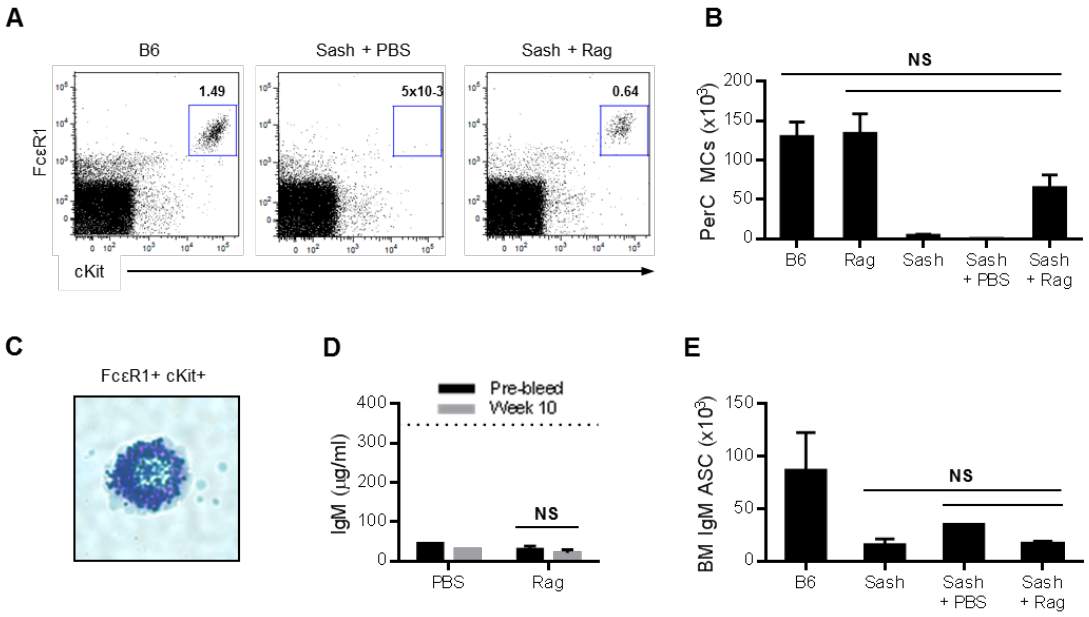

Figure 20: Restoration of PerC mast cells does not rescue nIgM production in Sash mice

10^6 total PerC cells from Rag1$^{-/-}$ mice were injected i.p. into Sash mice. Mice were analyzed 10 weeks later. (**A**) Representative flow plots of PerC cells, pre-gated on single live leukocytes. (**B**) Number of FcεR1$^+$cKit$^+$ mast cells (MCs) in the PerC. (**C**) Representative photograph of sorted, FcεR1$^+$cKit$^+$ PerC cells stained with toluidine blue. (**D**) Concentration of serum IgM measured by ELISA. Pre-bleed serum was taken prior to transfer, and week 10 serum taken at sacrifice. Dotted line indicates IgM concentration in the serum of normal B6 mice. (**E**) Number of IgM ASCs in the BM determined by ELISPOT. Data represent a total of two sash PerC-injected mice from one experiment, and show mean ± SEM.

different than those in B6 mice or Rag1-deficient controls ($p = 0.211$ and 0.133, respectively) (Figure 20A and B). To confirm that $Fc\varepsilon R1^{+}cKit^{+}$ cells were indeed MCs, I isolated the population from B6 mice by FACS, and examined the cells by microscopy. After staining with toluidine blue, $Fc\varepsilon R1^{+}cKit^{+}$ cells contained numerous dark, metachromatic granules, typical of mature MCs (Figure 20C) [243].

Despite restoration of PerC MCs, the low levels of serum IgM in Sash hosts remained unchanged throughout the course of the experiment, as did those in PBS injected controls (Figure 20D). Furthermore, 10 weeks following injection, the numbers of IgM ASCs in the BM of PerC cell-recipient mice were not different from those in untreated or PBS injected controls (Figure 20E). Collectively, these data indicate that the low serum IgM levels observed in Sash mice are not due to a lack of PerC MCs.

4.2.3.3 Sash mice have a B cell-intrinsic defect in nIgM-PC differentiation

To directly test whether the BM of MC-deficient Sash mice has the capacity to support nIgM PCs, I transferred $3x10^{6}$ CD45.1 WT PerC cells i.p. into Sash mice or Rag1 knockouts. After 10 weeks, the number of donor B1a cells in the PerC of $Rag1^{-/-}$ recipient mice was equal to that in CD45.1 donors, whereas the number in Sash recipients was 96% lower (Figure 21A). Furthermore, whereas PerC $CD11b^{-}$ B1 cell numbers were 30% of those in donors, they were 2% in Sash mice. Analysis of the BM revealed that $CD45.1^{+}$ nIgM PCs appeared in $Rag^{-/-}$ but not Sash recipient mice (Figure 21B). These data indicate that the PerC of Sash mice is non-permissive for the survival,

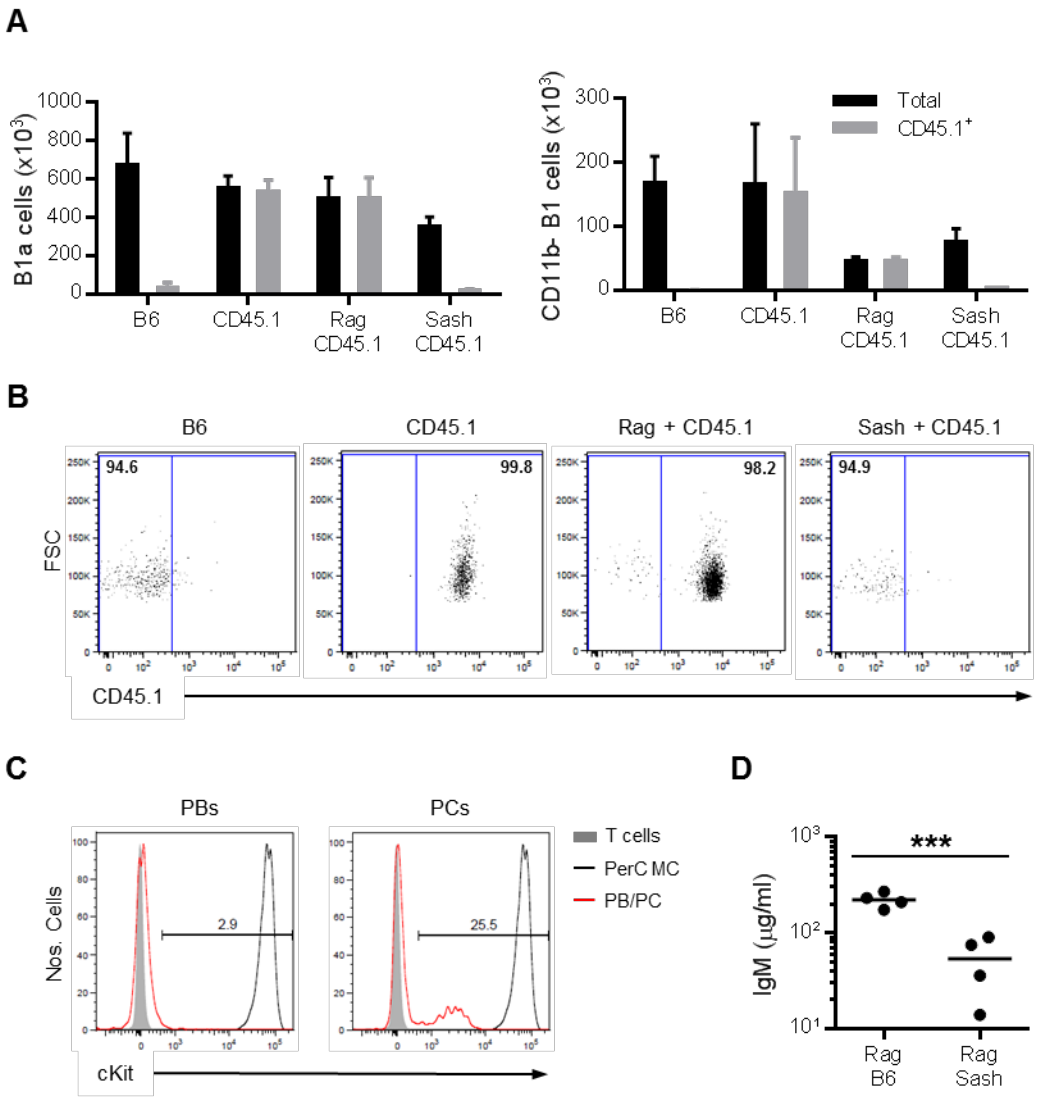

Figure 21: Sash mice have a B cell-intrinsic defect in nIgM-PC differentiation

(**A**) 3x10^6 total PerC cells from CD45.1$^+$ donor mice were injected i.p. into Rag1$^{-/-}$ or Sash mice. 10 weeks later the number of PerC B1a and CD11b$^-$ B1 cells was determined by flow cytometry. Data represent a total of four recipient mice in each group from two independent experiments, and show mean ± SEM. (**B**) Representative flow plots of live mIgM$^+$CD138$^+$B220$^{lo/-}$FSC^{hi} BM cells. (**C**) Representative flow plots of mIgM$^+$CD138$^+$B220^{lo}FSC^{hi} (PBs) and mIgM$^+$CD138$^+$B220$^-$FSC^{hi} (PCs) BM cells, with T cells and PerC mast cells as negative and positive controls, respectively. (**D**) 3x10^6 total PerC cells from B6 or Sash mice were injected i.p. into Rag1$^{-/-}$ mice. 10 weeks later the concentration of serum IgM was measured by ELISA. Each symbol represents an individual mouse, from two independent experiments.

homeostatic expansion, and differentiation of normal B1 cells.

I next considered whether the nIgM-deficient phenotype of Sash mice might result from a B cell-intrinsic defect. While stem cell factor (SCF), the ligand for the cKit receptor, does not support the *in vitro* survival of IgG-secreting cells [171], it may play a role in the maintenance of BM IgM PCs. Defective cKit expression in IgM PCs might thus inhibit their long-term survival in the BM. To test this possibility, I measured the frequency of BM IgM PCs that express cKit and compared the expression levels on positive cells to those of cKit$^+$ MCs. I found that 2.9% of IgM$^+$CD138$^+$B220^{lo}FSC^{hi} PBs and 25.5% of IgM$^+$CD138$^+$B220$^-$FSC^{hi} PCs were cKit$^+$, and that these positive cells expressed cKit at a level approximately 500-fold lower than PerC MCs (Figure 21C). Since IgM ASC numbers are reduced by 84% in the BM of Sash mice (Figure 19D), these data strongly suggest that loss of signaling through cKit on the quarter of BM IgM PCs that express the receptor is not responsible for producing the nIgM-deficient phenotype in Sash mice.

While cKit signaling is not thought to be required for B-cell development *per se*, either in the fetal liver or adult BM [239, 244], I tested whether fetal-lineage PerC B cells in Sash mice retained the capacity to differentiate into nIgM BM PCs by transferring $3x10^6$ unfractionated PerC cells from either B6 or Sash mice i.p. into Rag1-deficient mice. Ten weeks later, I found that serum IgM levels were fully restored in recipients of B6 PerC cells, whereas IgM titers were significantly lower (4-fold) in Sash recipients (Figure

21D). Collectively, my data indicate that PerC B cells in Sash mice are defective in their capacity to become nIgM PCs.

4.2.4 BM stromal cells retain nIgM PCs and support their survival

BM stromal cells express both adhesion molecules and survival factors, thus acting to both retain and support IgG PCs in the BM [1, 172, 174]. However, their primary role is to provide a scaffold on which survival niches are built in association with hematopoietic cells, such as eosinophils, which produce the bulk of the survival signals [122]. Thus, after ruling out the primary hematopoietic producers of IL-5, I turned to BM stromal cells as a possible niche cell. Indeed, BM stromal cells have been shown to produce IL-5 [245], and I detected substantial levels of IL-5 mRNA in the plastic-adherent (Ad) fraction of BM cells, exceeding even those in T_H2 culture-skewed $CD4^+$ splenic T cells (Figure 22A). In agreement with the results I obtained in the preceding part of this study, non-adherent (N-Ad) BM cells produced relatively little IL-5 (7-fold less than Ad cells), though slightly more than ex vivo $CD4^+$ splenic T cells, which served as a negative control. Similarly, IL-5 transcript was undetectable in N-Ad BM cells from $Rag1^{-/-}$ mice, whereas levels were very high in $Rag1^{-/-}$ Ad BM cells, higher even than B6 Ad BM (Figure 22A). This result is consistent with my transfer data showing that the BM of Rag1-deficient mice given B6 PerC cells harbors higher numbers of nIgM PCs than B6 control BM (Figure 9).

As IgG PCs are held in close connection with stromal cells in the BM,

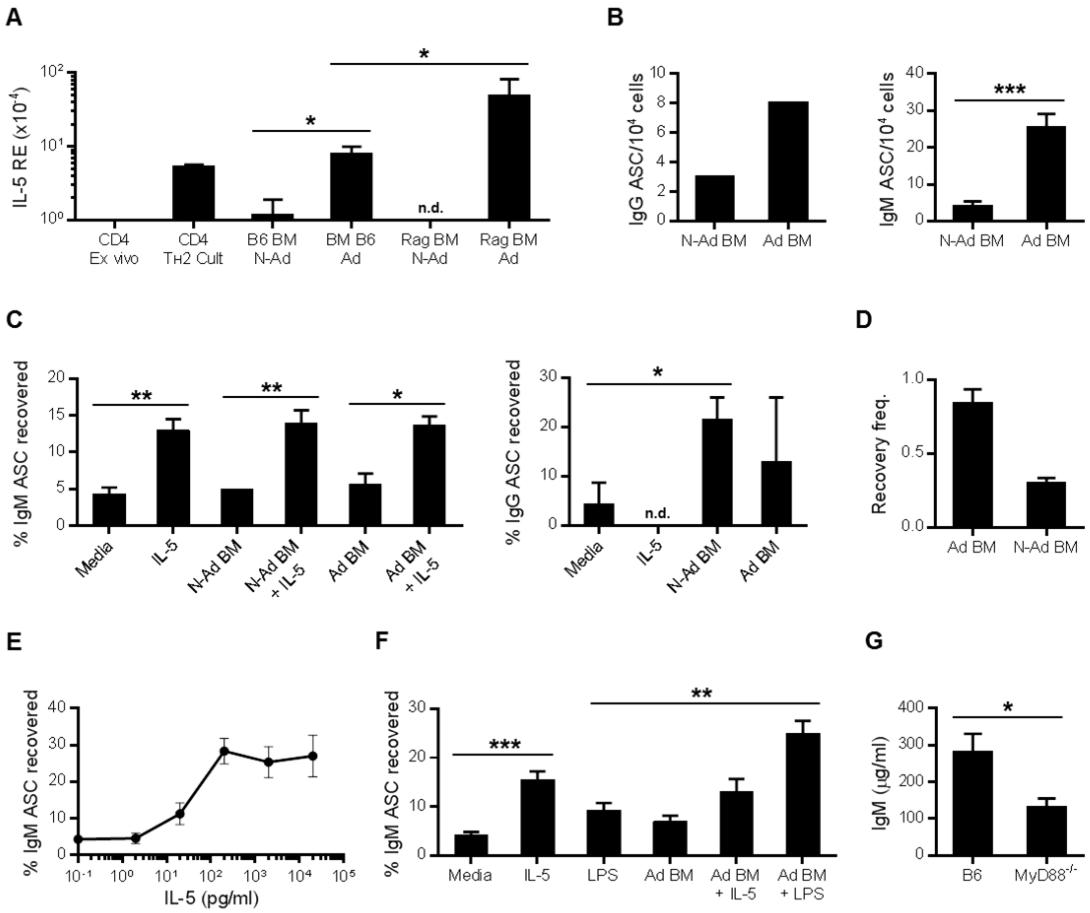

Figure 22: BM stromal cells express IL-5, retain nIgM PCs, and support nIgM PC survival when activated

(**A**) IL-5 expression relative to β-actin in *ex vivo* or TH2-skewed splenic CD4+ T cells, and N-Ad and Ad BM cells from B6 and Rag1-/- mice. (**B**) ELISPOT of N-Ad and Ad BM cells. (**C**) CD138+IgM+ (left) or CD138+IgM- (right) BM cells were cultured for 2 days in media alone, with 20 ng/ml IL-5, or with 10^4 N-Ad or Ad BM cells, with or without 20 ng/ml IL-5. IgM- and IgG-secreting cell input number was determined by ELISPOT of sorted cells at day 0 and was compared to the number detected in wells on day 2 to calculate percent recovery. (**D**) The frequency of trypan blue-excluding live cells remaining on day 2 of culture compared to the input cell number. (**E**) CD138+IgM+ BM cells were cultured for 2 days in media alone, or with 2, 20, 200 pg/ml, or 2 or 20 ng/ml IL-5. (**F**) CD138+IgM+ BM cells were cultured for 2 days in media alone or with 10^5 Ad BM cells, with or without 20 ng/ml IL-5 or 0.5 μg/ml LPS. (**G**) Serum IgM measured by ELISA, from eight mice. Data represent one to three independent experiments, and show mean ± SEM.

I hypothesized that IgM PCs are as well. ELISPOT assay revealed a higher frequency (2.6-fold) of IgG ASCs among Ad than N-Ad BM cells, as expected (Figure 22B). IgM ASCs followed a similar pattern, with a significant 6-fold higher frequency in the Ad BM fraction than the N-Ad population. This result suggests that IgM PCs, like IgG PCs, are retained in the BM by adhesion within the stromal cell reticulum.

To determine whether stromal cells had the capacity to support IgM PC survival, I placed sorted PCs on a layer of Ad BM cells, or among an equal number of N-Ad BM cells. In neither case did I observe recovery of IgM PCs above background, though addition of IL-5 to either culture increased survival significantly, similar to IL-5 alone, indicating that I was able to successfully recover ASCs from cultures with feeder cells (Figure 22C). I did find an enhanced recovery of IgG PCs cultured in the presence of non-adherent cells, presumably due to association with eosinophils. Thus, though Ad BM cells contain large amounts of IL-5 transcript, they failed to support nIgM PCs under the *in vitro* conditions I employed.

To determine whether Ad BM cells had died during the culture, I counted the number of live cells remaining following 2 days in culture. 84% of Ad cells persisted though the duration of the experiment, whereas 30% of N-Ad cells remained alive (Figure 22D). As the majority of Ad cells had not died, it was possible that they secreted a level of IL-5 too low to affect nIgM PC survival *in vitro*. To determine the sensitivity of nIgM PCs to IL-5 concentration, I titrated IL-5 in cultures of sorted nIgM PCs, and found

that the survival advantage disappeared at approximately 2 pg/ml (Figure 22E). By ELISA, I was unable to detect IL-5 in Ad BM culture supernatants above the detection limit of about 128 pg/ml (data not shown). Thus, although suboptimal levels of IL-5 may be secreted by Ad BM cells, they fail to support nIgM PCs in culture.

To enhance, therefore, the production of cytokines by the Ad BM fraction, I added LPS to the culture (Figure 22F). As before, IL-5 significantly enhanced the recovery of IgM ASCs, though LPS had minimal effect. Ad BM cells alone did not support IgM ASC survival, but did together with IL-5. Addition of LPS to Ad BM cultures significantly increased the survival of IgM ASCs compared to both LPS alone, as well as IL-5 addition (Figure. 22F). To determine whether PRR signaling plays a role in the support of nIgM PCs *in vivo*, I compared serum IgM levels in WT mice to those lacking a major PRR signaling molecule, MyD88, and found that levels were significantly lower (>2-fold) in the latter (Figure 22G). Collectively, my results indicate that nIgM PCs associate with adherent BM cells, which support their persistence by producing survival signals, including IL-5.

4.2.5 IL-5 is a redundant survival signal for nIgM PCs

I next tested whether IL-5 is required *in vivo* for the survival of nIgM PCs in the BM. Following 2 or 4 injections of either neutralizing anti-IL-5 or isotype control Ab every 3 days, I counted the number of ASCs in the BM and spleen by ELISPOT. The number of IgM ASCs remained unchanged in the BM of anti-IL-5 treated mice compared

to those receiving isotype control Ab, as did the number of BM IgG ASCs, and the number of IgM ASCs in the spleen (Figure 23A and B).

To confirm that the Ab I injected was able to reach the BM and sequester local IL-5, I counted the number of BM eosinophils. Eosinophils are dependent on IL-5 for generation, maintenance, and function [246]. Consistent with neutralization of IL-5 in the BM environment, I observed a significant 2.2-fold reduction in the number of eosinophils in the BM. Together with my previous results, these data suggest that IL-5 is a potent, but redundant survival signal for nIgM PCs in the BM. This is unsurprising, as similar observations have been reported for IgG PC survival factors, which independently enhance *in vitro* IgG PC survival, but are individually dispensable for the survival of some part of the BM IgG PC population [171, 173]. I conclude that nIgM PCs are also supported by multiple redundant factors, which together form a stable, long-term survival niche.

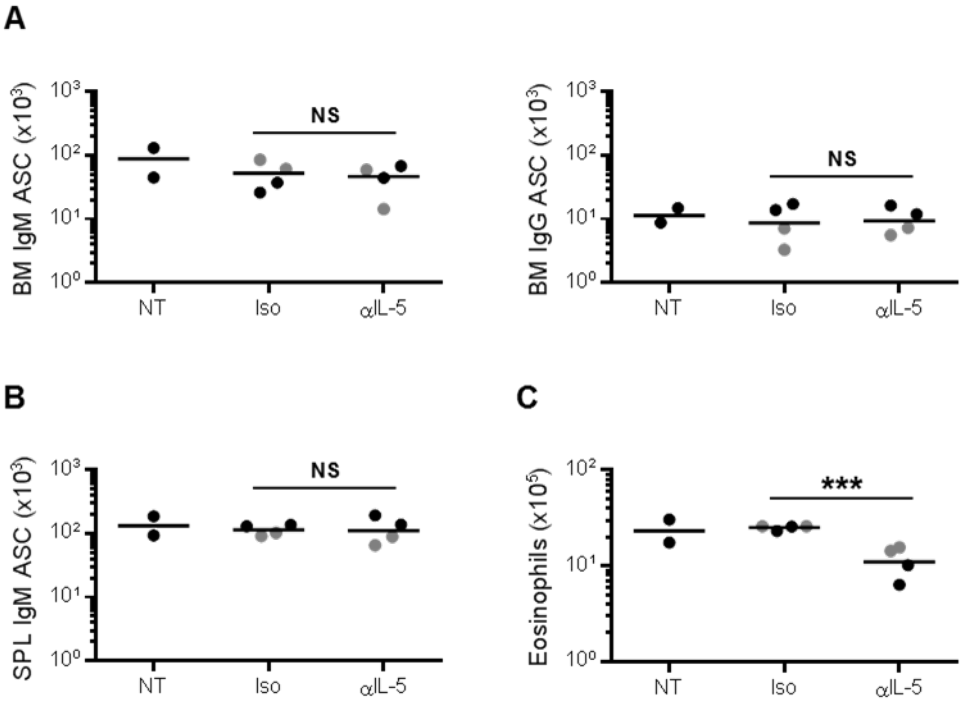

Figure 23: ***In vivo*** **IL-5 neutralization is insufficient to deplete BM nIgM PCs**

B6 mice were injected i.v. with 100 μg anti-IL-5 per injection every 3 days for 2 (black symbols) or 4 (gray symbols) injections, and analyzed 3 days following the final injection. (**A**) Number of IgM and IgG ASCs in the BM determined by ELISPOT. (**B**) Number of IgM ASCs in the spleen determined by ELISPOT. (**C**) Number of Siglec-$F^{+}SSC^{hi}$ eosinophils in the BM determined by flow cytometry. Each symbol represents an individual mouse, from two independent experiments.

5. The precursor of natural IgM PCs

In chapters 3 and 4, I showed that high titers of nIgM are maintained in the circulation by BM-resident PCs that survive long-term in a unique survival niche comprising IL-5-producing stromal cells. I also noted that these nIgM PCs differentiate from precursors in the PerC, but cannot be reconstituted by isolated B1a, B1b, or B2 cells. In this chapter, I describe my work to elucidate the identity and nature of nIgM PC precursors.

5.1 Introduction

nIgM production is strongly associated with B1a cells [109, 180-182]. Though B1a cells in the PerC do not make a substantial contribution to circulating nIgM levels, those in the spleen correlate with nIgM [189]. More recently BM B1a cells were also linked with nIgM [191]. Indeed, several populations certainly produce some amount of nIgM, but the primary source had never been confirmed as these studies failed to address the fundamental issue of whether the cells they described produced the bulk of nIgM. In chapter 3, I demonstrated that most nIgM is produced not by undifferentiated B1a cells, but by $CD5^-$ PBs and PCs in the BM; these cells are distinguished by a $CD138^+IgM^+B220^{lo/-}FSC^{hi}$ phenotype (Figures 7 and 8).

As PCs are terminally differentiated B cells, I sought to determine whether BM nIgM PCs differentiate from B1 or B2 cells. Following transfer of LN or PerC cells into Rag1-deficient mice, I found that only the latter restored serum IgM and nIgM PCs

(Figure 9). As LNs do not contain B1 cells, this result indicated that B1 cells give rise to nIgM PCs. Indeed, nIgM has long been connected with fetal-lineage B cells, and my own data support this connection (Figures 10 and 11). Nevertheless, transfer of neither purified B1a nor B1b cells reconstituted nIgM, in apparent contradiction to a number of experiments that link restoration of B1a cells to nIgM recovery [109, 180-182].

In this study, in order to identify the PerC B-cell population that gives rise to nIgM PCs, I transferred populations of PerC cells sorted according to CD19, CD5, and CD11b expression. Only mice receiving $CD19^+$, $CD19^+CD5^+$, or $CD19^+CD5^+CD11b^-$ cells recovered nIgM, while $CD19^-$, $CD19^+CD5^-$, or $CD19^+CD5^+CD11b^+$ cells did not, even though the last of these accumulated a normal number of PerC B1a cells. Thus, a distinct B1-cell population generates nIgM PCs. Furthermore, I show that interaction between $CD11b^-$ B1 cell subsets is likely required for nIgM-PC differentiation to occur, and that development in the fetal/neonatal environment is necessary for proper functional development of nIgM PC precursors. Finally, I found that a mutation affecting cKit expression likely diminishes the development and differentiation potential of nIgM PC precursors at a critical stage of development near birth. In summary, I have shown that $CD19^+CD5^+CD11b^-$ cells in the PerC comprise nIgM PC precursors, and develop their differentiation capacity in the neonatal environment.

5.2 Results

5.2.1 The phenotype of nIgM PC precursors in the PerC

5.2.1.1 The precursor of nIgM PCs is CD19$^+$

The PerC contains not only mature B-cell populations, but also stem cells with the capacity to differentiate into B cells [247]. To determine whether the PerC precursor of nIgM PCs is a committed CD19$^+$ B cell, or an earlier progenitor, I injected Rag1-deficient mice i.p. with 5x10^5 CD19$^+$ or CD19$^-$ cells sorted from pooled B6 PerC lavage (Figure 24A). Both fractions were isolated to a purity of over 98%.

Ten weeks following transfer, the number of IgM$^+$ B cells in the PerC of mice injected with CD19$^+$ cells was 22% of that detected in mice receiving unfractionated PerC, and only 0.1% of this number in CD19$^-$ cell recipients (Figure 24B). Furthermore, the number of B1a cells in the PerC of CD19$^+$ and total PerC cell recipient mice was not significantly different in 4 of 5 recipients, whereas PerC B1a cells were undetectable in 2 of 5 CD19$^-$ cell-recipient mice, and 92% lower in the others (Figure 24C).

As before (Figure 9; Table 1), serum IgM levels did not correlate with B1a cell reconstitution. In 2 of 5 mice receiving CD19$^+$ PerC cells, serum IgM reached levels comparable to those in mice receiving unfractionated PerC [2455 (±958) μg/ml and 1038 (±727) μg/ml, respectively], but in the other 3 CD19$^+$ cell-injected mice, levels were 99% lower; IgM was undetectable in the serum of all CD19$^-$ cell recipients (Figure 24D). Similarly, numbers of IgM ASCs were not significantly different between mice injected

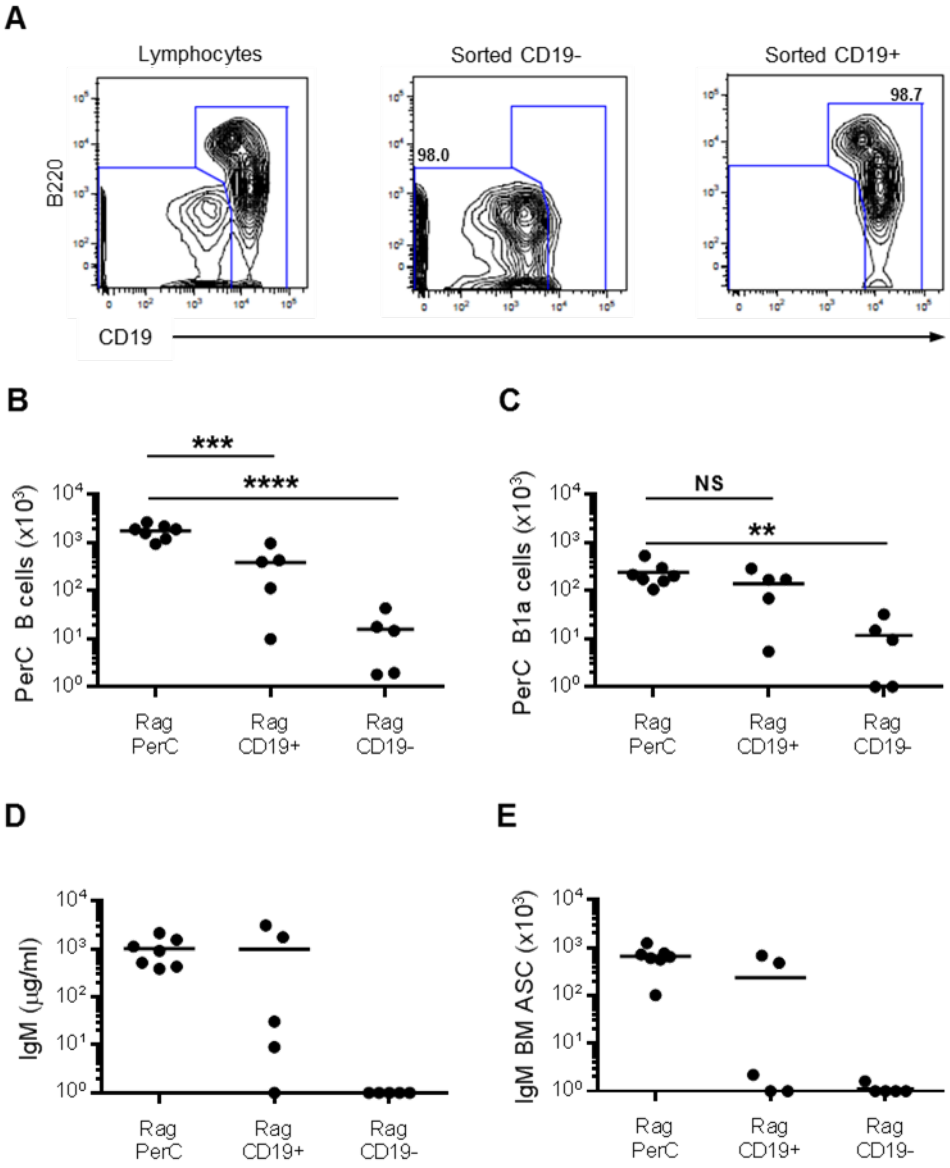

Figure 24: The precursor of nIgM PCs is CD19⁺

(Figure 24, continued) $5x10^5$ sorted $CD19^+$ or $CD19^-$ PerC cells from B6 mice were injected i.p. into $Rag1^{-/-}$ mice, which were then analyzed 10 weeks after transfer. (**A**) Representative flow plots of PerC lavage cells, pre-gated on single live leukocytes. (**B**) Number of PerC B cells (IgM^+) determined by flow cytometry. (**C**) Number of PerC B1a cells ($IgM^{hi}IgD^{lo}B220^{lo/-}CD11b^+CD23^-CD5^+$) determined by flow cytometry. (**D**) Serum IgM concentrations measured by ELISA. (**E**) Number of IgM ELISPOTs in the BM. Each symbol represents an individual mouse. Data represent three independent transfer experiments.

with total PerC cells and the 2 $CD19^+$ cell-recipient mice that recovered circulating IgM [65.4 (±36.8) x 10^4 vs. 58.2 (±14.5) x 10^4; p = 0.803], while IgM ASCs were essentially undetectable in the BM of the other 3 mice injected with $CD19^+$ PerC cells; IgM ASCs were undetectable or nearly so in the BM of all $CD19^-$ cell recipients (Figure 24E). These results indicate that the precursor of nIgM PCs is a $CD19^+$ cell. Moreover, they also confirm my previous finding that the presence of B1a cells does not correlate with nIgM PC numbers or serum IgM levels [194].

5.2.1.2 The precursor of nIgM PCs expresses CD5

PerC B cells can be divided by CD5 expression, with $CD5^+$ populations including B1a cells, and the $CD5^-$ compartments comprising B1b and B2. To determine whether the precursor of nIgM PCs expresses CD5, I injected 5x10^5 sorted PerC $CD19^+CD5^+$ or $CD19^+CD5^-$ cells i.p. into Rag1-deficient mice (Figure 25A). Both fractions were isolated to a purity of over 99%.

After 10 weeks, $CD19^+CD5^+$ cell-recipient mice and unfractionated PerC cell-recipient mice had indistinguishable numbers of IgM^+ PerC B cells (p = 0.101), whereas mice injected with $CD19^+CD5^-$ cells had 80% fewer (Figure 25B). In addition, the number of B1a cells in the PerC of $CD19^+CD5^+$ recipient mice was significantly higher than that in recipients of total PerC, whereas only 1 of 4 mice given $CD19^+CD5^-$ cells fully recovered B1a cell numbers (Figure 25C).

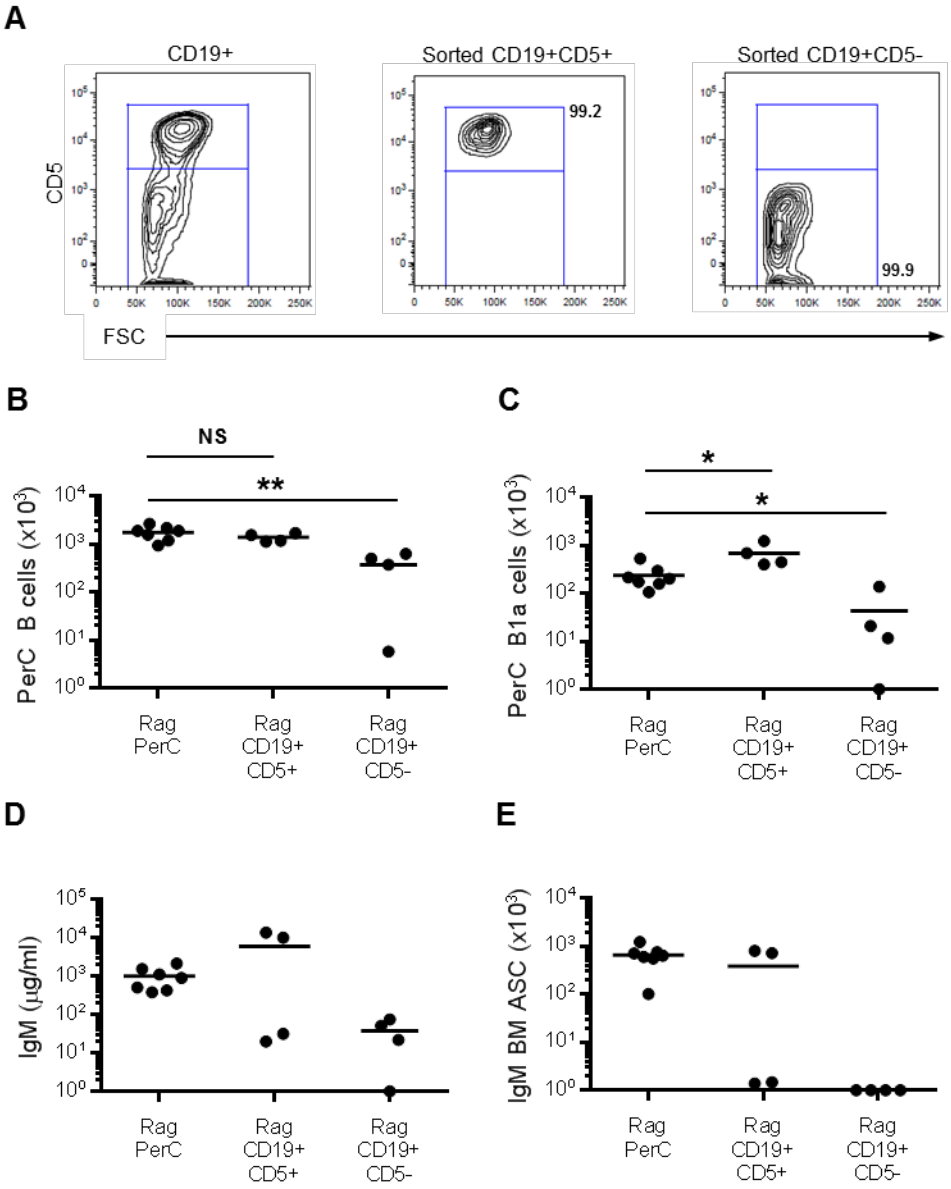

Figure 25: The precursor of nIgM PCs expresses CD5

(Figure 25, continued) $5x10^5$ sorted $CD19^+CD5^+$ or $CD19^+CD5^-$ PerC cells from B6 mice were injected i.p. into $Rag1^{-/-}$ mice, which were then analyzed 10 weeks after transfer. (**A**) Representative flow plots of PerC lavage cells, pre-gated on single live leukocytes. (**B**) Number of PerC B cells (IgM^+) determined by flow cytometry. (**C**) Number of PerC B1a cells ($IgM^{hi}IgD^{lo}B220^{lo/-}CD11b^+CD23^-CD5^+$) determined by flow cytometry. (**D**) Serum IgM concentrations measured by ELISA. (**E**) Number of IgM ELISPOTs in the BM. Each symbol represents an individual mouse. Data represent two independent transfer experiments.

Again, circulating IgM levels failed to correlate with B1a cell reconstitution. In 2 of 4 mice injected with $CD19^+CD5^+$ PerC cells, serum IgM levels were higher (12-fold) than those in mice receiving unfractionated PerC, but in the other two $CD19^+CD5^+$ cell-injected mice, levels were 97% lower; IgM was 96% lower in the serum of $CD19^+CD5^-$ cell recipients (Figure 25D). Consistent with these data, PerC cell-recipient mice and the 2 $CD19^+CD5^+$ cell-recipient mice with restored serum IgM had comparable numbers of BM IgM ASCs [65.4 (±36.8) x 10^4 vs. 77.7 (±6.0) x 10^4; p = 0.672], while IgM ASCs were nearly undetectable in the BM of the other 2 mice injected with $CD19^+CD5^+$ PerC cells; no IgM ASCs were detected in the BM of $CD19^+CD5^-$ cell recipients (Figure 25E). These data demonstrate that the $CD19^+$ precursor of nIgM PCs expresses $CD5^+$. They also further underscore my observation that the number of nIgM PCs is independent of the number of PerC B1a cells.

5.2.1.3 The $CD5^+CD11b^-$ PerC B-cell compartment comprises nIgM PC precursors

Although the precursor of nIgM PCs is contained within the $CD5^+$ PerC B-cell compartment, I previously found that purified B1a cells ($IgM^{hi}IgD^{lo}B220^{lo/-}CD11b^+CD23^-CD5^+$) do not reconstitute serum IgM (Figure 9). Nevertheless, the $CD5^+$ population is also known to contain B1a-like $CD11b^-$ cells that give rise to B1a cells [248, 249]. To determine whether the precursor of nIgM PCs expresses CD11b, I injected 5x10^5 sorted PerC $CD19^+CD5^+CD11b^+$ or $CD19^+CD5^+CD11b^-$ cells i.p. into Rag1-deficient mice (Figure

26A). The $CD19^+CD5^+CD11b^+$ fraction was isolated to a purity of over 98%, and $CD19^+CD5^+CD11b^-$ cells to over 80%.

Ten weeks later, IgM^+ B cell numbers in the PerC of mice injected with $CD19^+CD5^+CD11b^+$ cells, $CD19^+CD5^+CD11b^-$ cells, or total PerC cells were comparable (Figure 26B). The numbers of B1a cells in the PerC of both $CD19^+CD5^+CD11b^+$ and $CD19^+CD5^+CD11b^-$ cell-injected mice were higher even than those that had received unfractionated PerC cells (Figure 26C).

Consistent with my previous results, B1a cell recovery was not a predictor of serum IgM reconstitution. Circulating IgM concentrations in mice injected with $CD19^+CD5^+CD11b^+$ cells were 59-fold lower than in mice receiving unfractionated PerC, whereas in 1 of the 4 $CD19^+CD5^+CD11b^-$ cell-injected mice, levels were comparable to total PerC cell-recipients; the other three $CD19^+CD5^+CD11b^-$ cell recipients had 98% lower IgM levels (Figure 26D). In concert, $CD19^+CD5^+CD11b^+$ cell-recipient mice had 99.7% lower numbers of BM IgM ASCs than unfractionated PerC cell recipients, but 1 of the 4 mice injected with $CD19^+CD5^+CD11b^-$ cells had a fully recovered BM IgM ASC population, and the other 99% fewer (Figure 26E). From these results, I conclude that the precursor of nIgM PCs is in the $CD11b^-$ compartment.

5.2.1.4 Antibody-labeled and unlabeled PerC cells reconstitute nIgM with equal efficiency

Not all mice injected with a given fraction of PerC cells recovered serum IgM and BM IgM ASCs, despite consistent reconstitution of PerC B cells. To determine if Ab

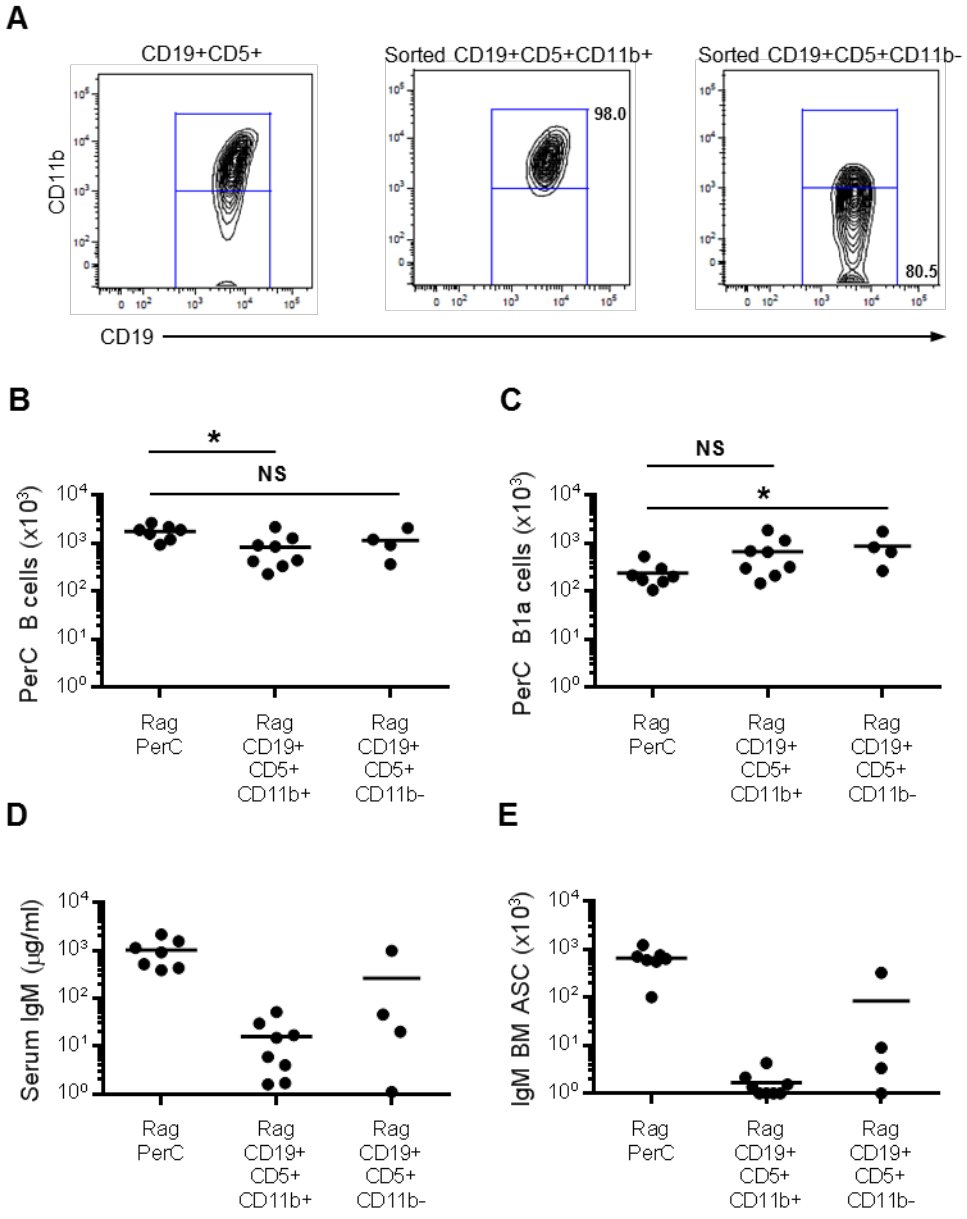

Figure 26: The CD5⁺CD11b⁻ PerC B-cell compartment comprises nIgM PC precursors

(Figure 26, continued) $5x10^5$ sorted $CD19^+CD5^+CD11b^+$ or $CD19^+CD5^+CD11b^-$ PerC cells from B6 mice were injected i.p. into $Rag1^{-/-}$ mice, which were then analyzed 10 weeks after transfer. (**A**) Representative flow plots of PerC lavage cells, pre-gated on single live leukocytes. (**B**) Number of PerC B cells (IgM^+) determined by flow cytometry. (**C**) Number of PerC B1a cells ($IgM^{hi}IgD^{lo}B220^{lo/-}CD11b^+CD23^-CD5^+$) determined by flow cytometry. (**D**) Serum IgM concentrations measured by ELISA. (**E**) Number of IgM ELISPOTs in the BM. Each symbol represents an individual mouse. Data represent four independent transfer experiments.

labeling of cells for FACS diminished the reconstitution potential of sorted populations, I transferred i.p. into Rag1-deficient mice 10^6 total PerC cells that were left unlabeled or were labeled with the identical panel of antibodies used in the preceding sort experiments.

10 weeks later, the level of IgM was not significantly different in the serum of mice injected with unlabeled or labeled cells, with 3 out of 4 unlabeled-cell recipients and 2 out of 3 labeled-cell recipients completely recovering serum IgM (Figure 27A). Corresponding IgM ASC numbers in the BM were also comparable between the two groups, with the same 3 out of 4 unlabeled-cell recipients and 2 out of 3 labeled-cell recipients accumulating more BM IgM ASCs than B6 controls (Figure 27B).

5.2.2 Titration of transferred PerC cells

My transfer experiments suggested that the precursor of nIgM PCs is rare, since the inconsistent recovery of serum IgM and nIgM PCs in mice given precursor-containing sorted cell populations was not due to negative functional modulation by labeling antibodies. I injected, therefore, decreasing numbers of unfractionated PerC cells i.p. into Rag1-deficient mice in order to deduce the number of precursor cells through limiting dilution [250].

Within 4 weeks, the levels of serum IgM in mice injected with either $3x10^6$ or $1x10^6$ PerC cells were comparable to those in normal B6 mice [434 (±88) μg/ml, 270 (±234) μg/ml, and 347 (±270) μg/ml, respectively] (Figure 28). In sharp contrast, mice receiving

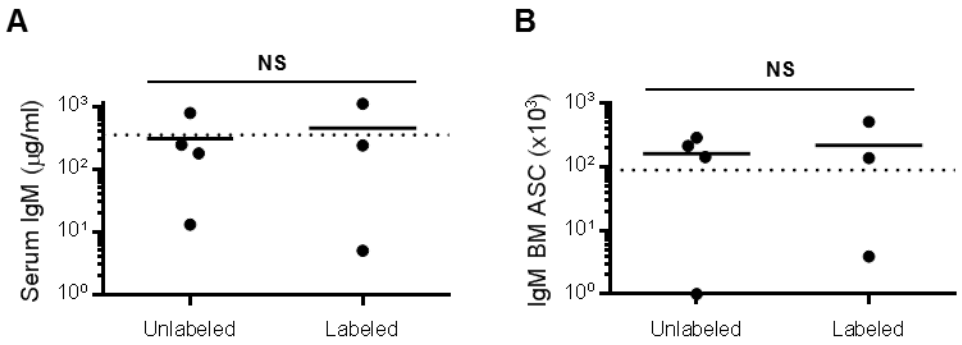

Figure 27: Antibody labeling of PerC cells does not affect their capacity to reconstitute nIgM in Rag1$^{-/-}$ mice

PerC cells from B6 mice were labeled with the same antibodies used in Figures 25-27, or left unlabeled and injected i.p. into Rag1$^{-/-}$ mice. Recipient mice were then analyzed 10 weeks after transfer. (**A**) Serum IgM concentrations measured by ELISA. (**B**) Number of IgM ELISPOTs in the BM. Each symbol represents an individual mouse, from one transfer experiment.

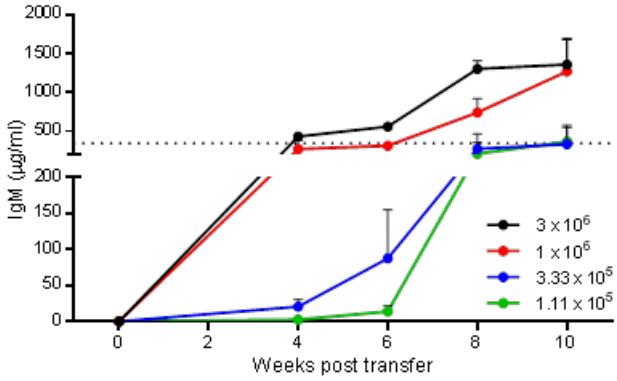

Figure 28: Transfer of decreasing numbers of unfractionated PerC cells into Rag1$^{-/-}$ mice

3-fold dilutions of 3 x 10^6 unfractionated PerC cells pooled from several B6 mice were injected i.p. into Rag1$^{-/-}$ mice. Shown are serum IgM concentrations 4, 6, 8, and 10 weeks after transfer. Dotted line indicates serum IgM level in normal B6 mice. Data represent four to six recipient mice of each transfer cell number from two independent experiments, and show mean ± SEM.

$3x10^5$ or $1x10^5$ PerC cells had 94% and 99% lower concentrations of serum IgM. After 6 weeks, serum IgM levels in recipients of $3x10^6$ or $1x10^6$ PerC cells remained near the B6 level, while those in $3x10^5$ cell-injected mice rose to 25% of B6, and to 4% in $1x10^5$ cell recipients. By week 8, all mice (except 1 of 6 recipients of $1x10^5$ cells) had circulating IgM levels comparable to or above B6 levels, and these levels were maintained or elevated after 10 weeks. These results show a dramatic shift in the rate, but not occurrence, of serum IgM reconstitution between stochastically sampled pools of 10^6 and $3x10^5$ PerC cells, indicating that cell-cell interaction between rare cells is required for nIgM PC formation.

5.2.3 Neonatal liver transfer

In chapter 3, I showed that nIgM PCs appear to differentiate from fetal-lineage B cells based on their V_H-gene usage and characteristics, and absence in B1-8i mice, a fetal B-cell non-permissive HC knockin strain (Figures 10 and 11). To determine if early B cells indeed supply nIgM PCs, I transferred $3x10^6$ total NL cells i.p. into Rag1-deficient hosts, as before.

Ten weeks following transfer, both B1a and $CD5^+CD11b^-$ B1 cell numbers were fully restored in NL recipients (Figure 29A). In contrast, numbers of B1b and B2 cells in the PerC of transfer recipients were significantly lower than those observed in B6 controls (57% and 79%, respectively). NL transfer also failed to reconstitute splenic MF and MZ B cells (Figure 29B). These results are in agreement with data showing that B1a

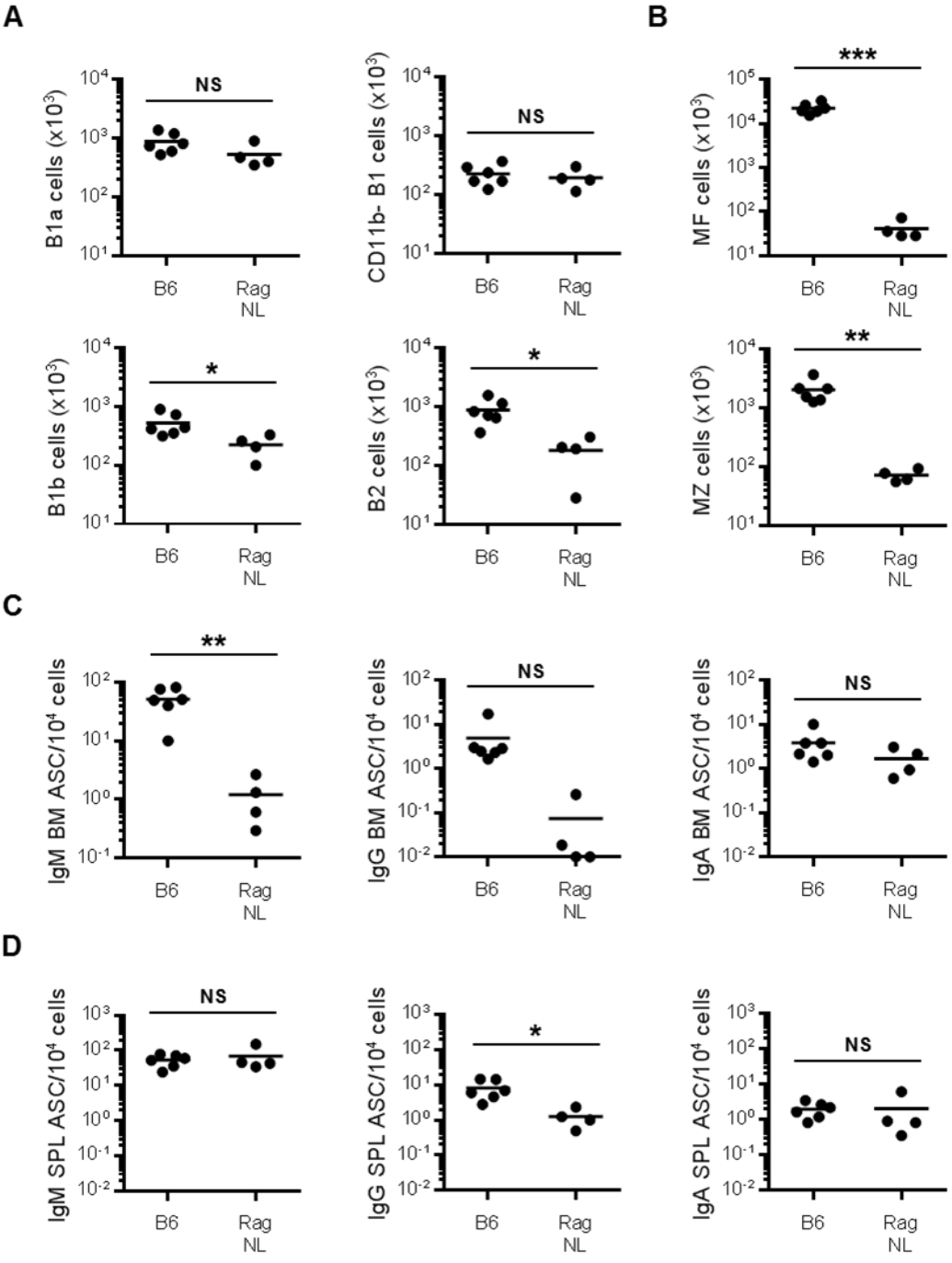

Figure 29: Transfer of NL i.p. fails to restore nIgM PCs in adult Rag1$^{-/-}$ mice

(Figure 29, continued) $3x10^6$ total liver cells from neonatal B6 mice were injected i.p. into $Rag1^{-/-}$ mice, which were then analyzed 10 weeks after transfer. (**A**) Number of B1a, $CD11b^-$ B1, B1b, and B2 cells in the PerC, determined by flow cytometry. (**B**) Number of MF and MZ B cells in the spleen determined by flow cytometry. (**C**) Frequency of IgM, IgG, and IgA ELISPOTs in the BM. (**D**) Frequency of IgM, IgG, and IgA ELISPOTs in the spleen. Each symbol represents an individual mouse from one transfer experiment.

cells are preferentially produced by fetal and neonatal liver, and suggest that i.p. transfer may inhibit B2 cell recovery, which normally occurs following i.v. infusion of NL cells [251, 252].

Despite the restoration of $CD5^{+}CD11b^{-}$ B1 cells in the PerC, NL recipients did not recover IgM ASCs in the BM (Figure 29C). Consistent with the presence of PerC B1a cells, but not PerC B2 or splenic MF B cells, IgG ASCs also failed to accumulate in the BM of NL recipient mice, while BM IgA ASCs reached numbers similar to those in B6 mice. Activated B1a cells undergoing class-switch preferentially switch to IgA, and give rise to IgA-producing cells [253, 254]. Furthermore, IgM and IgA ASC numbers were fully restored in the spleens of NL recipients, while IgG ASCs remained significantly lower than controls (Figure 29D). Collectively, these results suggest that removal from the fetal/neonatal liver environment alters the function of $CD5^{+}CD11b^{-}$ B1 cells but not B1a cells, leading to a lack of nIgM-PC differentiation in the adult PerC.

5.2.4 The role of cKit in the development of nIgM PC precursors

In light of my observation that nIgM PC precursors are defective in Sash mice, which as previously described carry an inversion mutation in the transcriptional regulatory elements upstream of the cKit gene, I compared the number of B1 cells in the PerC of Sash mice and B6 controls. Even though cKit signaling is not thought to be required for the development of fetal or BM B cells, I observed a reduction in the number of B1a (49%), $CD11b^{-}$ B1 (50%), and B1b (52%) cells in the PerC of Sash mice

(Figure 30A) [239, 244]. In contrast, PerC B2 cell numbers were dramatically elevated (370%) compared to B6 controls (Figure 30A).

To determine if the reduced number of B1 cells and their limited capacity to form nIgM PCs (Figure 21) was due to an altered Ig repertoire, I sorted B2, B1a, B1b, and CD11b$^-$ B1 cells from the PerC of B6 and Sash mice, and measured the ratio of V_H11 to V_H1 transcript levels, as before. I was unable to calculate the V_H11/V_H1 ratio in PerC B2 cells from B6 mice because V_H11 transcript levels were undetectable; however, the ratio in Sash B2 cells was low (1.8×10^{-3}) (Figure 30B), similar to that previously detected in class-switched BM PCs from B6 mice (6.1×10^{-3}) (Figure 12). The ratios of V_H11/V_H1 transcripts in the three B1 cell subsets were much higher, particularly in B1a and CD11b$^-$ B1 cells, with even higher levels detected in cells isolated from Sash mice (Figure 30B). These data indicate that the formation of the fetal B-cell repertoire is intact in Sash mice.

I next compared cKit density on the surface of B cells in the adult BM and FL from Sash and B6 mice. As expected, Lin$^-$Sca-1$^+$cKit$^+$ (LSK) cells, common myeloid progenitors (CMP), and MC precursors (MCp) expressed high levels of cKit, which dropped in the equivalent compartments in Sash mice by 17%, 37%, and 49%, respectively (Figure 31A). Developing B cells in adult BM from both strains, from pre-pro to immature, carried levels of cKit comparable to transitional and mature B cells, which do not express cKit (Figure 31A) [72]. In contrast, CD19$^+$ cells in embryonic day (E) 15.5 FL expressed substantial levels of cKit, approximately

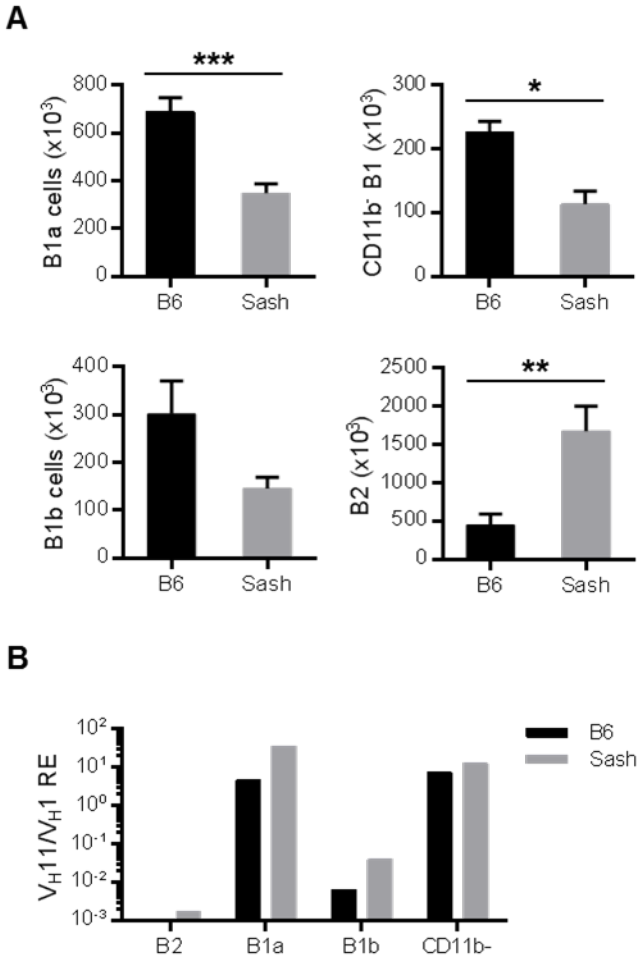

Figure 30: Analysis of B cells in the PerC of Sash mice

(**A**) Number of B1a, CD11b$^-$ B1, B1b, and B2 cells in the PerC of Sash mice, determined by flow cytometry. Data represent a total of six mice of each genotype, and show mean ± SEM. (**B**) Ratio of V_H11 to V_H1 expression relative to Igβ in sorted PerC B cell subsets, measured by quantitative real-time PCR. RE, relative expression.

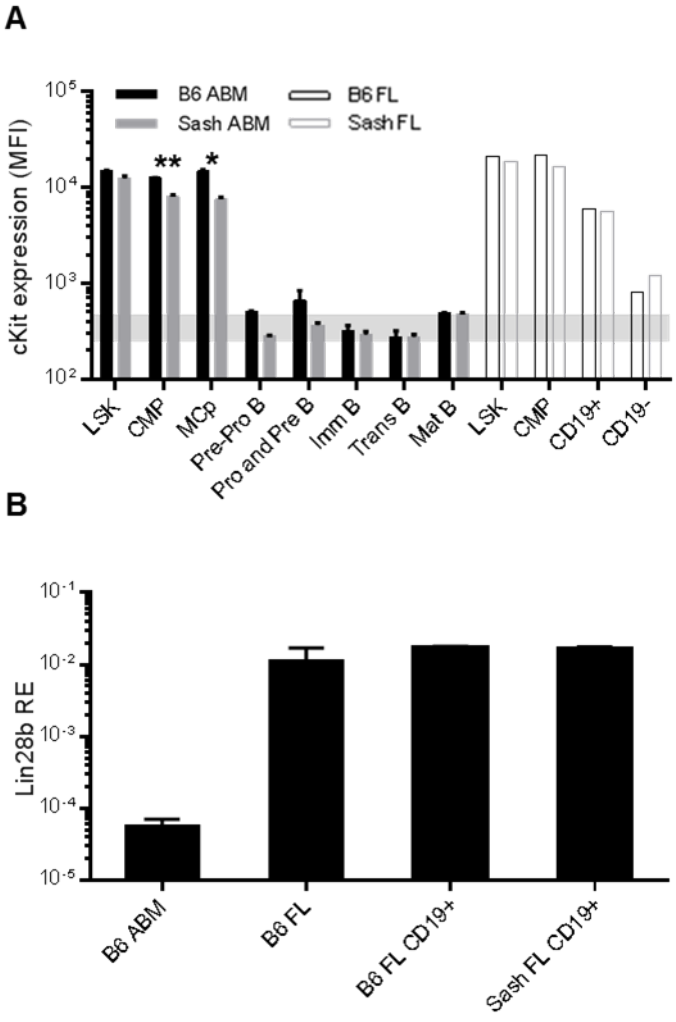

Figure 31: cKit and Lin28b expression by Sash B cells is unchanged

Adult BM (ABM) or E15.5 fetal liver (FL) cells from B6 and Sash mice were analyzed (**A**) by flow cytometry for cKit expression and (**B**) by quantitative PCR for Lin28b expression. LSK, $Lin^{-}Sca\text{-}1^{+}cKit^{+}$; CMP, common myeloid progenitor; MCp, mast cell progenitor. Data represent one or two experiments, and show mean ± SEM.

30% of that detected on FL LSK cells, while $CD19^-$ cells expressed levels much lower at less 4% (Figure 31A). I reasoned, therefore, that cKit expression may be required for proper development during fetal B-cell lymphopoiesis. Nevertheless, LSK, $CD19^+$, and $CD19^-$ cells from Sash FL expressed comparable levels of cKit to their B6 counterparts.

Though cKit levels were unchanged between B6 and Sash FL B cells, I compared transcript levels of the fetal lineage lymphocyte-determining factor Lin28b in cells from each strain [255]. As expected, Lin28b expression levels were more than 200-fold higher in FL than adult BM cells, and were similarly high in purified $CD19^+$ FL cells (Figure 31B). The relative amount of Lin28b transcript detected in $CD19^+$ cells from Sash FL was nearly identical to that in B6 controls. Thus, cKit is expressed on fetal B cells, and not dysregulated in Sash fetal liver. It is possible, however, that a loss of cKit may be observed at a later timepoint, such as in neonates, as MCs disappear from the skin of Sash pups most dramatically following birth [256].

6. Discussion and conclusion

Extensive investigation has revealed the vital role of nIgM in blocking infection as well as reducing the risk of autoimmunity. Nevertheless, the cells that supply the body with constitutive high titers of nIgM had not yet been identified. Prior to my work, the only widely accepted model linked nIgM with the B1 lineage. Within this broad categorization, various $CD5^+$ B1-cell populations were claimed as the source of nIgM, but a lack of rigorous experimentation and convincing evidence prevented consensus in the field. The source of nIgM, therefore, remained uncertain, and thus unstudied.

6.1 The source of nIgM

In the late 1980s, Bos *et al.* found that constitutive IgM ASCs exist in both the spleen and BM [17]. More recently, B1a cells within these organs were specifically shown to produce IgM [189-191]. Holodick and colleagues carefully described a population of IgM-secreting B1a cells in the spleen, and reasoned that splenic B1a cells must be the source of essentially all serum nIgM based on the following three premises: nIgM is linked with B1a cells, B1a cells exist only in PerC and spleen, and PerC B1a cells do not contribute to serum IgM [189]. Though this seems rational, the assumption that undifferentiated B1a cells are the immediate source of nIgM has never been demonstrated, but instead inferred from transfer experiments linking recovery of $CD5^+$ B1 cells to serum IgM [109, 180-182]. Moreover, the authors failed to determine if B1a cells make up the majority of splenic IgM ASCs, or even if splenic IgM ASCs constitute

most IgM ASCs in the body. Choi *et al.* used similar reasoning when they claimed that a novel population of B1a cells in the BM produces the majority of nIgM. It can be inferred from their data, however, that less than 1% of BM B1a cells secrete IgM, and that B1a cells make up no more than 5% of all IgM ASCs in the BM, thus discrediting their conclusion [191]. It is, therefore, extremely improbable that this compartment makes a substantial contribution to circulating nIgM titers.

By examining cells isolated from various tissues in ELISPOT assay, I found that 80% of IgM ASCs in naïve mice reside in the BM (Figure 7). ASCs contain large amounts of cytoplasmic Ig, so I used intracellular IgM staining to mark IgM ASCs by flow cytometry. cIgM^{hi} cells exhibited a CD138^{+}IgD^{-}IgM^{+}B220$^{lo/-}$FSC^{hi}CD5^{-} phenotype, consistent with differentiated PBs (B220^{lo}) and PCs (B220^{-}), but not B1a cells (Figures 7 and 8). BrdU uptake experiments confirmed that B220^{lo} cells are blasts, whereas their B220^{-} counterparts are quiescent and long-lived (Figure 13). Importantly, all IgM ASCs in the BM are CD138^{+}IgD^{-}IgM^{+}B220$^{lo/-}$FSC^{hi}CD5^{-} (Figure 7). I conclude that serum nIgM is maintained not by undifferentiated B1a cells in the spleen, but by LLPCs in the BM.

Though the mechanism by which nIgM titers are sustained quite reasonably mirrors that by which class-switched, Ag-specific Ab titers are preserved following infection or vaccination, it runs contrary to the paradigm that IgM ASCs are short-lived. Only ASCs that emerge from the GC in response to TD Ags are thought to become LLPCs, whereas those formed against TI Ags or early in TD reactions are short-lived and

do not provide long-term protection [118, 122, 162]. Nevertheless, recent evidence indicates that long-lived IgM ASCs can be generated following bacterial infection or immunization with TI polysaccharide Ag [257, 258]. I also find that nIgM titers remain intact in the absence of CD154, or even without T cells at all (Table 2; Figures 12 and 16). In light of the new model that appears to be emerging in which LLPCs are the source of long-term Ab of divergent origins, it is unsurprising that constitutive nIgM is also supplied by LLPCs.

nIgM is present even in germ-free mice; therefore, the signal that induces differentiation of nIgM PCs is likely of self-origin [18]. Such a mechanism is also predicted by the repertoire of nIgM, which exhibits low-level reactivity against endogenous ligands, primarily those found on apoptotic debris and senescent red blood cells [259]. These self-binding specificities incidentally mediate protection against infection, as they cross-react with similar epitopes on microorganisms; for example, anti-PC nIgM binds to apoptotic cells as well as the Gram-positive bacterium *streptococcus pneumoniae*, which displays cell wall carbohydrate-associated PC groups [198]. Consequently, it can be imagined that the differentiation of nIgM-producing cells is continuously induced by ubiquitous target Ag in the form of dead and dying cells, thereby generating a constant supply of Ab that both maintains tissue homeostasis and protects against infection.

6.2 Formation of nIgM PCs

My data show that B1a cells themselves do not supply serum nIgM (Figures 7 and 8). However, this result alone did not rule out the possibility that B1a cells in the PerC differentiate into PCs and migrate to the BM. Indeed, transfer studies have linked serum IgM with PerC B cells, specifically $CD5^+$ B1 cells [109, 180-182]. I performed, therefore, transfers of cells from B6 mice into Rag1-deficient recipients to identify the precursors of nIgM PCs. Transfer of B1-containing PerC, but not B1-deficient LN, fully reconstituted $CD5^+$ B1 cells, BM nIgM PCs, and serum nIgM, indicating that cells of the B1 lineage are upstream of nIgM PCs (Table 1; Figure 9) [110]. However, transfer of any of the three major PerC B-cell populations (B1a, B1b, or B2) did not restore nIgM (Figure 9). I transferred, therefore, PerC cells fractionated according to the B-cell subset markers CD19, CD5, and CD11b, and found that only the $CD19^+CD5^+CD11b^-$ compartment contained precursors of nIgM PCs (Figures 24-26). V_H-gene sequence analysis revealed that nIgM PCs in the BM carry Ig-genes typical of fetal-derived B cells, consistent with the loss of nIgM PCs in B1-deficient B1-8i knockin mice (Figures 10 and 11). As both B1a and B1b subsets are characterized by CD11b expression, I conclude that a distinct fetal B1 population generates nIgM PCs.

Previous studies transferred unfractionated PerC or sorted $CD5^+$ PerC cells, and thus overlooked the functional distinction between $CD11b^+$ and $CD11b^-$ subsets. My results are nevertheless consistent with studies showing that PerC cells preferentially

reconstitute $CD5^+$ B cells in recipient mice, concomitant with serum IgM restoration [25, 31, 109, 181, 201]. I also confirm the observations of Lalor *et al.*, who found that transfer of $CD5^+$ but not $CD5^-$ PerC cells restored serum IgM in B cell-depleted recipients [180].

$CD11b^-CD5^+$ PerC B cells have been characterized in only two publications prior to my work. Identified in 2006 by the Rothstein laboratory, the $CD11b^-$ subset exhibited V_H-gene usage similar to PerC B1a cells, which are by definition $CD11b^+$ [248]. The Herzenbergs later demonstrated that $CD11b^-CD5^+$ PerC B cells give rise to B1a cells following transfer [249]. I also observed PerC B1a cell recovery in mice injected with $CD11b^-$ B1 cells, and thus conclude that the $CD11b^-$ PerC B1-cell compartment comprises the precursors of both B1a cells and nIgM PCs (Figure 26). Though CD11b is considered a marker of PerC B1a cells, $CD11b^-CD5^+$ B cells in the spleen are confusingly called "splenic B1a" cells. These cells may also represent nIgM PC precursors, as transfer of spleen cells into SCID mice restores serum IgM [260]. In either case, my work attributes a distinct functional role to $CD11b^-$ PerC B1 cells for the first time, beyond their identification as an earlier developmental stage of B1a cells [249].

B cells accumulated in the PerC of every mouse (but one) injected with isolated $CD19^+$, $CD19^+CD5^+$, or $CD19^+CD5^+CD11b^-$ cells; nevertheless, nIgM PCs recovered in only some of these recipients, suggesting that cells with the capacity to become nIgM PCs are rare even within the $CD11b^-CD5^+$ compartment (Figures 24-26). The dramatic drop in the rate, but not occurrence, of nIgM reconstitution between mice injected with

10^6 and $3x10^5$ total PerC cells indicates that interaction between two functionally distinct subsets of $CD11b^-CD5^+$ B cells is likely required for the differentiation of nIgM PCs to occur (Figure 28). I propose two possible models. In the first, a rare subset produces nIgM PCs only in the presence of the other more abundant subset, which also gives rise to B1a cells. In the second, the abundant subset gives rise to B1a cells, which then differentiate into nIgM PCs only in the presence of the rare $CD11b^-$ subset. My data do not distinguish between these two possibilities.

Transfer of NL cells into the PerC of $Rag1^{-/-}$ mice failed to reconstitute nIgM PCs, even though the usage and characteristics of V_H-genes sequenced from nIgM PCs are consistent with a fetal origin, and nIgM PCs were missing in mice carrying a HC knockin that is non-permissive for fetal-lineage B-cell development (Figures 10, 11, and 29). In contrast, B1a cell numbers were fully restored in all recipients, in agreement with previous studies showing preferential reconstitution of $CD5^+$ B1 cells in mice injected with fetal or NL cells (Figure 29) [251, 252]. Indeed, B1a cells cannot be formed by adult BM [261]. I reason that by removing B1 precursors from the early hematopoietic microenvironment and placing them in an adult peripheral tissue, they are deprived of signals that are required for the proper functional development of nIgM PC precursors. B1a cells, however, appeared to develop normally, as they were able to form IgM and IgA ASCs in the spleen, and IgA ASCs in the BM (Figure 29).

Collectively, my data strongly dissociate the presence of ($CD11b^{+}CD5^{+}$) B1a cells from serum nIgM, and suggest a functional division of B1 cell subsets wherein B1a cells are poised to rapidly respond to environmental Ags, and a distinct population either gives rise to or induces the differentiation of nIgM PCs [184]. Thus, nIgM PCs produce constitutive high levels of serum nIgM, which acts as a pre-existing barrier against infection, and continuously opsonizes dead cells. On the other hand, B1a cells respond non-specifically to TI Ags and pathogen-associated molecular patterns (PAMPs), leading to a transient protective burst of spleen-derived IgM that mirrors the natural repertoire [111]. Indeed, injection of mice with LPS induces the formation of IgM ASCs in the spleen, some of which react with ChoP [202]. Furthermore, Choi and colleagues observed that only about 5% of IgM produced by B1a cells in response to influenza immunization actually binds influenza Ags [182]. The ease with which B1 cells differentiate into ASCs is likely a consequence of elevated Blimp-1 levels [185].

I found that nIgM PCs are characterized by a lack of CD5 expression, a molecule which defines nIgM PC precursors (Figure 8). Why downregulation of CD5 occurs during nIgM-PC differentiation is an intriguing question, and may be related to the continued expression of surface Ig on nIgM PCs, which is normally downregulated on class-switched PCs [143]. CD5 is a negative regulator of Ag-receptor signaling on both B cells and T cells through recruitment of the phosphatase Src homology 2 domain-containing phosphatase 1 (SHP-1), which dephosphorylates Ag-receptor signaling

components [262, 263]. It is thus thought that CD5 functions by thwarting the incessant activation of autoreactive B1 cells, which could lead to the generation of high-affinity autoAb-forming cells. Indeed, B1 cells do not proliferate in response to BCR ligation by anti-IgM Ab when CD5 is present, although they can be activated by LPS [263]. Perhaps the removal of CD5 from the surface of nIgM PCs allows pro-survival signaling through the BCR to occur by engagement of apoptotic developing lymphocytes, which are continuously formed in the BM but rapidly eliminated by macrophages and stromal cells [264].

The reduced number and function of B1 cells in Sash mice indicates that cKit plays a crucial role in fetal B-cell development (Figure 30). As the B1 cells that remain in the PerC of adult Sash mice exhibit an undisturbed V_H-gene repertoire, and yet have a severely reduced capacity to differentiate into nIgM PCs, it is likely that cKit signaling during fetal B-cell development endows B1 cells with this function (Figures 21 and 30). Indeed, cKit is not expressed on developing B cells in the adult BM, but is present at high densities on fetal B cells (Figure 31). cKit signals through, among other pathways, the MEK/ERK cascade, which positively regulates expression of the fetal lymphocyte-forming factor Lin28b [265, 266]. Though I did not observe a difference in the level of cKit on E15.5 fetal liver B cells from B6 and Sash mice, or altered expression of Lin28b, it is possible that the regulatory element mutated in Sash mice is not required to properly express cKit in B cells until near birth, as MC numbers in Sash mice decline with such

timing (Figure 31) [256]. In opposition to this hypothesis, transfer of WT fetal liver cells and those lacking surface expression of cKit formed equal numbers of $CD5^+$ B cells in the PerC of irradiated Rag2-deficient recipients [244]. Nevertheless, serum IgM levels were not measured in these experiments, and thus the functionality of the restored B1 cells was not determined.

6.3 Survival of nIgM PCs

Long-lived IgG PCs require external survival signals for their persistence [162, 171]. Thus, my observation that nIgM PCs are long-lived *in vivo*, but die rapidly upon isolation, prompted me to investigate the factors that mediate their long-term preservation (Figures 13 and 15). Not only were eosinophils, the main source of IgG PC survival signals, irrelevant for nIgM PC maintenance, but the potent IgG PC survival factor IL-6 also failed to contribute to nIgM PC survival (Figures 14 and 15). I hypothesized, therefore, that both the molecular and cellular components of the nIgM PC survival niche were unique, and indeed found that IL-5 significantly enhanced the recovery of nIgM PCs following isolation and culture, but had little effect on the recovery of IgG PCs (Figure 15). Whereas none of the three primary sources of IL-5 - T cells, ILC2s, and MCs – were responsible for maintaining nIgM PCs in the BM, I determined that BM stromal cells produce IL-5 and anchor nIgM PCs (Figures 16-22) [267]. Under stimulatory conditions, I found that Ad BM cells enhance the survival of nIgM PCs in culture (Figure 22). My work demonstrates for the first time that different

types of LLPCs reside in distinct survival niches, and along with my data showing that the frequency of $BrdU^+$ PCs ($B220^-$) increases at a slow but steady rate, suggest a model wherein constitutive nIgM titers are maintained in the serum by LLPCs that survive in the BM and are gradually replaced by newly generated PBs, as niche space becomes available.

The first hint that different populations of BM PCs reside in different niches came in 2010 with data showing that while a substantial fraction of IgG and IgA PCs co-localized with megakaryocytes, very few IgM PCs did so; accordingly, depletion of megakaryocytes had no effect on serum IgM levels, though IgA titers dropped significantly [178]. Following this study, Winter *et al.* proposed a model for niche-specialization in which stromal cells anchor PCs within the BM, and serve as a scaffold around which distinct supporting cells then gather to provide appropriate survival signals [268]. It was, however, possible that the IgM PCs they observed in the BM were short-lived and continually replaced by newly differentiated PBs, or that they had an intrinsic capacity to survive long-term. My work demonstrates for the first time that IgM PCs in the BM of naïve mice are long-lived cells that require external signals to persist, and that these signals are distinct from those described for IgG PCs.

That IL-5 serves as a strong promoter of nIgM PC survival is not surprising. IL-5 signaling upregulates expression of the anti-apoptotic molecule Mcl-1, and is crucial for the survival, self-renewal, and activation of B1 cells [221, 269]. Indeed, IL-5Rα knockouts

exhibit a 50% decline in circulating IgM, and injection of recombinant IL-5 boosts serum IgM levels 4-fold [221, 242]. Similarly, IL-6, which promotes the survival of both mouse and human IgG PCs, was originally called "B cell stimulating factor 2" for its role in enhancing the terminal differentiation of B2 cells and the transcription of Ig genes [171, 270-272]. Enforced expression of high levels of IL-6 in mice carrying IL-6 transgenes leads to IgG plasmacytosis, with IgG PC infiltration in numerous organs and over a 100-fold increase in circulating IgG (but not IgM) [224]. Thus, my studies have revealed a common theme in LLPC biology, wherein factors that promote the differentiation of a given PC subtype also support those PCs long-term.

The source of IL-5 in naïve mice was unlikely to be hematopoietic, as T cells, ILC2s, and MCs generally produce high levels of IL-5 only when activated, not at rest [230, 273, 274]. My results confirmed this notion, and instead support the role of stromal cells in both retaining and supporting nIgM PCs in the BM (Figure 22). Stromal cells and the matrix they generate form the structure of the BM, and provide a scaffold to spatially organize closely packed hematopoietic populations [275, 276]. Furthermore, stromal cells form distinct niches that support different stages and types of cells; for example, developing B cells rely on IL-7-producing stromal cells, whereas IgG PCs are supported by IL-6 and APRIL produced by an independent set of stromal cells and hematopoietic cells [172, 174, 268, 277]. My data confirm a report that BM stromal cells also make IL-5 (Figure 22) [245]. The correlation I observed between IL-5 levels in B6 and Rag1$^{-/-}$ stromal

cells and the size of the nIgM PC niche in the BM of these strains is particularly compelling (Figures 9 and 22).

As mentioned above, it is tempting to speculate that local apoptotic debris may serve as an additional survival signal through the BCR on nIgM PCs, as nIgM PCs retain surface IgM expression while eliminating CD5, and stromal cells are known scavengers of apoptotic material [264]. Moreover, the LPS-induced *in vitro* support of nIgM PCs by stromal cells may reflect an *in vivo* role for damage-associated molecular patterns (DAMPs) in enhancing the production of survival factors by stromal cells (Figure 22). Indeed, hematopoiesis in the BM can be influenced by PRR stimulation, and endogenous ligands have been found to trigger signaling through several PRRs called toll-like receptors (TLRs), including TLR4, the sensor of LPS [278, 279]. In support of this model, I found that mice lacking the TLR signaling molecule MyD88 have a two-fold reduction in serum IgM levels (Figure 22). Furthermore, IgG PC survival niches are also known to form in inflamed peripheral tissues [162].

In vivo neutralization of IL-5 failed to deplete nIgM PCs from the BM, supporting the notion that multiple redundant survival signals together preserve constitutive nIgM production (Figure 23). Such a system also hedges high-affinity, IgG humoral memory by preventing the IgG LLPCs that are generated during infection or vaccination from dying due to a temporary absence of one survival signal or niche cell, or an inherent deficiency in one of the factors in certain individuals [268]. The redundancy of LLPC

niche components has implications for the clinic, as for example in anti-IL-5 therapy, which is being tested as a treatment for asthmatic patients and those with hypereosinophilic syndrome [267]. On the other hand, cocktails of therapeutic agents might be used to selectively eliminate LLPC compartments, either those producing high-affinity, class-switched autoAbs, or in the case of xenotransplantation, nIgM-producing cells.

6.4 Concluding remarks

My work brings clarity to the study of nIgM, and provides a new framework by which to understand B1 cell biology (Figure 32). In contrast to the former model, wherein B1a cells produce both nIgM and "immune" IgM, I have demonstrated a functional division between $CD5^+$ B1 cell subsets. I have also established that nIgM is not produced by undifferentiated B1 cells, but by LLPCs in the BM. Finally, I show for the first time that distinct LLPC subsets in the BM reside in unique, specialized survival niches. My studies will guide the future direction of the field, and inform the development of therapeutic interventions such as those for humoral immunodeficiencies, autoimmune diseases, and PC malignancies.

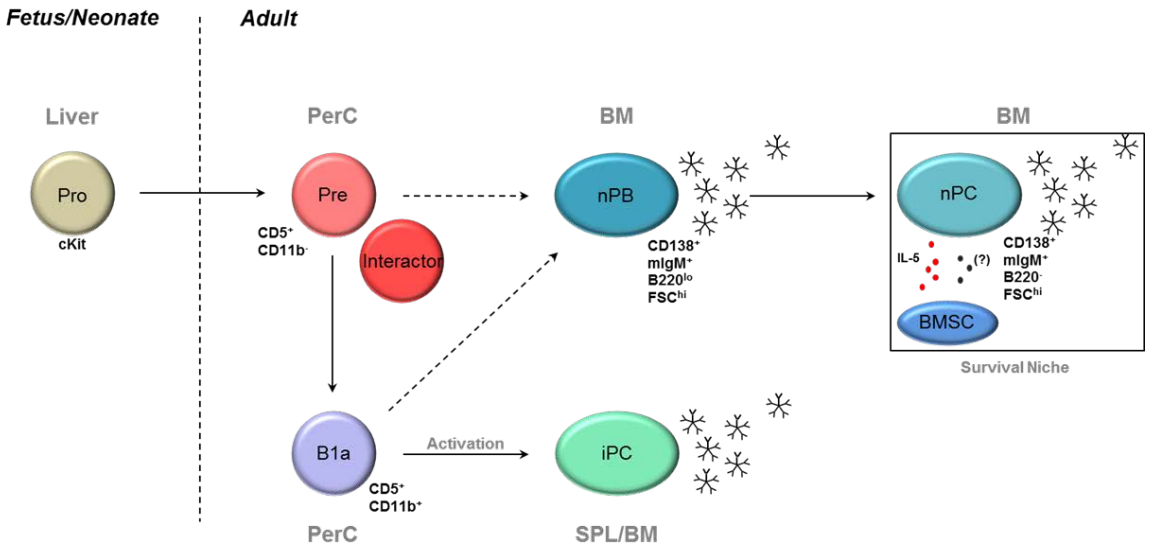

Figure 32: Model for the origin of natural antibody

Progenitors in the fetal/neonatal liver develop into $CD5^{+}CD11b^{-}$ precursor B cells, and in a cKit-dependent manner, $CD5^{+}CD11b^{-}$ interactor B cells in the PerC of the adult. $CD5^{+}CD11b^{-}$ precursor B cells give rise to $CD5^{+}CD11b^{+}$ B1a cells, which upon activation by exogenous stimuli differentiate into immune IgM-secreting PCs (iPCs) in the spleen and BM. $CD5^{+}CD11b^{-}$ interactor B cells induce $CD5^{+}CD11b^{-}$ precursors and/or B1a cells to differentiate into $CD138^{+}mIgM^{+}B220^{lo}FSC^{hi}$ nIgM PBs (nPB) in the BM. nPBs in turn maintain a full $CD138^{+}mIgM^{+}B220^{-}FSC^{hi}$ nIgM PC (nPC) population, which persists long-term in a niche comprising BM stromal cells (BMSC) that produce IL-5 (red circles) and other factors (black circles; ?).

References

1. Tangye, S.G., *Staying alive: regulation of plasma cell survival.* Trends Immunol, 2011. **32**(12): p. 595-602.

2. Plotkin, S.A., W.A. Orenstein, and P.A. Offit, *Vaccines*. Sixth edition. ed. xix, 1550 pages.

3. Centers for Disease, C. and Prevention, *Ten great public health achievements--worldwide, 2001-2010.* MMWR Morb Mortal Wkly Rep, 2011. **60**(24): p. 814-8.

4. von Behring, E. and S. Kitasato, *[The mechanism of diphtheria immunity and tetanus immunity in animals. 1890].* Mol Immunol, 1991. **28**(12): p. 1317, 1319-20.

5. Tiselius, A. and E.A. Kabat, *An Electrophoretic Study of Immune Sera and Purified Antibody Preparations.* J Exp Med, 1939. **69**(1): p. 119-31.

6. Fellah, J.S., et al., *Evolution of vertebrate IgM: complete amino acid sequence of the constant region of Ambystoma mexicanum mu chain deduced from cDNA sequence.* Eur J Immunol, 1992. **22**(10): p. 2595-601.

7. Williams, A.F. and A.N. Barclay, *The immunoglobulin superfamily--domains for cell surface recognition.* Annu Rev Immunol, 1988. **6**: p. 381-405.

8. Murphy, K., et al., *Janeway's immunobiology*. 8th ed. 2012, New York: Garland Science. xix, 868 p.

9. Schroeder, H.W., Jr. and L. Cavacini, *Structure and function of immunoglobulins.* J Allergy Clin Immunol, 2010. **125**(2 Suppl 2): p. S41-52.

10. Arnold, J.N., et al., *The impact of glycosylation on the biological function and structure of human immunoglobulins.* Annu Rev Immunol, 2007. **25**: p. 21-50.

11. Ravetch, J.V. and J.P. Kinet, *Fc receptors.* Annu Rev Immunol, 1991. **9**: p. 457-92.

12. Ravetch, J.V. and S. Bolland, *IgG Fc receptors.* Annu Rev Immunol, 2001. **19**: p. 275-90.

13. Woof, J.M. and J. Mestecky, *Mucosal immunoglobulins.* Immunol Rev, 2005. **206**: p. 64-82.

14. Fitzsimmons, C.M., F.H. Falcone, and D.W. Dunne, *Helminth Allergens, Parasite-Specific IgE, and Its Protective Role in Human Immunity.* Front Immunol, 2014. **5**: p. 61.

15. Gould, H.J., et al., *The biology of IGE and the basis of allergic disease.* Annu Rev Immunol, 2003. **21**: p. 579-628.

16. Ehrenstein, M.R. and C.A. Notley, *The importance of natural IgM: scavenger, protector and regulator.* Nat Rev Immunol, 2010. **10**(11): p. 778-86.

17. Bos, N.A., et al., *The influence of exogenous antigenic stimulation on the specificity repertoire of background immunoglobulin-secreting cells of different isotypes.* Cell Immunol, 1988. **112**(2): p. 371-80.

18. Haury, M., et al., *The repertoire of serum IgM in normal mice is largely independent of external antigenic contact.* Eur J Immunol, 1997. **27**(6): p. 1557-63.

19. Gronwall, C., J. Vas, and G.J. Silverman, *Protective Roles of Natural IgM Antibodies.* Front Immunol, 2012. **3**: p. 66.

20. Merbl, Y., et al., *Newborn humans manifest autoantibodies to defined self molecules detected by antigen microarray informatics.* J Clin Invest, 2007. **117**(3): p. 712-8.

21. Padilla, N.D., et al., *Levels of natural IgM antibodies against phosphorylcholine in healthy individuals and in patients undergoing isolated limb perfusion.* J Immunol Methods, 2004. **293**(1-2): p. 1-11.

22. Mouthon, L., et al., *Invariance and restriction toward a limited set of self-antigens characterize neonatal IgM antibody repertoires and prevail in autoreactive repertoires of healthy adults.* Proc Natl Acad Sci U S A, 1995. **92**(9): p. 3839-43.

23. Avrameas, S., *Natural autoantibodies: from 'horror autotoxicus' to 'gnothi seauton'.* Immunol Today, 1991. **12**(5): p. 154-9.

24. Ochsenbein, A.F., et al., *Control of early viral and bacterial distribution and disease by natural antibodies.* Science, 1999. **286**(5447): p. 2156-9.

25. Chou, M.Y., et al., *Oxidation-specific epitopes are dominant targets of innate natural antibodies in mice and humans.* J Clin Invest, 2009. **119**(5): p. 1335-49.

26. Silverman, G.J., et al., *Genetic imprinting of autoantibody repertoires in systemic lupus erythematosus patients.* Clin Exp Immunol, 2008. **153**(1): p. 102-16.

27. Casali, P. and A.L. Notkins, *CD5+ B lymphocytes, polyreactive antibodies and the human B-cell repertoire.* Immunol Today, 1989. **10**(11): p. 364-8.

28. Shaw, P.X., et al., *Natural antibodies with the T15 idiotype may act in atherosclerosis, apoptotic clearance, and protective immunity.* J Clin Invest, 2000. **105**(12): p. 1731-40.

29. Boes, M., et al., *A critical role of natural immunoglobulin M in immediate defense against systemic bacterial infection.* Journal of Experimental Medicine, 1998. **188**(12): p. 2381-6.

30. Zhou, Z.H., et al., *The broad antibacterial activity of the natural antibody repertoire is due to polyreactive antibodies.* Cell Host Microbe, 2007. **1**(1): p. 51-61.

31. Baumgarth, N., et al., *B-1 and B-2 cell-derived immunoglobulin M antibodies are nonredundant components of the protective response to influenza virus infection.* J Exp Med, 2000. **192**(2): p. 271-80.

32. Jayasekera, J.P., E.A. Moseman, and M.C. Carroll, *Natural antibody and complement mediate neutralization of influenza virus in the absence of prior immunity.* J Virol, 2007. **81**(7): p. 3487-94.

33. Baxendale, H.E., et al., *Natural human antibodies to pneumococcus have distinctive molecular characteristics and protect against pneumococcal disease.* Clin Exp Immunol, 2008. **151**(1): p. 51-60.

34. Brown, J.S., et al., *The classical pathway is the dominant complement pathway required for innate immunity to Streptococcus pneumoniae infection in mice.* Proc Natl Acad Sci U S A, 2002. **99**(26): p. 16969-74.

35. Subramaniam, K.S., et al., *The absence of serum IgM enhances the susceptibility of mice to pulmonary challenge with Cryptococcus neoformans.* J Immunol, 2010. **184**(10): p. 5755-67.

36. Rajan, B., T. Ramalingam, and T.V. Rajan, *Critical role for IgM in host protection in experimental filarial infection.* J Immunol, 2005. **175**(3): p. 1827-33.

37. Norrby-Teglund, A., K.N. Haque, and L. Hammarstrom, *Intravenous polyclonal IgM-enriched immunoglobulin therapy in sepsis: a review of clinical efficacy in relation to microbiological aetiology and severity of sepsis.* J Intern Med, 2006. **260**(6): p. 509-16.

38. Czajkowsky, D.M. and Z. Shao, *The human IgM pentamer is a mushroom-shaped molecule with a flexural bias.* Proc Natl Acad Sci U S A, 2009. **106**(35): p. 14960-5.

39. deCathelineau, A.M. and P.M. Henson, *The final step in programmed cell death: phagocytes carry apoptotic cells to the grave.* Essays Biochem, 2003. **39**: p. 105-17.

40. Quartier, P., et al., *Predominant role of IgM-dependent activation of the classical pathway in the clearance of dying cells by murine bone marrow-derived macrophages in vitro.* Eur J Immunol, 2005. **35**(1): p. 252-60.

41. Chen, Y., et al., *IgM antibodies to apoptosis-associated determinants recruit C1q and enhance dendritic cell phagocytosis of apoptotic cells.* J Immunol, 2009. **182**(10): p. 6031-43.

42. Notley, C.A., et al., *Natural IgM is required for suppression of inflammatory arthritis by apoptotic cells.* J Immunol, 2011. **186**(8): p. 4967-72.

43. Cox, K.O. and S.J. Hardy, *Autoantibodies against mouse bromelain-modified RBC are specifically inhibited by a common membrane phospholipid, phosphatidylcholine.* Immunology, 1985. **55**(2): p. 263-9.

44. Hardy, R.R. and K. Hayakawa, *Development of B cells producing natural autoantibodies to thymocytes and senescent erythrocytes.* Springer Semin Immunopathol, 2005. **26**(4): p. 363-75.

45. Chen, Y., et al., *Regulation of dendritic cells and macrophages by an anti-apoptotic cell natural antibody that suppresses TLR responses and inhibits inflammatory arthritis.* J Immunol, 2009. **183**(2): p. 1346-59.

46. Ehrenstein, M.R., H.T. Cook, and M.S. Neuberger, *Deficiency in serum immunoglobulin (Ig)M predisposes to development of IgG autoantibodies.* J Exp Med, 2000. **191**(7): p. 1253-8.

47. Boes, M., et al., *Accelerated development of IgG autoantibodies and autoimmune disease in the absence of secreted IgM.* Proc Natl Acad Sci U S A, 2000. **97**(3): p. 1184-9.

48. Gronwall, C., et al., *IgM autoantibodies to distinct apoptosis-associated antigens correlate with protection from cardiovascular events and renal disease in patients with SLE.* Clin Immunol, 2012. **142**(3): p. 390-8.

49. Mehrani, T. and M. Petri, *IgM anti-beta2 glycoprotein I is protective against lupus nephritis and renal damage in systemic lupus erythematosus.* J Rheumatol, 2011. **38**(3): p. 450-3.

50. Witte, T., et al., *IgM anti-dsDNA antibodies in systemic lupus erythematosus: negative association with nephritis. SLE Study Group.* Rheumatol Int, 1998. **18**(3): p. 85-91.

51. Forger, F., et al., *Clinical significance of anti-dsDNA antibody isotypes: IgG/IgM ratio of anti-dsDNA antibodies as a prognostic marker for lupus nephritis.* Lupus, 2004. **13**(1): p. 36-44.

52. Shaw, P.X., et al., *The autoreactivity of anti-phosphorylcholine antibodies for atherosclerosis-associated neo-antigens and apoptotic cells.* J Immunol, 2003. **170**(12): p. 6151-7.

53. Lewis, M.J., et al., *Immunoglobulin M is required for protection against atherosclerosis in low-density lipoprotein receptor-deficient mice.* Circulation, 2009. **120**(5): p. 417-26.

54. Karvonen, J., et al., *Immunoglobulin M type of autoantibodies to oxidized low-density lipoprotein has an inverse relation to carotid artery atherosclerosis.* Circulation, 2003. **108**(17): p. 2107-12.

55. Fiskesund, R., et al., *Low levels of antibodies against phosphorylcholine predict development of stroke in a population-based study from northern Sweden.* Stroke, 2010. **41**(4): p. 607-12.

56. Gronlund, H., et al., *Low levels of IgM antibodies against phosphorylcholine predict development of acute myocardial infarction in a population-based cohort from northern Sweden.* Eur J Cardiovasc Prev Rehabil, 2009. **16**(3): p. 382-6.

57. Eriksson, U.K., et al., *Low levels of antibodies against phosphorylcholine in Alzheimer's disease.* J Alzheimers Dis, 2010. **21**(2): p. 577-84.

58. Binder, C.J., et al., *Pneumococcal vaccination decreases atherosclerotic lesion formation: molecular mimicry between Streptococcus pneumoniae and oxidized LDL.* Nat Med, 2003. **9**(6): p. 736-43.

59. Cesena, F.H., et al., *Immune-modulation by polyclonal IgM treatment reduces atherosclerosis in hypercholesterolemic apoE-/- mice.* Atherosclerosis, 2012. **220**(1): p. 59-65.

60. Werwitzke, S., et al., *Inhibition of lupus disease by anti-double-stranded DNA antibodies of the IgM isotype in the (NZB x NZW)F1 mouse.* Arthritis Rheum, 2005. **52**(11): p. 3629-38.

61. Jiang, C., et al., *Activation-induced deaminase-deficient MRL/lpr mice secrete high levels of protective antibodies against lupus nephritis.* Arthritis Rheum, 2011. **63**(4): p. 1086-96.

62. Kulik, L., et al., *Pathogenic natural antibodies recognizing annexin IV are required to develop intestinal ischemia-reperfusion injury.* J Immunol, 2009. **182**(9): p. 5363-73.

63. Haas, M.S., et al., *Blockade of self-reactive IgM significantly reduces injury in a murine model of acute myocardial infarction.* Cardiovasc Res, 2010. **87**(4): p. 618-27.

64. Ghumra, A., et al., *Identification of residues in the Cmu4 domain of polymeric IgM essential for interaction with Plasmodium falciparum erythrocyte membrane protein 1 (PfEMP1).* J Immunol, 2008. **181**(3): p. 1988-2000.

65. Milland, J. and M.S. Sandrin, *ABO blood group and related antigens, natural antibodies and transplantation.* Tissue Antigens, 2006. **68**(6): p. 459-66.

66. Cooper, M.D., R.D.A. Peterson, and R.A. Good, *Delineation of the thymic and bursal lymphoid systems in the chicken.* Nature, 1965. **205**(4967): p. 143-146.

67. Cooper, M.D., et al., *The functions of the thymus system and the bursa system in the chicken.* J Exp Med, 1966. **123**(1): p. 75-102.

68. LeBien, T.W. and T.F. Tedder, *B lymphocytes: how they develop and function.* Blood, 2008. **112**(5): p. 1570-80.

69. Conley, M.E., et al., *Primary B cell immunodeficiencies: comparisons and contrasts.* Annu Rev Immunol, 2009. **27**: p. 199-227.

70. Froland, S., J.B. Natvig, and P. Berdal, *Surface-bound immunoglobulin as a marker of B lymphocytes in man.* Nat New Biol, 1971. **234**(51): p. 251-2.

71. Fuentes-Panana, E.M., G. Bannish, and J.G. Monroe, *Basal B-cell receptor signaling in B lymphocytes: mechanisms of regulation and role in positive selection, differentiation, and peripheral survival.* Immunol Rev, 2004. **197**: p. 26-40.

72. Hardy, R.R. and K. Hayakawa, *B cell development pathways.* Annu Rev Immunol, 2001. **19**: p. 595-621.

73. Lander, E.S., et al., *Initial sequencing and analysis of the human genome.* Nature, 2001. **409**(6822): p. 860-921.

74. Mouse Genome Sequencing, C., et al., *Initial sequencing and comparative analysis of the mouse genome.* Nature, 2002. **420**(6915): p. 520-62.

75. Tonegawa, S., *Somatic generation of antibody diversity.* Nature, 1983. **302**(5909): p. 575-81.

76. Honjo, T., *Immunoglobulin genes.* Annu Rev Immunol, 1983. **1**: p. 499-528.

77. Early, P., et al., *An immunoglobulin heavy chain variable region gene is generated from three segments of DNA: VH, D and JH.* Cell, 1980. **19**(4): p. 981-92.

78. de Bono, B., M. Madera, and C. Chothia, *VH gene segments in the mouse and human genomes.* J Mol Biol, 2004. **342**(1): p. 131-43.

79. Kindt, T.J., et al., *Kuby immunology*. 6th ed. 2007, New York: W.H. Freeman. xxii, 574, A-31, G-12, AN-27, I-27 p.

80. Shimizu, A., et al., *Organization of the constant-region gene family of the mouse immunoglobulin heavy chain.* Cell, 1982. **28**(3): p. 499-506.

81. Hofker, M.H., M.A. Walter, and D.W. Cox, *Complete physical map of the human immunoglobulin heavy chain constant region gene complex.* Proc Natl Acad Sci U S A, 1989. **86**(14): p. 5567-71.

82. Market, E. and F.N. Papavasiliou, *V(D)J recombination and the evolution of the adaptive immune system.* PLoS Biol, 2003. **1**(1): p. E16.

83. van Gent, D.C., et al., *Initiation of V(D)J recombination in a cell-free system.* Cell, 1995. **81**(6): p. 925-34.

84. Mombaerts, P., et al., *RAG-1-deficient mice have no mature B and T lymphocytes.* Cell, 1992. **68**(5): p. 869-77.

85. Shinkai, Y., et al., *RAG-2-deficient mice lack mature lymphocytes owing to inability to initiate V(D)J rearrangement.* Cell, 1992. **68**(5): p. 855-67.

86. Bassing, C.H., W. Swat, and F.W. Alt, *The mechanism and regulation of chromosomal V(D)J recombination.* Cell, 2002. **109 Suppl**: p. S45-55.

87. Alt, F.W. and D. Baltimore, *Joining of immunoglobulin heavy chain gene segments: implications from a chromosome with evidence of three D-JH fusions.* Proc Natl Acad Sci U S A, 1982. **79**(13): p. 4118-22.

88. Osmond, D.G., A. Rolink, and F. Melchers, *Murine B lymphopoiesis: towards a unified model.* Immunol Today, 1998. **19**(2): p. 65-8.

89. Kondo, M., I.L. Weissman, and K. Akashi, *Identification of clonogenic common lymphoid progenitors in mouse bone marrow.* Cell, 1997. **91**(5): p. 661-72.

90. Li, Y.S., et al., *Identification of the earliest B lineage stage in mouse bone marrow.* Immunity, 1996. **5**(6): p. 527-35.

91. Allman, D., J. Li, and R.R. Hardy, *Commitment to the B lymphoid lineage occurs before DH-JH recombination.* J Exp Med, 1999. **189**(4): p. 735-40.

92. Karasuyama, H., A. Kudo, and F. Melchers, *The proteins encoded by the VpreB and lambda 5 pre-B cell-specific genes can associate with each other and with mu heavy chain.* J Exp Med, 1990. **172**(3): p. 969-72.

93. Geier, J.K. and M.S. Schlissel, *Pre-BCR signals and the control of Ig gene rearrangements.* Semin Immunol, 2006. **18**(1): p. 31-9.

94. Karasuyama, H., A. Rolink, and F. Melchers, *Surrogate light chain in B cell development.* Adv Immunol, 1996. **63**: p. 1-41.

95. Raff, M.C., et al., *Early production of intracellular IgM by B-lymphocyte precursors in mouse.* Nature, 1976. **259**(5540): p. 224-6.

96. Chung, J.B., M. Silverman, and J.G. Monroe, *Transitional B cells: step by step towards immune competence.* Trends Immunol, 2003. **24**(6): p. 343-9.

97. Hieter, P.A., et al., *Human immunoglobulin kappa light-chain genes are deleted or rearranged in lambda-producing B cells.* Nature, 1981. **290**(5805): p. 368-72.

98. Goodnow, C.C., et al., *Cellular and genetic mechanisms of self tolerance and autoimmunity.* Nature, 2005. **435**(7042): p. 590-7.

99. Stavnezer, J., J.E. Guikema, and C.E. Schrader, *Mechanism and regulation of class switch recombination.* Annu Rev Immunol, 2008. **26**: p. 261-92.

100. Allman, D., et al., *Resolution of three nonproliferative immature splenic B cell subsets reveals multiple selection points during peripheral B cell maturation.* J Immunol, 2001. **167**(12): p. 6834-40.

101. Cerutti, A., M. Cols, and I. Puga, *Marginal zone B cells: virtues of innate-like antibody-producing lymphocytes.* Nat Rev Immunol, 2013. **13**(2): p. 118-132.

102. Mackay, F. and J.L. Browning, *BAFF: a fundamental survival factor for B cells.* Nat Rev Immunol, 2002. **2**(7): p. 465-75.

103. Li, Y.S., K. Hayakawa, and R.R. Hardy, *The regulated expression of B lineage associated genes during B cell differentiation in bone marrow and fetal liver.* J Exp Med, 1993. **178**(3): p. 951-60.

104. Wasserman, R., et al., *A novel mechanism for B cell repertoire maturation based on response by B cell precursors to pre-B receptor assembly.* J Exp Med, 1998. **187**(2): p. 259-64.

105. Kantor, A.B., et al., *An unbiased analysis of V(H)-D-J(H) sequences from B-1a, B-1b, and conventional B cells.* J Immunol, 1997. **158**(3): p. 1175-86.

106. Kantor, A.B., *V-gene usage and N-region insertions in B-1a, B-1b and conventional B cells.* Semin Immunol, 1996. **8**(1): p. 29-35.

107. Hayakawa, K., et al., *Positive selection of natural autoreactive B cells.* Science, 1999. **285**(5424): p. 113-6.

108. Wang, H. and S.H. Clarke, *Positive selection focuses the VH12 B-cell repertoire towards a single B1 specificity with survival function.* Immunol Rev, 2004. **197**: p. 51-9.

109. Forster, I. and K. Rajewsky, *Expansion and functional activity of Ly-1+ B cells upon transfer of peritoneal cells into allotype-congenic, newborn mice.* Eur J Immunol, 1987. **17**(4): p. 521-8.

110. Hayakawa, K., R.R. Hardy, and L.A. Herzenberg, *Peritoneal Ly-1 B cells: genetic control, autoantibody production, increased lambda light chain expression.* Eur J Immunol, 1986. **16**(4): p. 450-6.

111. Baumgarth, N., *The double life of a B-1 cell: self-reactivity selects for protective effector functions.* Nat Rev Immunol, 2011. **11**(1): p. 34-46.

112. Zhong, X., et al., *A novel subpopulation of B-1 cells is enriched with autoreactivity in normal and lupus-prone mice.* Arthritis Rheum, 2009. **60**(12): p. 3734-43.

113. Enghard, P., et al., *Class switching and consecutive loss of dsDNA-reactive B1a B cells from the peritoneal cavity during murine lupus development.* Eur J Immunol, 2010. **40**(6): p. 1809-18.

114. Murakami, M., et al., *Prevention of autoimmune symptoms in autoimmune-prone mice by elimination of B-1 cells.* Int Immunol, 1995. **7**(5): p. 877-82.

115. Haskins, K., J. Kappler, and P. Marrack, *The major histocompatibility complex-restricted antigen receptor on T cells.* Annu Rev Immunol, 1984. **2**: p. 51-66.

116. Banchereau, J. and R.M. Steinman, *Dendritic cells and the control of immunity.* Nature, 1998. **392**(6673): p. 245-52.

117. Janeway, C.A., Jr. and R. Medzhitov, *Innate immune recognition.* Annu Rev Immunol, 2002. **20**: p. 197-216.

118. McHeyzer-Williams, L.J. and M.G. McHeyzer-Williams, *Antigen-specific memory B cell development.* Annu Rev Immunol, 2005. **23**: p. 487-513.

119. Lanzavecchia, A., *Antigen-specific interaction between T and B cells.* Nature, 1985. **314**(6011): p. 537-539.

120. Mond, J.J., A. Lees, and C.M. Snapper, *T cell-independent antigens type 2.* Annual Review of Immunology, 1995. **13**(1): p. 655-692.

121. Mosier, D.E. and B. Subbarao, *Thymus-independent antigens: complexity of B-lymphocyte activation revealed.* Immunol Today, 1982. **3**(8): p. 217-22.

122. Chu, V.T. and C. Berek, *The establishment of the plasma cell survival niche in the bone marrow.* Immunol Rev, 2013. **251**(1): p. 177-88.

123. Eisen, H.N. and G.W. Siskind, *Variations in affinities of antibodies during the immune response.* Biochemistry, 1964. **3**: p. 996.

124. Weigert, M.G., et al., *Variability in the lambda light chain sequences of mouse antibody.* Nature, 1970. **228**(276): p. 1045-7.

125. Jacob, J., et al., *Intraclonal generation of antibody mutants in germinal centres.* Nature, 1991. **354**(6352): p. 389-92.

126. MacLennan, I.C., *Germinal centers.* Annual Review of Immunology, 1994. **12**: p. 117-39.

127. Muramatsu, M., et al., *Class switch recombination and hypermutation require activation-induced cytidine deaminase (AID), a potential RNA editing enzyme.* Cell, 2000. **102**(5): p. 553-63.

128. Victora, G.D. and M.C. Nussenzweig, *Germinal centers.* Annu Rev Immunol, 2012. **30**: p. 429-57.

129. Mandel, T.E., et al., *Long-term antigen retention by dendritic cells in the popliteal lymph node of immunized mice.* Immunology, 1981. **43**(2): p. 353-62.

130. Jacobson, E.B., L.H. Caporale, and G.J. Thorbecke, *Effect of thymus cell injections on germinal center formation in lymphoid tissues of nude (thymusless) mice.* Cell Immunol, 1974. **13**(3): p. 416-30.

131. Han, S., et al., *In situ studies of the primary immune response to (4-hydroxy-3-nitrophenyl)acetyl. IV. Affinity-dependent, antigen-driven B cell apoptosis in germinal centers as a mechanism for maintaining self- tolerance.* J Exp Med, 1995. **182**(6): p. 1635-44.

132. Renshaw, B.R., et al., *Humoral immune responses in CD40 ligand-deficient mice.* J Exp Med, 1994. **180**(5): p. 1889-900.

133. Kurosaki, T., K. Kometani, and W. Ise, *Memory B cells.* Nat Rev Immunol, 2015. **15**(3): p. 149-159.

134. Taylor, J.J., K.A. Pape, and M.K. Jenkins, *A germinal center-independent pathway generates unswitched memory B cells early in the primary response.* J Exp Med, 2012. **209**(3): p. 597-606.

135. Yang, Y., et al., *Antigen-specific memory in B-1a and its relationship to natural immunity.* Proc Natl Acad Sci U S A, 2012. **109**(14): p. 5388-93.

136. Alugupalli, K.R., et al., *B1b lymphocytes confer T cell-independent long-lasting immunity.* Immunity, 2004. **21**(3): p. 379-90.

137. Kometani, K., et al., *Repression of the transcription factor Bach2 contributes to predisposition of IgG1 memory B cells toward plasma cell differentiation.* Immunity, 2013. **39**(1): p. 136-47.

138. Dogan, I., et al., *Multiple layers of B cell memory with different effector functions.* Nat Immunol, 2009. **10**(12): p. 1292-9.

139. Maruyama, M., K.P. Lam, and K. Rajewsky, *Memory B-cell persistence is independent of persisting immunizing antigen.* Nature, 2000. **407**(6804): p. 636-42.

140. Takahashi, Y., H. Ohta, and T. Takemori, *Fas is required for clonal selection in germinal centers and the subsequent establishment of the memory B cell repertoire.* Immunity, 2001. **14**(2): p. 181-92.

141. Pape, K.A., et al., *Different B Cell Populations Mediate Early and Late Memory During an Endogenous Immune Response.* Science, 2011.

142. Yu, X., et al., *Neutralizing antibodies derived from the B cells of 1918 influenza pandemic survivors.* Nature, 2008. **455**(7212): p. 532-6.

143. Oracki, S.A., et al., *Plasma cell development and survival.* Immunol Rev, 2010. **237**(1): p. 140-59.

144. Jacob, J. and G. Kelsoe, *In situ studies of the primary immune response to (4-hydroxy-3- nitrophenyl)acetyl. II. A common clonal origin for periarteriolar lymphoid sheath-associated foci and germinal centers.* J Exp Med, 1992. **176**(3): p. 679-87.

145. Sze, D.M., et al., *Intrinsic constraint on plasmablast growth and extrinsic limits of plasma cell survival.* J Exp Med, 2000. **192**(6): p. 813-21.

146. Smith, K.G., et al., *The phenotype and fate of the antibody-forming cells of the splenic foci.* Eur J Immunol, 1996. **26**(2): p. 444-8.

147. Dilosa, R.M., et al., *Germinal center B cells and antibody production in the bone marrow.* J Immunol, 1991. **146**(12): p. 4071-7.

148. Bjorneboe, M., H. Gormsen, and F. Lundquist, *Further Experimental Studies on the Role of the Plasma Cells as Antibody Producers.* Journal of Immunology, 1947. **55**(2): p. 121-129.

149. Calame, K.L., *Plasma cells: finding new light at the end of B cell development.* Nat Immunol, 2001. **2**(12): p. 1103-8.

150. Koda, J.E., A. Rapraeger, and M. Bernfield, *Heparan-Sulfate Proteoglycans from Mouse Mammary Epithelial-Cells - Cell-Surface Proteoglycan as a Receptor for Interstitial Collagens.* Journal of Biological Chemistry, 1985. **260**(13): p. 8157-8162.

151. Saunders, S. and M. Bernfield, *Cell surface proteoglycan binds mouse mammary epithelial cells to fibronectin and behaves as a receptor for interstitial matrix.* J Cell Biol, 1988. **106**(2): p. 423-30.

152. Sanderson, R.D., P. Lalor, and M. Bernfield, *B lymphocytes express and lose syndecan at specific stages of differentiation.* Cell Regul, 1989. **1**(1): p. 27-35.

153. Kallies, A., et al., *Plasma cell ontogeny defined by quantitative changes in blimp-1 expression.* J Exp Med, 2004. **200**(8): p. 967-77.

154. Turner, C.A., Jr., D.H. Mack, and M.M. Davis, *Blimp-1, a novel zinc finger-containing protein that can drive the maturation of B lymphocytes into immunoglobulin-secreting cells.* Cell, 1994. **77**(2): p. 297-306.

155. Shapiro-Shelef, M., et al., *Blimp-1 is required for the formation of immunoglobulin secreting plasma cells and pre-plasma memory B cells.* Immunity, 2003. **19**(4): p. 607-20.

156. Reimold, A.M., et al., *Transcription factor B cell lineage-specific activator protein regulates the gene for human X-box binding protein 1.* J Exp Med, 1996. **183**(2): p. 393-401.

157. Yoshida, H., et al., *XBP1 mRNA is induced by ATF6 and spliced by IRE1 in response to ER stress to produce a highly active transcription factor.* Cell, 2001. **107**(7): p. 881-91.

158. Iwakoshi, N.N., et al., *Plasma cell differentiation and the unfolded protein response intersect at the transcription factor XBP-1.* Nat Immunol, 2003. **4**(4): p. 321-9.

159. Yoshida, T., et al., *Memory B and memory plasma cells.* Immunol Rev, 2010. **237**(1): p. 117-39.

160. Lin, Y., K. Wong, and K. Calame, *Repression of c-myc transcription by Blimp-1, an inducer of terminal B cell differentiation.* Science, 1997. **276**(5312): p. 596-9.

161. Hargreaves, D.C., et al., *A coordinated change in chemokine responsiveness guides plasma cell movements.* J Exp Med, 2001. **194**(1): p. 45-56.

162. Radbruch, A., et al., *Competence and competition: the challenge of becoming a long-lived plasma cell.* Nat Rev Immunol, 2006. **6**(10): p. 741-50.

163. Benner, R., W. Hijmans, and J.J. Haaijman, *The bone marrow: the major source of serum immunoglobulins, but still a neglected site of antibody formation.* Clin Exp Immunol, 1981. **46**(1): p. 1-8.

164. Slifka, M.K., et al., *Humoral immunity due to long-lived plasma cells.* Immunity, 1998. **8**(3): p. 363-72.

165. Amanna, I.J., N.E. Carlson, and M.K. Slifka, *Duration of humoral immunity to common viral and vaccine antigens.* New England Journal of Medicine, 2007. **357**(19): p. 1903-1915.

166. Vieira, P. and K. Rajewsky, *The half-lives of serum immunoglobulins in adult mice.* European Journal of Immunology, 1988. **18**(2): p. 313-6.

167. Slifka, M.K. and R. Ahmed, *Long-lived plasma cells: a mechanism for maintaining persistent antibody production.* Current Opinion in Immunology, 1998. **10**(3): p. 252-8.

168. Manz, R.A., et al., *Survival of long-lived plasma cells is independent of antigen.* Int Immunol, 1998. **10**(11): p. 1703-11.

169. DiLillo, D.J., et al., *Maintenance of long-lived plasma cells and serological memory despite mature and memory B cell depletion during CD20 immunotherapy in mice.* J Immunol, 2008. **180**(1): p. 361-71.

170. Manz, R.A., A. Thiel, and A. Radbruch, *Lifetime of plasma cells in the bone marrow.* Nature, 1997. **388**(6638): p. 133-4.

171. Cassese, G., et al., *Plasma cell survival is mediated by synergistic effects of cytokines and adhesion-dependent signals.* J Immunol, 2003. **171**(4): p. 1684-90.

172. Minges Wols, H.A., et al., *The role of bone marrow-derived stromal cells in the maintenance of plasma cell longevity.* J Immunol, 2002. **169**(8): p. 4213-21.

173. Benson, M.J., et al., *Cutting edge: the dependence of plasma cells and independence of memory B cells on BAFF and APRIL.* J Immunol, 2008. **180**(6): p. 3655-9.

174. Belnoue, E., et al., *APRIL is critical for plasmablast survival in the bone marrow and poorly expressed by early-life bone marrow stromal cells.* Blood, 2008. **111**(5): p. 2755-64.

175. O'Connor, B.P., et al., *BCMA is essential for the survival of long-lived bone marrow plasma cells.* J Exp Med, 2004. **199**(1): p. 91-8.

176. Peperzak, V., et al., *Mcl-1 is essential for the survival of plasma cells.* Nat Immunol, 2013. **14**(3): p. 290-7.

177. Chu, V.T., et al., *Eosinophils are required for the maintenance of plasma cells in the bone marrow.* Nat Immunol, 2011. **12**(2): p. 151-9.

178. Winter, O., et al., *Megakaryocytes constitute a functional component of a plasma cell niche in the bone marrow.* Blood, 2010. **116**(11): p. 1867-75.

179. Baumgarth, N., J.W. Tung, and L.A. Herzenberg, *Inherent specificities in natural antibodies: a key to immune defense against pathogen invasion.* Springer Semin Immunopathol, 2005. **26**(4): p. 347-62.

180. Lalor, P.A., et al., *Feedback regulation of murine Ly-1 B cell development.* Eur J Immunol, 1989. **19**(3): p. 507-13.

181. Baumgarth, N., et al., *Innate and acquired humoral immunities to influenza virus are mediated by distinct arms of the immune system.* Proc Natl Acad Sci U S A, 1999. **96**(5): p. 2250-5.

182. Choi, Y.S. and N. Baumgarth, *Dual role for B-1a cells in immunity to influenza virus infection.* J Exp Med, 2008. **205**(13): p. 3053-64.

183. Kearney, J.F., et al., *Natural antibody repertoires: development and functional role in inhibiting allergic airway disease.* Annu Rev Immunol, 2015. **33**: p. 475-504.

184. Yang, Y., et al., *Division and differentiation of natural antibody-producing cells in mouse spleen.* Proc Natl Acad Sci U S A, 2007. **104**(11): p. 4542-6.

185. Fairfax, K.A., et al., *Different kinetics of blimp-1 induction in B cell subsets revealed by reporter gene.* J Immunol, 2007. **178**(7): p. 4104-11.

186. Kawahara, T., et al., *Peritoneal cavity B cells are precursors of splenic IgM natural antibody-producing cells.* J Immunol, 2003. **171**(10): p. 5406-14.

187. Baumgarth, N., *Innate-like B cells and their rules of engagement.* Adv Exp Med Biol, 2013. **785**: p. 57-66.

188. Tumang, J.R., et al., *Spontaneously Ig-secreting B-1 cells violate the accepted paradigm for expression of differentiation-associated transcription factors.* J Immunol, 2005. **174**(6): p. 3173-7.

189. Holodick, N.E., J.R. Tumang, and T.L. Rothstein, *Immunoglobulin secretion by B1 cells: differential intensity and IRF4-dependence of spontaneous IgM secretion by peritoneal and splenic B1 cells.* Eur J Immunol, 2010. **40**(11): p. 3007-16.

190. Holodick, N.E., T. Vizconde, and T.L. Rothstein, *Splenic B-1a Cells Expressing CD138 Spontaneously Secrete Large Amounts of Immunoglobulin in Naive Mice.* Front Immunol, 2014. **5**: p. 129.

191. Choi, Y.S., et al., *B-1 cells in the bone marrow are a significant source of natural IgM.* Eur J Immunol, 2012. **42**(1): p. 120-9.

192. Silverman, G.J., *Regulatory natural autoantibodies to apoptotic cells: pallbearers and protectors.* Arthritis Rheum, 2011. **63**(3): p. 597-602.

193. Ueda, Y., et al., *T-independent activation-induced cytidine deaminase expression, class-switch recombination, and antibody production by immature/transitional 1 B cells.* J Immunol, 2007. **178**(6): p. 3593-601.

194. Reynolds, A.E., M. Kuraoka, and G. Kelsoe, *Natural IgM is produced by CD5- plasma cells that occupy a distinct survival niche in bone marrow.* J Immunol, 2015. **194**(1): p. 231-42.

195. Rapaka, R.R., et al., *Conserved natural IgM antibodies mediate innate and adaptive immunity against the opportunistic fungus Pneumocystis murina.* J Exp Med, 2010. **207**(13): p. 2907-19.

196. Boes, M., *Role of natural and immune IgM antibodies in immune responses.* Mol Immunol, 2000. **37**(18): p. 1141-9.

197. Racine, R. and G.M. Winslow, *IgM in microbial infections: taken for granted?* Immunol Lett, 2009. **125**(2): p. 79-85.

198. Briles, D.E., et al., *Antiphosphocholine antibodies found in normal mouse serum are protective against intravenous infection with type 3 streptococcus pneumoniae.* J Exp Med, 1981. **153**(3): p. 694-705.

199. Kyaw, T., et al., *B1a B lymphocytes are atheroprotective by secreting natural IgM that increases IgM deposits and reduces necrotic cores in atherosclerotic lesions.* Circ Res, 2011. **109**(8): p. 830-40.

200. Wardemann, H., et al., *B-1a B cells that link the innate and adaptive immune responses are lacking in the absence of the spleen.* J Exp Med, 2002. **195**(6): p. 771-80.

201. Thurnheer, M.C., et al., *B1 cells contribute to serum IgM, but not to intestinal IgA, production in gnotobiotic Ig allotype chimeric mice.* J Immunol, 2003. **170**(9): p. 4564-71.

202. Hayakawa, K., et al., *Ly-1 B cells: functionally distinct lymphocytes that secrete IgM autoantibodies.* Proc Natl Acad Sci U S A, 1984. **81**(8): p. 2494-8.

203. Hooijkaas, H., et al., *Frequency analysis of the antibody specificity repertoire of mitogen-reactive B cells and "spontaneously" occurring "background" plaque-forming cells in nude mice.* Cell Immunol, 1985. **92**(1): p. 154-62.

204. Ohdan, H., et al., *Mac-1-negative B-1b phenotype of natural antibody-producing cells, including those responding to Gal alpha 1,3Gal epitopes in alpha 1,3-galactosyltransferase-deficient mice.* J Immunol, 2000. **165**(10): p. 5518-29.

205. Boggs, D.R., *The total marrow mass of the mouse: a simplified method of measurement.* Am J Hematol, 1984. **16**(3): p. 277-86.

206. Underhill, G.H., et al., *IgG plasma cells display a unique spectrum of leukocyte adhesion and homing molecules.* Blood, 2002. **99**(8): p. 2905-12.

207. Rozanski, C.H., et al., *Sustained antibody responses depend on CD28 function in bone marrow-resident plasma cells.* J Exp Med, 2011. **208**(7): p. 1435-46.

208. Hayakawa, K., et al., *The "Ly-1 B" cell subpopulation in normal immunodefective, and autoimmune mice.* J Exp Med, 1983. **157**(1): p. 202-18.

209. Kantor, A.B. and L.A. Herzenberg, *Origin of murine B cell lineages.* Annu Rev Immunol, 1993. **11**: p. 501-38.

210. Carmack, C.E., et al., *Rearrangement and selection of VH11 in the Ly-1 B cell lineage.* J Exp Med, 1990. **172**(1): p. 371-4.

211. Vollmers, H.P. and S. Brandlein, *Natural IgM antibodies: the orphaned molecules in immune surveillance.* Adv Drug Deliv Rev, 2006. **58**(5-6): p. 755-65.

212. Seidl, K.J., et al., *Predominant VH genes expressed in innate antibodies are associated with distinctive antigen-binding sites.* Proc Natl Acad Sci U S A, 1999. **96**(5): p. 2262-7.

213. Hayakawa, K., et al., *Positive selection of anti-thy-1 autoreactive B-1 cells and natural serum autoantibody production independent from bone marrow B cell development.* J Exp Med, 2003. **197**(1): p. 87-99.

214. Chumley, M.J., et al., *A VH11V kappa 9 B cell antigen receptor drives generation of CD5+ B cells both in vivo and in vitro.* J Immunol, 2000. **164**(9): p. 4586-93.

215. Lam, K.P. and K. Rajewsky, *B cell antigen receptor specificity and surface density together determine B-1 versus B-2 cell development.* J Exp Med, 1999. **190**(4): p. 471-7.

216. Sonoda, E., et al., *B cell development under the condition of allelic inclusion.* Immunity, 1997. **6**(3): p. 225-33.

217. Manz, R.A., et al., *Humoral immunity and long-lived plasma cells.* Curr Opin Immunol, 2002. **14**(4): p. 517-21.

218. Lindsley, R.C., et al., *Generation of peripheral B cells occurs via two spatially and temporally distinct pathways.* Blood, 2007. **109**(6): p. 2521-8.

219. Ho, F., et al., *Distinct short-lived and long-lived antibody-producing cell populations.* Eur J Immunol, 1986. **16**(10): p. 1297-301.

220. Yu, C., et al., *Targeted deletion of a high-affinity GATA-binding site in the GATA-1 promoter leads to selective loss of the eosinophil lineage in vivo.* J Exp Med, 2002. **195**(11): p. 1387-95.

221. Moon, B.G., et al., *The role of IL-5 for mature B-1 cells in homeostatic proliferation, cell survival, and Ig production.* J Immunol, 2004. **172**(10): p. 6020-9.

222. Yoshida, T., et al., *Defective B-1 cell development and impaired immunity against Angiostrongylus cantonensis in IL-5R alpha-deficient mice.* Immunity, 1996. **4**(5): p. 483-94.

223. Kopf, M., et al., *IL-5-deficient mice have a developmental defect in CD5+ B-1 cells and lack eosinophilia but have normal antibody and cytotoxic T cell responses.* Immunity, 1996. **4**(1): p. 15-24.

224. Suematsu, S., et al., *IgG1 plasmacytosis in interleukin 6 transgenic mice.* Proc Natl Acad Sci U S A, 1989. **86**(19): p. 7547-51.

225. Tominaga, A., et al., *Transgenic mice expressing a B cell growth and differentiation factor gene (interleukin 5) develop eosinophilia and autoantibody production.* J Exp Med, 1991. **173**(2): p. 429-37.

226. Dooldeniya, M.D. and A.N. Warrens, *Xenotransplantation: where are we today?* J R Soc Med, 2003. **96**(3): p. 111-7.

227. Qamar, N. and R.L. Fuleihan, *The hyper IgM syndromes.* Clin Rev Allergy Immunol, 2014. **46**(2): p. 120-30.

228. Zhang, W., et al., *Essential role of LAT in T cell development.* Immunity, 1999. **10**(3): p. 323-32.

229. Walker, J.A. and A.N. McKenzie, *Development and function of group 2 innate lymphoid cells.* Curr Opin Immunol, 2013. **25**(2): p. 148-55.

230. Brickshawana, A., et al., *Lineage(-)Sca1+c-Kit(-)CD25+ cells are IL-33-responsive type 2 innate cells in the mouse bone marrow.* J Immunol, 2011. **187**(11): p. 5795-804.

231. Halim, T.Y., et al., *Retinoic-acid-receptor-related orphan nuclear receptor alpha is required for natural helper cell development and allergic inflammation.* Immunity, 2012. **37**(3): p. 463-74.

232. Spits, H., et al., *Innate lymphoid cells--a proposal for uniform nomenclature.* Nat Rev Immunol, 2013. **13**(2): p. 145-9.

233. Walker, J.A., J.L. Barlow, and A.N. McKenzie, *Innate lymphoid cells--how did we miss them?* Nat Rev Immunol, 2013. **13**(2): p. 75-87.

234. Monticelli, L.A., et al., *Innate lymphoid cells promote lung-tissue homeostasis after infection with influenza virus.* Nat Immunol, 2011. **12**(11): p. 1045-54.

235. Hepworth, M.R., et al., *Innate lymphoid cells regulate CD4+ T-cell responses to intestinal commensal bacteria.* Nature, 2013. **498**(7452): p. 113-7.

236. Saenz, S.A., et al., *IL-25 simultaneously elicits distinct populations of innate lymphoid cells and multipotent progenitor type 2 (MPPtype2) cells.* J Exp Med, 2013. **210**(9): p. 1823-37.

237. Abraham, S.N. and A.L. St John, *Mast cell-orchestrated immunity to pathogens.* Nat Rev Immunol, 2010. **10**(6): p. 440-52.

238. da Silva, E.Z., M.C. Jamur, and C. Oliver, *Mast cell function: a new vision of an old cell.* J Histochem Cytochem, 2014. **62**(10): p. 698-738.

239. Grimbaldeston, M.A., et al., *Mast cell-deficient W-sash c-kit mutant Kit W-sh/W-sh mice as a model for investigating mast cell biology in vivo.* Am J Pathol, 2005. **167**(3): p. 835-48.

240. Chu, Y.T., et al., *Mast cell-macrophage dynamics in modulation of dengue virus infection in skin.* Immunology, 2015. **146**(1): p. 163-72.

241. Reber, L.L., et al., *Contribution of mast cell-derived interleukin-1beta to uric acid crystal-induced acute arthritis in mice.* Arthritis Rheumatol, 2014. **66**(10): p. 2881-91.

242. Hitoshi, Y., et al., *IL-5 receptor positive B cells, but not eosinophils, are functionally and numerically influenced in mice carrying the X-linked immune defect.* Int Immunol, 1993. **5**(9): p. 1183-90.

243. Jamur, M.C., et al., *Identification and characterization of undifferentiated mast cells in mouse bone marrow.* Blood, 2005. **105**(11): p. 4282-9.

244. Takeda, S., T. Shimizu, and H.R. Rodewald, *Interactions between c-kit and stem cell factor are not required for B-cell development in vivo.* Blood, 1997. **89**(2): p. 518-25.

245. Hogan, M.B., D. Piktel, and K.S. Landreth, *IL-5 production by bone marrow stromal cells: implications for eosinophilia associated with asthma.* J Allergy Clin Immunol, 2000. **106**(2): p. 329-36.

246. Takatsu, K. and H. Nakajima, *IL-5 and eosinophilia.* Curr Opin Immunol, 2008. **20**(3): p. 288-94.

247. Shen, J., et al., *Novel source of human hematopoietic stem cells from peritoneal dialysis effluents.* Stem Cell Res, 2015. **15**(2): p. 299-304.

248. Hastings, W.D., et al., *CD5+/Mac-1- peritoneal B cells: a novel B cell subset that exhibits characteristics of B-1 cells.* Immunol Lett, 2006. **105**(1): p. 90-6.

249. Ghosn, E.E., et al., *CD11b expression distinguishes sequential stages of peritoneal B-1 development.* Proc Natl Acad Sci U S A, 2008. **105**(13): p. 5195-200.

250. Lefkovits, I. and H. Waldmann, *Limiting dilution analysis of cells of the immune system*. 2nd ed. 1999, Oxford [England] ; New York: Oxford University Press. xvi, 285 p.

251. Hayakawa, K., R.R. Hardy, and L.A. Herzenberg, *Progenitors for Ly-1 B cells are distinct from progenitors for other B cells.* J Exp Med, 1985. **161**(6): p. 1554-68.

252. Hardy, R.R. and K. Hayakawa, *A developmental switch in B lymphopoiesis.* Proc Natl Acad Sci U S A, 1991. **88**(24): p. 11550-4.

253. Kroese, F.G., et al., *Many of the IgA producing plasma cells in murine gut are derived from self-replenishing precursors in the peritoneal cavity.* Int Immunol, 1989. **1**(1): p. 75-84.

254. Kaminski, D.A. and J. Stavnezer, *Enhanced IgA class switching in marginal zone and B1 B cells relative to follicular/B2 B cells.* J Immunol, 2006. **177**(9): p. 6025-9.

255. Yuan, J., et al., *Lin28b reprograms adult bone marrow hematopoietic progenitors to mediate fetal-like lymphopoiesis.* Science, 2012. **335**(6073): p. 1195-200.

256. Yamazaki, M., et al., *C-kit gene is expressed by skin mast cells in embryos but not in puppies of Wsh/Wsh mice: age-dependent abolishment of c-kit gene expression.* Blood, 1994. **83**(12): p. 3509-16.

257. Racine, R., et al., *IgM production by bone marrow plasmablasts contributes to long-term protection against intracellular bacterial infection.* J Immunol, 2011. **186**(2): p. 1011-21.

258. Foote, J.B., et al., *Long-term maintenance of polysaccharide-specific antibodies by IgM-secreting cells.* J Immunol, 2012. **188**(1): p. 57-67.

259. Bendelac, A., M. Bonneville, and J.F. Kearney, *Autoreactivity by design: innate B and T lymphocytes.* Nat Rev Immunol, 2001. **1**(3): p. 177-86.

260. Riggs, J.E., R.S. Stowers, and D.E. Mosier, *The immunoglobulin allotype contributed by peritoneal cavity B cells dominates in SCID mice reconstituted with allotype-disparate mixtures of splenic and peritoneal cavity B cells.* J Exp Med, 1990. **172**(2): p. 475-85.

261. Lalor, P.A., et al., *Permanent alteration of the murine Ly-1 B repertoire due to selective depletion of Ly-1 B cells in neonatal animals.* Eur J Immunol, 1989. **19**(3): p. 501-6.

262. Sen, G., et al., *Negative regulation of antigen receptor-mediated signaling by constitutive association of CD5 with the SHP-1 protein tyrosine phosphatase in B-1 B cells.* Eur J Immunol, 1999. **29**(10): p. 3319-28.

263. Berland, R. and H.H. Wortis, *Origins and functions of B-1 cells with notes on the role of CD5.* Annu Rev Immunol, 2002. **20**: p. 253-300.

264. Dogusan, Z., E. Montecino-Rodriguez, and K. Dorshkind, *Macrophages and stromal cells phagocytose apoptotic bone marrow-derived B lineage cells.* J Immunol, 2004. **172**(8): p. 4717-23.

265. Wandzioch, E., et al., *Activation of the MAP kinase pathway by c-Kit is PI-3 kinase dependent in hematopoietic progenitor/stem cell lines.* Blood, 2004. **104**(1): p. 51-7.

266. Dangi-Garimella, S., et al., *Raf kinase inhibitory protein suppresses a metastasis signalling cascade involving LIN28 and let-7.* EMBO J, 2009. **28**(4): p. 347-58.

267. Takatsu, K., *Interleukin-5 and IL-5 receptor in health and diseases.* Proc Jpn Acad Ser B Phys Biol Sci, 2011. **87**(8): p. 463-85.

268. Winter, O., E. Mohr, and R.A. Manz, *Alternative cell types form a Multi-Component-Plasma-Cell-Niche.* Immunol Lett, 2011. **141**(1): p. 145-6.

269. Huang, H.M., C.J. Huang, and J.J. Yen, *Mcl-1 is a common target of stem cell factor and interleukin-5 for apoptosis prevention activity via MEK/MAPK and PI-3K/Akt pathways.* Blood, 2000. **96**(5): p. 1764-71.

270. Jourdan, M., et al., *IL-6 supports the generation of human long-lived plasma cells in combination with either APRIL or stromal cell-soluble factors.* Leukemia, 2014. **28**(8): p. 1647-56.

271. Tanner, J.E. and G. Tosato, *Regulation of B-cell growth and immunoglobulin gene transcription by interleukin-6.* Blood, 1992. **79**(2): p. 452-9.

272. Kishimoto, T. and T. Hirano, *Molecular regulation of B lymphocyte response.* Annu Rev Immunol, 1988. **6**: p. 485-512.

273. Masuda, A., et al., *Th2 cytokine production from mast cells is directly induced by lipopolysaccharide and distinctly regulated by c-Jun N-terminal kinase and p38 pathways.* J Immunol, 2002. **169**(7): p. 3801-10.

274. Williams, C.M. and J.W. Coleman, *Induced expression of mRNA for IL-5, IL-6, TNF-alpha, MIP-2 and IFN-gamma in immunologically activated rat peritoneal mast cells: inhibition by dexamethasone and cyclosporin A.* Immunology, 1995. **86**(2): p. 244-9.

275. Tokoyoda, K., et al., *Organization of immunological memory by bone marrow stroma.* Nat Rev Immunol, 2010. **10**(3): p. 193-200.

276. Nagasawa, T., *Microenvironmental niches in the bone marrow required for B-cell development.* Nat Rev Immunol, 2006. **6**(2): p. 107-16.

277. Tokoyoda, K., et al., *Cellular niches controlling B lymphocyte behavior within bone marrow during development.* Immunity, 2004. **20**(6): p. 707-18.

278. Erridge, C., *Endogenous ligands of TLR2 and TLR4: agonists or assistants?* J Leukoc Biol, 2010. **87**(6): p. 989-99.

279. Nagai, Y., et al., *Toll-like receptors on hematopoietic progenitor cells stimulate innate immune system replenishment.* Immunity, 2006. **24**(6): p. 801-12.

Biography

Alex was born in Mineola, NY on the 2nd day of November, 1986. His scientific pursuits began early in life when he became fascinated by birds around age 10. Growing up he spent innumerable hours making observations, gathering data, and participating in citizen-science projects. At 18, Alex entered Cornell University to study biology in the College of Agriculture and Life Sciences. After his second year, he carried out his first independent academic research project under the mentorship of Dr. David Winkler, studying the foraging behavior of Tree Swallows (*Tachycineta bicolor*). The desire to increase the breadth of his experience led him to pursue a second research opportunity the following summer in the distant field of immunology. It was through a project in the laboratory of Dr. Christopher Mariani at North Carolina State University that Alex was introduced to the fascinating world of the immune system. Through his work on Granulomatous Meningoencephalitis, he developed a keen interest in the body's defense system, and took a series of courses on immunology during his final year at Cornell. In 2009, he graduated *cum laude* with a Bachelor's degree in Biological Sciences, and began his graduate studies in the Department of Immunology at Duke University.

Alex has received the Duke University Dean's Graduate Fellowship (2009), two Trainee Abstract Awards from the American Association of Immunologists (2013 and 2014), a Duke Immunology Department Bernard Amos Research Lecture Poster Session

Award (2015), and a Trainee Poster Award from the American Association of Immunologists (2015).

Publications

Reynolds AE, Kuraoka M, Kelsoe G. (2015). *Natural IgM is produced by CD5$^-$ plasma cells that occupy a distinct survival niche in bone marrow.* Journal of Immunology 1;194(1):231-42.

Kuraoka M, Holl TM, Liao D, Womble M, Cain DW, **Reynolds AE**, Kelsoe G. (2011). *Activation-induced cytidine deaminase mediates central tolerance in B cells.* Proc Natl Acad Sci USA 12;108(28):11560-5.

Nojima T, Kuraoka M, **Reynolds AE**, Kitamura D, Kelsoe G. *Tracing Self-Reactive B Cells in Normal Mice*. (manuscript in preparation).